

**Functional changes in connectivity induced by differential manipulations of activity in
Drosophila tonic versus phasic motoneurons**

by
Nicole Ann Aponte Santiago
B.Sc. in Cell and Molecular Biology
University of Puerto Rico – Río Piedras, 2013

SUBMITTED TO THE DEPARTMENT OF BIOLOGY IN PARTIAL FULFILLMENT OF
THE REQUIREMENTS FOR THE DEGREE OF

DOCTOR OF PHILOSOPHY IN BIOLOGY
AT THE
MASSACHUSETTS INSTITUTE OF TECHNOLOGY
May 2020

© 2020 Nicole Ann Aponte Santiago. All rights reserved.

The author hereby grants to MIT permission to reproduce and to distribute
publicly paper and electronic copies of this thesis document in whole or in part in any medium now
known or hereafter created

Signature of Author:

Certified by: **Signature redacted** x Department of Biology
May 6th, 2020

Accepted by: **Signature redacted** x Dr. J. Troy Littleton
Professor of Biology
Thesis Supervisor

x Dr. Stephen Bell
Professor of Biology
Chairman of the Graduate Committee

Functional changes in connectivity induced by differential manipulations of activity in *Drosophila* tonic versus phasic motoneurons

by
Nicole Ann Aponte Santiago

Submitted to the Department of Biology on May 15, 2020 in Partial Fulfillment of the Requirements for the Degree of Doctor of Philosophy in Biology

Abstract

Structural and functional plasticity induced by neuronal competition is a common feature of developing nervous systems. However, the rules governing how postsynaptic cells differentiate between presynaptic inputs are unclear. In this thesis, I characterized synaptic interactions following manipulations of Ib tonic or Is phasic glutamatergic motoneurons that co-innervate postsynaptic muscles at *Drosophila* neuromuscular junctions (NMJs). After identifying drivers for each neuronal subtype, I performed ablation or genetic manipulations to alter neuronal activity and examined the effects on synaptic innervation and function. Ablation of either Ib or Is resulted in decreased muscle response, with some functional compensation occurring in the tonic Ib input when Is was missing. In contrast, the phasic Is terminal failed to show functional or structural changes following loss of the co-innervating Ib input. Decreasing the activity of the Ib or Is neuron with tetanus toxin light chain resulted in structural changes in muscle innervation. Decreased Ib activity resulted in reduced active zone (AZ) number and decreased postsynaptic subsynaptic reticulum (SSR) volume, with the emergence of filopodial-like protrusions from synaptic boutons of the Ib input. Decreased Is activity did not induce structural changes at its own synapses, but the co-innervating Ib motoneuron increased the number of synaptic boutons and AZs it formed. These findings indicate tonic and phasic neurons respond independently to changes in activity, with either functional or structural alterations in the tonic motoneuron occurring following loss or reduced activity of the co-innervating phasic input, respectively. This thesis work contributes to the understanding of how multiple neuronal inputs innervating one postsynaptic muscle interact.

Thesis Supervisor: J. Troy Littleton

Title: Professor of Biology

Acknowledgments:

I am grateful for the people in my life that have encouraged me to foster my love for science, learning, and discovery. Thanks to my dad, Raul Aponte Machin, for introducing me to science and to my mom, Lanette Ann Santiago Cardona, for encouraging me to be my best self. Thank you to my sister, Linette Ann Aponte Santiago, who always challenges me and who I admire. Thank you to the strong women in my family, who showed me that anything is possible.

I want to thank my teachers for encouraging me to seek to learn more than what is required in a curriculum and to continue to ask questions. I want to thank my friends for always looking out for me. Thanks to GWAMIT for giving me a platform, a sense of belonging, and encouragement. To MSRP and Mandana Sassanfar for believing in me and my potential. I want to thank my scientific mentors for pushing me to think outside the box and for believing in my potential. I want to thank J. Troy Littleton for his guidance and mentoring. I thank the Littleton lab members for encouraging me to give my best every day. To MIT and the Biology Department, thank you for giving me a supportive environment to grow as a scientist.

Finally, I want to thank my husband, Emir Avilés Pagán, for always being there for me and for being by my side as we learned what it takes to be a scientist and partners in life. I look forward to our future adventures.

TABLE OF CONTENTS

Abstract.....	2
Acknowledgments.....	3
Table of Contents.....	4
Chapter 1: Neuronal Plasticity of Tonic and Phasic Motoneuron.....	7
Introduction.....	8
Different Types of Synaptic Plasticity and Their Contribution to Animal Behavior.....	9
Distinctions Between Vertebrate and Invertebrate Neuronal Plasticity.....	11
The Drosophila NMJ as a Model Glutamatergic Synapse.....	12
Different Types of Motoneurons at the Drosophila NMJ.....	15
General Overview of Tonic and Phasic Neuronal Properties.....	16
Tonic and Phasic Motoneurons at the Drosophila NMJ.....	18
Tonic and Phasic Motoneuron Morphology Differences at the Drosophila NMJ.....	18
Tonic and Phasic Differential Neurotransmission.....	20
Differential Homeostatic Regulation.....	21
Pathways Implicated in Synapse Formation and Growth in Drosophila.....	23
Conclusion.....	28
Bibliography.....	30
Chapter 2: Functional changes in connectivity induced by differential manipulations of activity in Drosophila tonic versus phasic motoneurons.....	53

Abstract.....	54
Introduction.....	55
Results.....	59
Screen for Ib and Is motoneuron-specific GAL4 drivers.....	59
Establishment of MN1-Ib and MN-Is synaptic connections during development.....	60
Role of MN1-Ib and MNIs in muscle excitability and contraction.....	63
Lack of Ib and Is synaptic competition during NMJ development.....	65
Ablation of MNIs triggers increased evoked release from the remaining MN1-Ib input...	66
Imbalances in MN1-Ib or MNIs neuronal activity reveal structural plasticity of tonic Ib inputs.....	69
Discussion.....	73
Plasticity of target choice by motoneurons at Drosophila NMJs.....	73
Different plasticity rules for tonic versus phasic motoneurons.....	76
Molecular pathways underlying structural and functional plasticity in motoneurons.....	78
Materials and Methods.....	81
Drosophila stocks.....	81
Transgenic constructs.....	81
Immunocytochemistry.....	81
Motoneuron GAL4 driver screen.....	82
Quantification of confocal images.....	83
Live imaging of Ib and Is innervation and synaptic growth.....	83
Electrophysiology.....	84
Muscle force contraction measurements.....	84

Statistical analysis.....	85
Acknowledgements.....	86
Figures.....	87
References.....	122
Chapter 3: Conclusions and future directions.....	143
Conclusion.....	144
Future Directions.....	147
Different levels of plasticity between Ib and Is motoneurons.....	147
Muscle innervation by multiple Ib or Is motoneurons.....	148
Differences between Ib motoneurons.....	149
Disruption of retrograde signals involved in muscle-triggered Ib plasticity.....	150
Transcriptional profiles of Ib and Is motoneurons.....	153
Possible Parallels to Mammalian Tonic and Phasic Neurons.....	154
Bibliography.....	155

Chapter 1: Neuronal Plasticity of Tonic and Phasic Motoneuron

Nicole A. Aponte-Santiago, J. Troy Littleton

The Picower Institute for Learning and Memory, Department of Biology and Department of Brain and Cognitive Sciences, Massachusetts Institute of Technology, Cambridge, MA 02139

Introduction

Brain plasticity can be mediated through both structural and functional changes in synaptic wiring. The ability of the nervous system to alter its functional connectivity is key to processes such as learning and memory. Disruptions in plasticity mechanisms can result in neurodevelopmental diseases and impaired rewiring after adult brain injury. A widespread and prominent form of plasticity occurs during neuronal development, where dynamic neuronal activity changes and behavioral experiences merge to shape how connections are formed and stabilized. Although several vertebrate systems have been used to study activity-dependent synaptic plasticity during development, the molecular underpinnings that mediate neuronal and synaptic changes are still being characterized. As such, *Drosophila* provides a powerful genetic toolkit that can be employed to define both the types and molecular mechanisms that can contribute to activity-dependent neuronal and circuit development.

The motor system has been a useful model to study activity-dependent synaptic interactions, with synapse elimination at vertebrate neuromuscular junctions (NMJs) representing a paradigm for neuronal competition. It has been difficult to address whether similar types of plasticity may occur at *Drosophila* motor synapses due to limited genetic access to individual motoneuron subtypes. Two glutamatergic motoneurons co-innervate most larval muscle fibers. These two motoneurons are a Ib “tonic” neuron, which shows facilitation, increasing release over time, and maintaining release after high-frequency stimulation, while a stronger type Is “phasic” neuron shows depression, reduction in the release after long high-frequency stimulation. Several properties of these two classes of motoneurons have been previously characterized, with the Is and Ib neurons showing different morphological and electrophysiological properties. In addition, each

Ib neuron innervates only a single muscle, while a Is neuron innervates a subset of muscles to coordinate the contraction of distinct muscle groups. Synaptic strength and plasticity are thought to be input specific for these neuronal subclasses at the *Drosophila* NMJ, but how they interact is poorly understood. If and how the postsynaptic muscle can differentiate between these two inputs, and how it might preferentially regulate them, is unclear. In my thesis, I describe my graduate work to create a genetic toolbox for differentially labeling and manipulating the presence or activity of the Ib and Is motoneuron subclasses. Using this genetic toolkit, I characterized if the Ib and Is inputs that innervate a single muscle fiber, muscle 1, cooperate or compete for synaptic innervation and drive to the postsynaptic cell. Moreover, I examined if and how developmental plasticity occurred when there was an input imbalance between the neuronal subtypes. These experiments have provided a foundation to use the *Drosophila* NMJ as a model system for exploring how the same postsynaptic cell can identify and differentially control presynaptic inputs from unique motoneuron subclasses.

Different Types of Synaptic Plasticity and Their Contribution to Animal Behavior

Functional and structural changes in neuronal circuits can occur in response to environmental stimuli, learning and injury. The synapse is a site for communication where information is transferred from one neuron to another cell. The synapse can be formed, eliminated, and modified by activity-dependent changes, resulting in the rewiring of neuronal circuits (Holtmaat & Svoboda, 2009). Therefore, synapses, are commonly modified to change their function and structure to alter local information flow or circuit plasticity.

Synaptic growth, stability, and maintenance requires plasticity at the molecular and neuronal level, as well as integration on a larger circuit-level to maintain overall output within an

acceptable range. Defects in synaptic plasticity can affect memory storage and contribute to phenotypes observed in various neurodegenerative diseases (Mayford et al., 2012). Yet this flexibility is in itself destabilizing and if unbalanced, may result in disorders such as autism, schizophrenia and intellectual disability (Eichler & Meier, 2008; Hunt et al., 2017; Melom & Littleton, 2011; Osses & Juan, 2015; Styr & Slutsky, 2018). Many developmental mechanisms are also re-employed during regeneration following neuronal injury, with failures to reorganize synapses disrupting regeneration, linking synapse disorganization to disease and neural dysfunction (Ivakhnitskaia et al., 2018). Therefore, it is crucial to understand synaptic plasticity in a pathological context.

Both vertebrate and invertebrate nervous systems can alter their functional connectivity in response to changes in neuronal firing patterns or behavioral experiences, even though some invertebrates, like insects, have relatively small nervous systems in comparison to mammals (Cognigni et al., 2018; Davis, 2006; Ghelani and Sigrist, 2018; Giurfa, 2013; Mayford et al., 2012). For example, the brain of *Drosophila melanogaster*, a type of fruit fly, contains approximately 100,000 neurons and the bee brain contains one million neurons. In contrast, the human brain contains ~100 billion neurons (Chiang et al., 2011; Herculano-Houzel, 2009). Despite these reductions in overall neuronal number, insects are capable of concept learning, pessimistic biases, fear conditioning and attention-like processes (Giurfa, 2013). Furthermore, numerous single gene mutations have been found that disrupt both short and long-term memory in *Drosophila*, many of which cause similar defects in mammalian learning (Androschuk et al., 2015; R. L. Davis, 2005). These findings suggest that many of the underlying mechanisms of neuronal plasticity, learning, and memory may have similar molecular players that arose early in brain evolution.

Across most vertebrate and invertebrate species, neuronal plasticity can occur through various mechanisms, including through increasing or decreasing synaptic strength (Mayford et al., 2012). Reversible changes in synapses during learning are thought to be primarily generated due to activity-dependent changes. These changes must be stabilized for them to become permanent, a process known as memory consolidation, transitioning short-term memory to long-term memory. For long-term memory, protein synthesis and changes in synaptic morphology occur, resulting in structural plasticity (Lamprecht & LeDoux, 2004). In the sea slug, *Aplysia*, studies have shown that changes in synapse morphology and synapse number occur during non-associative learning (Bailey & Chen, 1988b, 1988a; Lamprecht & LeDoux, 2004). Furthermore, this type of experience-dependent plasticity has been documented in rodents, raccoons, non-human primates, and humans (Foeller & Feldman, 2004). Therefore, activity-dependent plasticity mechanisms are widespread and general types of plastic change appear to be conserved across many species.

Distinctions Between Vertebrate and Invertebrate Neuronal Plasticity

Synapses are maintained and shaped with neuronal activity playing an important role (Saneyoshi et al., 2010). Dynamic synaptic alterations due to activity are referred to as activity-dependent plasticity, allowing neuronal circuits to mature and perform properly in the face of distinct and changing environmental stimuli. In addition, perturbations in neuronal activity during development can lead to profound functional rewiring of brain circuits. For example, changes in sensitivity to sensory input or experience during mammalian brain development at temporal windows, known as critical periods, can result in physiological and morphological changes in the developing brain (Wiesel et al., 1963). Furthermore, several models for synaptic competition, a refinement process of neural circuits where more robust synaptic inputs are conserved while

weaker inputs are eliminated, have been well-described in vertebrate systems. Hubel and Wiesel pioneered studies in the cat visual system, establishing the concept of activity-dependence for a type of structural plasticity in the central nervous system (CNS) termed ocular dominance plasticity (ODP) (Hubel & Wiesel, 1970; Wiesel et al., 1963). With monocular deprivation, active axons from the open eye outcompete inactive axons to take over synaptic space in the visual cortex. More recently, synaptic competition at developing mammalian neuromuscular junctions (NMJs) has become a widely studied model (Arzan Zarin & Labrador, 2019; Walsh & Lichtman, 2003).

At the mammalian NMJ, muscles are initially innervated by several motoneurons. During development, motor neurons compete for innervation through an activity-dependent process until each muscle fiber is innervated by a single neuron (Walsh & Lichtman, 2003). Furthermore, activity-dependent refinement and pruning of synaptic connections can be disrupted in neurodevelopmental disease states (Doll & Broadie, 2014) and are important to limit rewiring after adult injury or stroke (Nahmani & Turrigiano, 2014). Invertebrates also show neuronal plasticity due to changes in activity. Unilateral deafferentation, destruction or interruption of incoming connections of olfactory receptor neurons (ORNs) in the *Drosophila* CNS results in a significant increase of axon density of contralateral projections from the intact antenna (Berdnik, 2006). Therefore, ORNs axons are capable of enhanced axonal and synaptic growth. In addition, exposure of flies to a long-term odor results in olfactory adaptation and a decrease in volume of specific glomeruli, linking structural brain plasticity and learning in *Drosophila* (Devaud et al., 2001). Furthermore, the ablation of specific motor neurons can result in axonal sprouting of neighboring motor neurons at the fly NMJ that can form connections onto de-innervated muscles (Chang & Keshishian, 1996). Although several systems have been characterized for activity-dependent

synaptic competition, how plasticity of inputs from distinct neuronal classes are regulated by postsynaptic cells is unclear.

The *Drosophila* NMJ as a Model Glutamatergic Synapse

The *Drosophila* neuromuscular junction is a well-established model for glutamatergic synapses with strong evolutionary conservation of the molecular components that mediate synapse formation and function. Taking advantage of the genetic tractability of the fruit fly, Seymour Benzer and his lab pioneered the use of *Drosophila* to identify and characterize mutants in genes involved in behavior (Benzer, 1967), neuronal excitability and synaptic plasticity. These studies lead to a widespread effort to identify the molecular underpinnings of not only neuronal and synaptic function, but also complex behavioral outputs. Together with biochemical and ultrastructural approaches, an understanding of the basis of neuronal communication emerged. The main features of a synapse are the presynaptic active zone, synaptic vesicles, a synaptic cleft and a postsynaptic density (PSD), which must function properly for synaptic communication to occur. Synaptic communication at the *Drosophila* NMJ can be measured in the postsynaptic muscle cell through whole cell muscle recordings of excitatory postsynaptic potentials (EPSPs) and miniature EPSPs (mEPSPs) (Jan LY & Jan YN., 1976). EPSPs are a measure of the muscle's response to evoked release of vesicles from the presynaptic neuron, while mEPSPs represent spontaneous fusion events of single vesicles (one quantum). The coupling of electrophysiological recordings of *Drosophila* larvae with neuronal mutants such as *Shaker* (*Sh*) and *shibire* (*shi*) propelled the glutamatergic neuromuscular junction (NMJ) to become a powerful system to study synapse development and plasticity (Ikeda et al., 1976; Jan LY & Jan YN., 1976; Kaplan & Trout, 1969).

Neurotransmitter release onto the postsynaptic cell occurs at a specialized region of the presynaptic terminal known as the active zone (AZ). AZs contain docked vesicles, a cluster of voltage-gated calcium channels, a cytomatrix of the active zone (CAZ), and an organization platform for proteins with roles in synapse regulation and assembly. The *Drosophila* CAZ is easily identifiable by electron microscopy (EM) as a T-bar structure attached to the plasma membrane that is approximately 200 nm wide and 50 nm high. From the T-bar's core, filaments with synaptic vesicles (SVs) extend (Jiao et al., 2010). The principal structural component of the T-bar is the scaffolding protein Bruchpilot (BRP), with an average CAZ containing ~137 BRP molecules (Ehmann et al., 2014). BRP is homolog to the ELKS/CAST protein family, which includes important scaffolding protein across species (Hida & Ohtsuka, 2010). Loss of BRP results in defects in short-term plasticity, reduced neurotransmitter release, and defective calcium channel enrichment at AZs (Wagh et al., 2006). Therefore, disruption of the CAZ results in defective synaptic communication to the postsynaptic cell.

The postsynaptic cell also has a specialized domain with proteins that bind neurotransmitters and promote anterograde and retrograde signaling. This domain is called the postsynaptic density (PSD) and is recognizable as an electron density by EM. At the type I NMJ boutons, the postsynaptic muscle membrane undergoes various folds and invaginations that form the subsynaptic reticulum (SSR), a complex membrane structure. Within the SSR and apposed to active zones are numerous PSD proteins, including glutamate receptors (GluRs), scaffolding molecules, adhesion molecules, ion channels, and signaling complexes. In the muscle, the GluRs are excitatory ionotropic non-NMDA-type receptors. GluRs are tetrameric receptors that assemble into two possible tetrameric configurations containing GluR-IIC, GluR-IID and GluR-IIE subunits with a fourth GluRIIA (A-type) or GluR-IIB (B-type) subunit (Featherstone et al., 2005; Marrus

et al., 2004; Petersen et al., 1997; Qin et al., 2005; Schuster et al., 1991). The A-type and B-type GluRs exhibit different distributions and have distinct quantal size and desensitization, (Akbergenova et al., 2018; Diantonio et al., 1999). In addition, the GluRIIA and GluRIIB incorporation into the GluR tetramer is plastic, as the expression of tetanus toxic light chain (TeTXLC) suppresses evoked release and increases GluRIIA incorporation (Schmid et al., 2008). PSDs with more GluRIIA incorporation appose AZs with high synaptic vesicle release (P_r) (Akbergenova et al., 2018). GluRIIB changes its distribution during development of the PSD, forming a ring around a central core of GluRIIA as apposed AZs increase their P_r (Akbergenova et al., 2018). This plasticity of the PSD allows the postsynaptic cell to increase the strength of the PSD over development given the GluRIIA receptors conduct more current than their GluRIIB counterparts.

Unlike the synaptic re-organization that occurs at mammalian NMJs, the *Drosophila* NMJ is hardwired. During development of the NMJ, axons exit from motoneurons in the central nervous system and pathfind to the appropriate target muscle in the periphery. At the end of the terminal, the growth cone makes contact with muscles, looking for an appropriate synaptic target (Hoang & Chiba, 2001; Ruiz-Cañada & Budnik, 2006). GluRs redistribute from the muscle surface to the new synapse at the end of embryogenesis. Furthermore, initial innervation by the motorneuron does not require glutamate release (Broadie et al., 1993; Daniels et al., 2006; Featherstone et al., 2002; Saitoe et al., 1997; Schmid et al., 2006). At the NMJ, the growth cone is segregated into varicosities that form the initial synaptic boutons. The boutons contain spaced AZs with GluRs opposing them in the muscle. There is a correlation between the number of boutons and the strength of the NMJ (Reiff et al., 2002; Sanyal et al., 2002; Schuster, 2006; Sigrist et al., 2000, 2003). Several different types of motoneurons, easily distinguishable by their structure and unique

properties, are generated during neurogenesis and pathfind to target muscles early in development (Arzan Zarin & Labrador, 2019). These motoneurons receive input from central pattern generators (CPGs) and local interneurons to form the larval motor system that drives larval locomotion.

Different Types of Motoneurons at the *Drosophila* NMJ

The *Drosophila* NMJ has stereotypical segmental development with each abdominal half-segment containing 30 skeletal muscles innervated precisely by 36 easily identifiable motoneurons (Arzan Zarin & Labrador, 2019). These motoneurons form 4 unique subclasses that were initially defined by their unique presynaptic bouton structure and innervation pattern at NMJs. Type I boutons are glutamatergic, releasing the neurotransmitter glutamate and are sub-divided into two categories. Type-I Ib (“big”) boutons are 3-6 μm in diameter, while the type-I Is (“small”) boutons have a diameter at 2-4 μm . The Type II boutons are small, at 1-2 μm in diameter, and release the biogenic amine octopamine (Monastirioti et al., 1995). Type III boutons are 1-2 μm in diameter and release insulin-like peptide, and are only found at muscle 12 (Hoang & Chiba, 2001). This extensive characterization of the NMJ allows for the study of synapse development and plasticity.

General Overview of Tonic and Phasic Neuronal Properties

The mechanisms that allow inputs from distinct neuronal classes to be integrated into one postsynaptic target is poorly understood. Much of the work in the field has focused on the interplay between excitatory and inhibitory inputs that control the overall excitability of neuronal outputs. Among interactions between excitatory inputs, tonic and phasic neurons have been shown to co-innervate many postsynaptic targets and provide distinct patterns of excitatory drive. Crustacea muscles have been a model for this type of co-innervation, where two types of input important for

muscle control have been described: a “tonic,” slowly contracting, sustained, fatigue-resistant contraction cycle; and a “phasic” cycle producing very quick, twitch-like, non-sustained contractions (H. Atwood, 2008; Kennedy & Takeda, 1965). This system involves two types of motoneurons with different properties. In crayfish, phasic neurons are imperative during escape behaviors. The phasic neuron innervates powerful and large muscles in the abdomen. On the other hand, tonic neurons project to thin muscles maintaining spontaneous activity for locomotion and posture and are low-threshold, just like their mammalian counterparts (H. Atwood, 2008). Tonic and phasic motoneurons can also innervate the same target muscle, as occurs in the *Drosophila* motor system.

The first studies of phasic (“slow”) and tonic (“twitch”) motoneurons were described in amphibians (Kuffler & Williams, 1953). Yet, crayfish studies were the first to link the inputs to behavioral context, making the crayfish a popular model for phasic and tonic studies (H. Atwood, 2008). In crayfish abdominal muscles, the tonic system is linked to postural adjustments, while the phasic system is needed for vigorous escape responses (H. Atwood, 2008; Kennedy & Takeda, 1965). Subsequent studies in the medial gastrocnemius muscle of the cat discovered another phasic and tonic parallel where tonic and phasic synapses are involved in posture and walking, and 60% of the fast-fatigable muscle fibers are needed for jumping (Burke, 1980). Tonic and phasic neurons have also been observed in the prefrontal cortex (PFC) of mammals, where they contribute to behavior flexibility. Dopamine neurons play an important role in the decision process of changing a new task or maintaining a learned behavior (Durstewitz et al., 2000; Durstewitz & Seamans, 2008; Floresco et al., 2006; Puig & Miller, 2012, 2015; Seamans et al., 1998; St. Onge et al., 2011; Stefani & Moghaddam, 2006). Tonic patterns of stimulation from dopamine neurons from the ventral tegmental area (VTA) innervating the PFC cause mice to maintain their learned behavior.

In contrast, rewards can produce phasic increases in the activity of dopaminergic VTA-PFC fibers, with phasic stimulation leading to changes in previously learned associations (Ellwood et al., 2017). In addition, in the mammalian brain, tonic and phasic inhibition interact to maintain homeostatic inhibition. GABA_A receptors, located both in synaptic and extrasynaptic membranes, are the main inhibitory receptors in the brain. Synaptic GABA_A receptors mediate phasic inhibition, while extrasynaptic GABA_A receptors mediate tonic inhibition. Tonic inhibition increases in the cerebellum on the first postpartum month, while phasic inhibition decreases (Brickley et al., 1996; Wall & Usowicz, 1997). Dysfunction in tonic or phasic inhibition has been associated with epilepsy, depression, and anxiety (Brickley & Mody, 2012; Fritschy, 2008; Hines et al., 2012; Macdonald et al., 2010).

Tonic and Phasic Motoneurons at the *Drosophila* NMJ

Two glutamatergic motor neurons innervate most larval muscle fibers, a type Ib “tonic” motoneuron, and the type Is “phasic” motoneuron (Hoang & Chiba, 2001). The Is and Ib neurons have different morphological and electrophysiological properties that are important to sustain muscle contraction (H. L. Atwood et al., 1993a; Hoang & Chiba, 2001; Jia et al., 1993; Kurdyak et al., 1994; Lnenicka & Keshishian, 2000; Lu et al., 2016; Newman et al., 2017). Each Ib neuron innervates only a single muscle, while the Is neurons innervate a subset of muscles to coordinate the contraction of distinct muscle groups. Elimination of Is motoneurons disrupt contraction wave coordination between multiple segments (Newman et al., 2017; Suster et al., 2003). Prior studies have suggested Ib and Is motoneurons have distinct synaptic strengths, short term plasticity outputs, and responses to homeostatic plasticity at the *Drosophila* NMJ (Ashley & Budnik, 2017;

Newman et al., 2017). However, how the postsynaptic muscle differentiates between these two inputs, and how it preferentially regulate their properties is unclear.

Tonic and Phasic Motoneuron Morphology Differences at the *Drosophila* NMJ

One major morphological difference between Ib and Is neurons is how the muscle postsynaptic membrane is organized. The subsynaptic reticulum (SSR) are large infoldings of the muscle postsynaptic membrane that develop around presynaptic boutons over the course of larval development. Mature Ib boutons have a bigger SSR than the Is counterparts. Disc large (Dlg) is a well-known postsynaptic scaffolding protein that is abundant in the SSR, and is a member of the membrane-associated guanylate kinase (MAGUK) family. Similar MAGUK proteins like PSD-95 have roles in the organization of the PSD and regulation of mammalian ionotropic glutamate receptors (Elias & Nicoll, 2007; Zheng et al., 2011). Dlg recruits other PSD proteins, including the adhesion protein Fasciclin II (FasII), the K⁺ channel Shaker and the postsynaptic t-SNARE Gtaxis (Gtx) that regulates SSR development and expansion (Gorczyca et al., 2007; Thomas et al., 1997; Zito et al., 1997). The differential distribution of the SSR between Ib and Is boutons suggests that the muscle is capable of distinguishing these two inputs and forming distinct postsynaptic specializations. In addition, there are differences in the abundance of specific postsynaptic glutamate receptor subunits, with the GluRIIA subtype enriching more at Ib terminals (Petersen et al., 1997). Therefore, the postsynaptic cell may distinguish between these two inputs and differentially regulate them.

Synaptic bouton shape is also different between Ib and Is motoneurons. The bigger boutons in Ib motoneurons have increased mitochondrial and synaptic vesicle number than Is terminals (H. L. Atwood et al., 1993a; Jia et al., 1993). This difference have been suggested to alter calcium

buffering and ATP production. Ib synapses have a faster clearance of Ca^{2+} than Is neurons (He et al., 2009). This is consistent with the higher firing frequency of the Ib during fictive crawling in semi-intact larvae preparations (40–60 Hz in Ib vs 10–20 Hz in type Is) (Cattaert & Birman, 2001; Chouhan et al., 2010). Therefore, the Ib input may require a more robust Ca^{2+} clearing system than the Is to prevent intracellular Ca^{2+} buildup. Ib neurons also require more ATP metabolism, consistent with their larger pool of mitochondria compared to phasic Is terminals (H. L. Atwood et al., 1993a; Jia et al., 1993; X. Xing & Wu, 2018). The same is true for the tonic and phasic motoneurons in crayfish (Msghina et al., 1998, 1999; P. V. Nguyen et al., 1997). Therefore, bouton shape affects several important properties of the Ib and Is motoneurons.

Tonic and Phasic Differential Neurotransmission

The tonic Ib and phasic Is synapses have different physiological properties. The tonic Ib synapse has smaller quantal size, more spontaneous release, and lower P_r than the phasic Is (Newman et al., 2017). The Ib exhibits short-term facilitation while Is has short-term depression during high frequency trains (Lnenicka & Keshishian, 2000; Lu et al., 2016). Also, synaptic strength, short-term plasticity, and synaptic homeostasis are synapse specific (Newman et al., 2017). Ib inputs have a large number of silent active zones that can be recruited, which is important for plasticity during stimulation trains. Phasic Is synapses have a larger quantal amplitude due to 30% larger synaptic vesicle size. In contrast, Ib synapses have more spontaneous release, yet spontaneous release only accounts for less than 1% of the total postsynaptic calcium signal at the NMJ (Karunanithi et al., 2002; Newman et al., 2017; C. T. Nguyen & Stewart, 2016). In contrast, action potential (AP) response sites are more numerous in Ib synapses, although single AP-evoked

quantal size is larger in Is synapses (Newman et al., 2017). If and how the muscle differentially contributes to these specific presynaptic properties is poorly understood.

Tonic Ib and phasic Is motoneurons also have different membrane excitability profiles (X. Xing & Wu, 2018). The tonic Ib neuron's capability of sustained neurotransmission results in Ib synaptic activity beginning and ending before phasic Is activity (Choi et al., 2004; Schaefer et al., 2010). Ib neurons have a lower spike threshold than Is neurons, and the distal Is motoneuron (MNISN-Is) has a longer delay-to-spike than Ib in whole-cell recordings during fictive locomotion (Schaefer et al., 2010). In addition, different excitatory and inhibitory interneurons regulate the recruitment of motoneurons between and within hemisegments (Heckscher et al., 2015; Zwart et al., 2016). Therefore, a combination of circuitry and intrinsic properties of Ib and Is motoneurons results in complex behavioral motor outputs (Newman et al., 2017).

Short-term plasticity is also different between tonic Ib and phasic Is synapses. Overall release facilitates in Ib synapses while it depresses in Is synapses. Phasic Is synapses have a higher probability of release, which makes them more energy-efficient, but incapable of sustaining release during long periods (Lu et al., 2016). Furthermore, Ib synapses have a larger number of silent synapses that are recruited for short-term plasticity while Is boutons have a large number of active zones that depress (Newman et al., 2017). Also, calcium sensitivity is different between Ib and Is synapses, with Ib synapses having less sensitivity to external calcium. Ib has lower release probability at low calcium, and increases in extracellular calcium can increase Ib synapses release rate to match or exceed the release rate of Is synapses (Genç & Davis, 2019).

Differential Homeostatic Regulation

Synaptic activity must be stabilized through homeostatic mechanisms in a variety of organisms from invertebrates to humans (Pozo & Goda, 2010). Perturbations that destabilize neurotransmitters are offset by changes to postsynaptic receptors (synaptic scaling) and/or changing presynaptic neurotransmission to maintain levels of output within a set range (G. W. Davis & Müller, 2015; Turrigiano, 2012). This stabilizing yet flexible mechanism is termed homeostatic synaptic plasticity (Turrigiano, 2012). Reduction of postsynaptic glutamate receptor (GluR) function through genetic or pharmaceutical manipulation results in presynaptic homeostatic potentiation (PHP) at the *Drosophila* NMJ, where the presynaptic cell receives a retrograde signal resulting in a compensatory enhancement in neurotransmitter release (Frank, 2014). This process is important for bringing neurotransmission back to baseline levels. Another mechanism to maintain neurotransmission at baseline is presynaptic homeostatic depression (PHD). PHD is where increased vesicle size results in a reduction of synaptic vesicle release (quantal content) which reduces basal levels of neurotransmission (C. K. Chen et al., 2014; Dickman et al., 2005; Marie et al., 2004; Verstreken et al., 2002). PHD is hypothesized to be an autocrine adaptive response to baseline glutamate (Daniels et al., 2004; X. Li et al., 2018). Failure of homeostatic plasticity can result in synaptic imbalance and neurodevelopmental disorders. Disruptions in GluR function reduce muscle response, which might also occur when an input is eliminated or silenced. As such, similar pathways could be engaged.

Both Ib and Is synapses are capable of homeostatic compensation. Yet, Ib and Is synapses differentially express presynaptic homeostatic potentiation (PHP) at low calcium, with Ib inputs being more responsive to homeostatic compensation (Genç & Davis, 2019). Even though a disruptive mutation of GluR results in a reduction of quantal size in both Ib and Is synapses, only the Ib input produced the compensatory response of increasing neurotransmitter release at low

calcium. Also, in these conditions, CaMKII, a proposed signaling component of this pathway, was reduced in the post-synaptic terminal of Ib inputs, but not Is inputs (Newman et al., 2017). Ib and Is synapses respond differently to presynaptic homeostatic potentiation (PHP) due to acute or chronic neurotransmitter perturbations. Acute PHP is created by a 10-minute incubation of the larvae preparation in the glutamate receptor antagonist phillanthotoxin (PhTx), which binds to glutamate receptors, causing a decrease in ionic conductance and a decrease in average miniature excitatory postsynaptic potential (mEPSP). This conductance change induces PHP through the promotion of an increase in presynaptic neurotransmitter (Orr et al., 2017). PHP is more robust in Is synapses, but more variable and less robust in Ib synapses at low calcium conditions. This discrepancy may be due to Ib synapses having a lower probability of release. In addition, increasing external calcium concentration to 3.0 mM resulted in a robust acute PHP response in both Ib and Is synapses. During chronic induction of PHP due to deletion of the GluRIIA subunit, a presynaptic reorganization of active zones occur (N. Harris et al., 2018; Marie et al., 2010). At low extracellular calcium (0.5 mM), chronic PHP is absent from Is synapses, but is present and as robust as PHP in Ib synapses at high extracellular calcium (3.0 mM). This indicates that the muscle may be capable of distinguishing Ib and Is inputs under specific conditions.

One way that the muscle may distinguish the Ib from the Is input is by reacting to the differential amount of calcium influx around postsynaptic Ib synapses. Ib inputs have more extended periods of activity, elevating the calcium accumulation around Ib during larvae locomotion. CAMKII may respond to this calcium accumulation differentially in the postsynaptic compartment of the two input types (Stratton et al., 2013). Yet, even if CAMKII is downregulated, only the Ib responds with homeostatic compensation (Newman et al., 2017).

Pathways Implicated in Synapse Formation and Growth in Drosophila

At the Drosophila NMJ, each motoneuron innervates a specific muscle fiber, but the precise branching pattern and bouton organization is distinct in each animal. Pathways involved in NMJ structural plasticity may also be involved in input specific regulation. These pathways include the regulation of excitability, anterograde, retrograde, and autocrine signaling and involve both pre- and post-synaptic partners through changes in the cytoskeleton, extracellular matrix and vesicle trafficking. During the larval stages, the NMJ undergoes significant growth, with the muscle surface area increasing over 100-fold in five days of larval development (H. L. Atwood et al., 1993b; Menon et al., 2013; Schuster et al., 1996). To maintain proper innervation, the presynaptic motoneuron expands the size of its terminal arbor and the number of synapses. Live imaging through the cuticle of bouton growth during growing larvae revealed that new boutons are either added onto the ends of the arbor or form between existing boutons (Zito et al., 1999). In addition, rapid presynaptic bouton budding can occur in the presynaptic arbor in response to elevated neuronal activity (Ataman et al., 2008; Piccioli & Littleton, 2014). Below I describe some of the key molecular pathways that have been shown to control structural growth of Drosophila NMJ synapses.

Two major pathways involved in activity-dependent plasticity through transsynaptic signaling are the Bone morphogenic proteins (BMP) and Wnt pathway. These are involved in early development but have additional roles at the NMJ (K. P. Harris et al., 2015). Bone morphogenic proteins (BMPs) are conserved differentiation and growth factors that are part of the transforming growth factor-beta (TGF- β) superfamily. Initiating the BMP signaling pathway, the BMP ligand is secreted from muscle. It binds to two type-II BMP receptors at the presynaptic membrane, which phosphorylate type-I BMP receptors. Phosphorylated type-I BMP receptors phosphorylate

cytoplasmic R-Smads, which recruits co-Smads, forming a Smad complex. Finally, the Smad complex regulates the transcription of target genes after translocating to the nucleus. At the *Drosophila* NMJ, mutants affecting this pathway have been identified, affecting synaptic growth as well as exhibiting reduced neurotransmitter release. Some examples of these mutants include a BMP type-II receptor *wishful thinking* (*wit*), the BMP ligand Glass bottom boat (*Gbb*), the type I receptors Thickveins (*Tkv*) and Saxophone (*Sax*), the R-Smad Mothers against decapentaplegic (*Mad*), the co-Smad Medea (*Med*) and a direct transcription target of this pathway, the Rho-type guanine nucleotide exchange factor (GEF) *trio* (Aberle et al., 2002; K. P. Harris et al., 2015; Marqués et al., 2002; Marqués & Zhang, 2006; McCabe et al., 2003, 2004; Rawson et al., 2003). During a critical period at the first larval instar, Mad signaling is necessary for NMJ growth and activity-dependent plasticity (Berke et al., 2013). Furthermore, BMP signaling functions in both retrograde and anterograde directions at the synapse (Dudu et al., 2006; Fuentes-Medel et al., 2012). It is unknown if BMP signaling functions differently between different inputs to the postsynaptic cell.

Another conserved pathway from early development with an important function at the NMJ is the Wnt pathway. Wnts are secreted glycoproteins with roles in tissue patterning as well as in post-mitotic neurons, dendrite development, axon pathfinding, and synaptogenesis (Budnik & Salinas, 2011). Loss of Wnt/Wingless (*Wg*) shows a decrease in bouton number, irregular and large boutons, SSR depletion, increase in the number of ghost boutons (irregular boutons without neurotransmission machinery and a postsynaptic scaffold), an increase in GluRIIA clustering, and abnormal microtubule organization in the presynaptic cytoskeleton (Ataman et al., 2006; Kerr et al., 2014; Korkut et al., 2009; Packard et al., 2002; Speese et al., 2012). In the canonical Wnt pathway, β -catenin is imported to the nucleus and regulates the transcription of targeted genes. At

the NMJ, Wg is secreted from the neuron and binds to its receptor Frizzled-2 (Fz2) in both the neuron and muscle, making Wnt signaling bidirectional. If Wg is secreted by the neurons and binds in the postsynaptic side, Fz2 is endocytosed, cleaved, and a C-terminal fragment of Fz2 is delivered to the nucleus (Mathew et al., 2005). If Wg binds Fz2 in the presynaptic cell, the pathway is independent of β -catenin, unlike the canonical pathway, and acts locally at the synaptic terminal. Disruption of the presynaptic pathway results in disruption of the microtubule organization, reduced bouton number, and irregular bouton morphology (Mathew et al., 2005). Differential regulation of Wg to different inputs may be another mechanism that the muscle uses to differentially regulate its inputs.

Another transsynaptic signal for synapse growth regulation is controlled by the postsynaptic calcium sensor, synaptotagmin 4 (SYT4), which is required for synaptic overgrowth in hyperexcitable mutants, induction of presynaptic miniature release after high-frequency stimulation, and the induction of ghost boutons (Barber et al., 2009; Korkut et al., 2013; Piccioli & Littleton, 2014; Yoshihara et al., 2005). SYT4 is transferred transsynaptically from the presynaptic terminal on exosomes, which are signaling vesicles released from cells that contribute to cell-cell communications (Cocucci & Meldolesi, 2015; Korkut et al., 2013). Differential retrograde signaling through SYT4 could also be used by the postsynaptic cell to regulate different types of innervation.

Another critical form of signaling at the NMJ is neurotrophic signaling, which has been shown to control synaptic plasticity, synaptic targeting, neuronal survival, proliferation, and differentiation. Neurotrophins (NTs) in *Drosophila*, DNT1, and DNT2, are required for neuronal survival (Zhu et al., 2008). Neurotrophin receptors in *Drosophila* are encoded by Toll paralogs that function in development and immunity. *Toll-6* and *Toll-7* are expressed in locomotion centers

in the adult brain, motoneurons, and interneurons of the embryonic central pattern generator. The central pattern generator is the CNS circuit required for proper locomotion. Finally, Toll-7 and Toll-6 regulate movement, motor axon targeting, and neuronal survival by promiscuously binding to DNT1 and DNT2, respectively (Mcilroy et al., 2013). Therefore, neurotrophin signaling may be another candidate pathway by which the muscle regulates its inputs.

Transsynaptic adhesion also regulate synaptic morphology and apposition, as well as active zone density, bouton growth, and the postsynaptic density. One transsynaptic adhesion pair is Neurexin (Nrx) and Neuroligin (Nlg), which regulate formation, maturation, and organization of synapses across species (Bang & Owczarek, 2013). There is one *nrx* gene (*nrx-1*) and four *nlg* genes in *Drosophila*. Mutants of *nlg-1* contain boutons without postsynaptic specialization called orphan boutons (Banovic et al., 2010; Y. C. Chen et al., 2012; Sun et al., 2011; G. Xing et al., 2014). Mutants for *nrx-1*, *nlg-1*, and *nlg-2* have decreased bouton number, while *nlg-3* mutants show bouton overgrowth (Banovic et al., 2010; J. L. Chen et al., 2012; J. Li et al., 2007; Sun et al., 2011; G. Xing et al., 2014). Also, *nlg-1* and *nlg-2* boutons are bigger and irregularly shaped (Y. C. Chen et al., 2012). Another transsynaptic pair, the Teneurins (ten), interact with Nrx-1 and Nlg-1. Loss of teneurins results in similar phenotype to *nrx-1* and *nlg-1* mutants with AZ/GluR spacing and size defects, disruption of the postsynaptic cytoskeleton and of the presynaptic microtubules, and loss of SSR (Banovic et al., 2010; J. Li et al., 2007; Mosca et al., 2012). Loss of ten-A (presynaptic) or ten-M (postsynaptic) also show a decrease in bouton number with irregularly shaped large boutons (Mosca et al., 2005). Therefore, adhesion connections could play a role in regulating different presynaptic inputs onto a postsynaptic cell.

Increasing larval locomotion or inducing neuronal seizures can also result in increased nerve terminal growth and elevated synaptic bouton number (Guan et al., 2005; Sigrist et al., 2003).

Activity-dependent increases in bouton number can also be mediated by increased calcium/cAMP signaling. Bouton overgrowth is observed in hyperexcitable double mutants of voltage-gated K⁺ channels, *sh*, and *ether a go-go (eag)* (Budnik et al., 1990). Other mutants with overgrowth are those affecting the K⁺ channel *slowpoke (slo)*, a calcium-activated BK channel, and a voltage-dependent ERG channel *seizure (sei)* (Lee & Wu, 2010). Loss of adenylyl cyclase, *rutabaga (rut)*, suppresses overgrowth in *eag*, *Sh*, *slo*, or *sei* mutant backgrounds (Lee & Wu, 2010; Zhong et al., 1992). Also, loss of a cAMP-specific phosphodiesterase, *dunce (dnc)*, suppresses overgrowth in *sei* and *slo* mutants. Therefore, cAMP levels are important for activity-dependent overgrowth. Another way to increase bouton number is by increasing larvae locomotion (Sigrist et al., 2003). It is unknown if different types of motoneurons respond differently to activity dependent changes and whether synaptic growth pathways specifically regulate distinct types of motoneurons.

Conclusion

As described above, changes in neuronal activity can lead to rewiring of brain circuits through alterations in structure or function. These dynamic alterations in synapses allow neuronal circuits to mature and perform properly in the face of distinct environmental stimuli. How postsynaptic targets independently regulate the plasticity of inputs from distinct neuronal classes is unclear. Therefore, the goal of this thesis is to establish a system to manipulate and characterize synaptic interactions between motoneuron subclasses in *Drosophila*.

In the mammalian NMJ, multiple neurons of the same class innervate one muscle fiber. These neurons compete until the most active motoneuron becomes the driver for the muscle. In contrast, the *Drosophila* motor circuit is hardwired, with most muscles innervated by two distinct

glutamatergic motoneuron classes. The tonic Ib motoneurons sustain long periods of contraction of individual muscles, while the stronger Is phasic motoneurons serve to regulation coordinated contraction of specific muscle groups. How muscles differentially regulate these tonic and phasic inputs is poorly understood. In addition, how phasic Is and tonic Ib motoneurons alter their properties in response to changes in the co-innervating input is unknown.

The *Drosophila* musculature is organized in repeating abdominal hemisegments and has a hardwired innervation pattern with easy access for electrophysiology and imaging. In addition to the ease of genetic manipulation and imaging, multiple forms of acute and chronic synaptic plasticity have been described in *Drosophila*. In addition, two principal glutamatergic motoneuron classes, the tonic Ib and phasic Is neurons, innervate the muscles and have distinct synaptic properties.

In my thesis work, I focused on charactering how the tonic Ib and phasic Is motoneurons innervating muscle 1 (M1) develop, function and interact during larval development. Are there changes in connectivity when the activity of one of these neurons is altered or the neuron is absent? Are these changes dependent on which neuron is being manipulated? What are the resulting functional and/or structural changes when this dual innervation system is perturbed? In this thesis, I describe the rules I identified when there is only one input, when one input has less activity (silencing), or when one input has more activity (stimulation). These results provided a foundation for understanding how tonic and phasic motoneurons differentially respond to activity manipulations during *Drosophila* larval development.

Bibliography:

- Aberle, H., Haghghi, A. P., Fetter, R. D., McCabe, B. D., Magalhães, T. R., & Goodman, C. S. (2002). Wishful thinking encodes a BMP type II receptor that regulates synaptic growth in *Drosophila*. *Neuron*, *33*(4), 545–558. [https://doi.org/10.1016/S0896-6273\(02\)00589-5](https://doi.org/10.1016/S0896-6273(02)00589-5)
- Akbergenova, Y., Cunningham, K. L., Zhang, Y. V., Weiss, S., & Littleton, J. T. (2018). *Characterization of developmental and molecular factors underlying release heterogeneity at Drosophila synapses*. 1–37.
- Androschuk, A., Al-Jabri, B., & Bolduc, F. V. (2015). From learning to memory: What flies can tell us about intellectual disability treatment. *Frontiers in Psychiatry*, *6*(JUN), 1–16. <https://doi.org/10.3389/fpsy.2015.00085>
- Arzan Zarin, A., & Labrador, J. P. (2019). Motor axon guidance in *Drosophila*. *Seminars in Cell and Developmental Biology*, *85*, 36–47. <https://doi.org/10.1016/j.semcdb.2017.11.013>
- Ashley, J., & Budnik, V. (2017). A Tale of Two Inputs. *Neuron*, *93*(6), 1245–1247. <https://doi.org/10.1016/j.neuron.2017.03.013>
- Ataman, B., Ashley, J., Gorczyca, M., Ramachandran, P., Fouquet, W., Sigrist, S. J., & Budnik, V. (2008). Rapid Activity-Dependent Modifications in Synaptic Structure and Function Require Bidirectional Wnt Signaling. *Neuron*, *57*(5), 705–718. <https://doi.org/10.1016/j.neuron.2008.01.026>
- Ataman, B., Budnik, V., & Thomas, U. (2006). *Scaffolding Proteins at the Drosophila Neuromuscular Junction* (Vol. 75, pp. 181–216). Elsevier. <http://linkinghub.elsevier.com/retrieve/pii/S0074774206750097>
- Atwood, H. (2008). Parallel “phasic” and “tonic” motor systems of the crayfish abdomen. In *Journal of Experimental Biology* (Vol. 211, Issue 14, pp. 2193–2195).

<https://doi.org/10.1242/jeb.010868>

Atwood, H. L., Govind, C. K., & Wu, C.-F. (1993a). Differential ultrastructure of synaptic terminals on ventral longitudinal abdominal muscles in *Drosophila* larvae. *Journal of Neurobiology*, 24(8), 1008–1024.

<http://onlinelibrary.wiley.com/doi/10.1002/neu.480240803/full>

Atwood, H. L., Govind, C. K., & Wu, C.-F. (1993b). Differential ultrastructure of synaptic terminals on ventral longitudinal abdominal muscles in *Drosophila* larvae. *Journal of Neurobiology*, 24(8), 1008–1024.

<http://onlinelibrary.wiley.com/doi/10.1002/neu.480240803/full>

Bailey, C. H., & Chen, M. (1988a). Long-term sensitization in *Aplysia* increases the number of presynaptic contacts onto the identified gill motor neuron L7. *Proceedings of the National Academy of Sciences of the United States of America*, 85(23), 9356–9359.

<https://doi.org/10.1073/pnas.85.23.9356>

Bailey, C. H., & Chen, M. (1988b). Morphological basis of short-term habituation in *Aplysia*. *Journal of Neuroscience*, 8(7), 2452–2459. <https://doi.org/10.1523/jneurosci.08-07-02452.1988>

Bang, M. L., & Owczarek, S. (2013). A matter of balance: Role of neurexin and neuroligin at the synapse. *Neurochemical Research*, 38(6), 1174–1189. <https://doi.org/10.1007/s11064-013-1029-9>

Banovic, D., Khorramshahi, O., Oswald, D., Wichmann, C., Riedt, T., Fouquet, W., Tian, R., Sigrist, S. J., & Aberle, H. (2010). *Drosophila* Neuroligin 1 Promotes Growth and Postsynaptic Differentiation at Glutamatergic Neuromuscular Junctions. *Neuron*, 66(5), 724–738. <https://doi.org/10.1016/j.neuron.2010.05.020>

- Barber, C. F., Jorquera, R. A., Melom, J. E., & Littleton, J. T. (2009). Postsynaptic regulation of synaptic plasticity by synaptotagmin 4 requires both C2 domains. *Journal of Cell Biology*, *187*(2), 295–310. <https://doi.org/10.1083/jcb.200903098>
- Benzer, S. (1967). BEHAVIORAL MUTANTS OF *Drosophila* ISOLATED BY COUNTERCURRENT DISTRIBUTION. *Proceedings of the National Academy of Sciences*, *58*(3), 1112–1119. <https://doi.org/10.1073/pnas.58.3.1112>
- Berdnik, D. (2006). Wiring Stability of the Adult *Drosophila* Olfactory Circuit after Lesion. *Journal of Neuroscience*, *26*(13), 3367–3376. <https://doi.org/10.1523/JNEUROSCI.4941-05.2006>
- Berke, B., Wittnam, J., McNeill, E., Vactor, D. L. Van, & Keshishian, H. (2013). *Retrograde BMP Signaling at the Synapse : A Permissive Signal for Synapse Maturation and Activity-Dependent Plasticity*. *33*(45), 17937–17950. <https://doi.org/10.1523/JNEUROSCI.6075-11.2013>
- Brickley, S. G., Cull-Candy, S. G., & Farrant, M. (1996). Development of a tonic form of synaptic inhibition in rat cerebellar granule cells resulting from persistent activation of GABAA receptors. *Journal of Physiology*, *497*(3), 753–759. <https://doi.org/10.1113/jphysiol.1996.sp021806>
- Brickley, S. G., & Mody, I. (2012). Extrasynaptic GABA A Receptors: Their Function in the CNS and Implications for Disease. *Neuron*, *73*(1), 23–34. <https://doi.org/10.1016/j.neuron.2011.12.012>
- Broadie, K. S., Bate, M., & Broadie, S. (1993). Development of the Embryonic Neuromuscular Synapse of *Drosophila melanogaster*. *The Journal of Neuroscience*, *13*(1), 144–166. <http://www.ncbi.nlm.nih.gov/pubmed/8093713>

- Budnik, V., & Salinas, P. C. (2011). Wnt signaling during synaptic development and plasticity. *Current Opinion in Neurobiology*, *21*(1), 151–159.
<https://doi.org/10.1016/j.conb.2010.12.002>
- Budnik, V., Zhong, Y., & Wu, C. F. (1990). Morphological plasticity of motor axons in *Drosophila* mutants with altered excitability. *Journal of Neuroscience*, *10*(11), 3754–3768.
<https://doi.org/10.1523/jneurosci.10-11-03754.1990>
- Burke, R. E. (1980). Motor unit types: functional specializations in motor control. *Trends in Neurosciences*, *3*(11 C), 255–258. [https://doi.org/10.1016/0166-2236\(80\)90095-8](https://doi.org/10.1016/0166-2236(80)90095-8)
- Cattaert, D., & Birman, S. (2001). Blockade of the central generator of locomotor rhythm by noncompetitive NMDA receptor antagonists in *Drosophila* larvae. *Journal of Neurobiology*, *48*, 58–73. <https://doi.org/10.1002/neu.1042>
- Chang, T. N., & Keshishian, H. (1996). Laser ablation of *Drosophila* embryonic motoneurons causes ectopic innervation of target muscle fibers. *The Journal of Neuroscience : The Official Journal of the Society for Neuroscience*, *16*(18), 5715–5726.
- Chen, C. K., Bregere, C., Paluch, J., Lu, J. F., Dickman, D. K., & Chang, K. T. (2014). Activity-dependent facilitation of Synaptojanin and synaptic vesicle recycling by the Minibrain kinase. *Nature Communications*, *5*(May). <https://doi.org/10.1038/ncomms5246>
- Chen, J. L., Villa, K. L., Cha, J. W., So, P. T. C., Kubota, Y., & Nedivi, E. (2012). Clustered Dynamics of Inhibitory Synapses and Dendritic Spines in the Adult Neocortex. *Neuron*, *74*(2), 361–373. <https://doi.org/10.1016/j.neuron.2012.02.030>
- Chen, Y. C., Lin, Y. Q., Banerjee, S., Venken, K., Li, J., Ismat, A., Chen, K., Duraine, L., Bellen, H. J., & Bhat, M. A. (2012). *Drosophila* neuroligin 2 is required presynaptically and postsynaptically for proper synaptic differentiation and synaptic transmission. *Journal of*

- Neuroscience*, 32(45), 16018–16030. <https://doi.org/10.1523/JNEUROSCI.1685-12.2012>
- Chiang, A. S., Lin, C. Y., Chuang, C. C., Chang, H. M., Hsieh, C. H., Yeh, C. W., Shih, C. T., Wu, J. J., Wang, G. T., Chen, Y. C., Wu, C. C., Chen, G. Y., Ching, Y. T., Lee, P. C., Lin, C. Y., Lin, H. H., Wu, C. C., Hsu, H. W., Huang, Y. A., ... Hwang, J. K. (2011). Three-dimensional reconstruction of brain-wide wiring networks in drosophila at single-cell resolution. *Current Biology*, 21(1), 1–11. <https://doi.org/10.1016/j.cub.2010.11.056>
- Choi, J. C., Park, D., & Griffith, L. C. (2004). Electrophysiological and morphological characterization of identified motor neurons in the *Drosophila* third instar larva central nervous system. *Journal of Neurophysiology*, 91(5), 2353–2365. <https://doi.org/10.1152/jn.01115.2003>
- Chouhan, A. K., Zhang, J., Zinsmaier, K. E., & Macleod, G. T. (2010). Presynaptic mitochondria in functionally different motor neurons exhibit similar affinities for Ca²⁺ but exert little influence as Ca²⁺ buffers at nerve firing rates in situ. *Journal of Neuroscience*, 30(5), 1869–1881. <https://doi.org/10.1523/JNEUROSCI.4701-09.2010>
- Cocucci, E., & Meldolesi, J. (2015). Ectosomes and exosomes: Shedding the confusion between extracellular vesicles. *Trends in Cell Biology*, 25(6), 364–372. <https://doi.org/10.1016/j.tcb.2015.01.004>
- Daniels, R. W., Collins, C. a., Chen, K., Gelfand, M. V., Featherstone, D. E., & DiAntonio, A. (2006). A single vesicular glutamate transporter is sufficient to fill a synaptic vesicle. *Neuron*, 49(1), 11–16. <https://doi.org/10.1016/j.neuron.2005.11.032>
- Daniels, R. W., Collins, C. A., Gelfand, M. V., Dant, J., Brooks, E. S., Krantz, D. E., & Diantonio, A. (2004). *Increased Expression of the Drosophila Vesicular Glutamate Transporter Leads to Excess Glutamate Release and a Compensatory Decrease in Quantal*

- Content*, 24(46), 10466–10474. <https://doi.org/10.1523/JNEUROSCI.3001-04.2004>
- Davis, G. W., & Müller, M. (2015). Homeostatic Control of Presynaptic Neurotransmitter Release. *Annual Review of Physiology*, 77(1), 251–270. <https://doi.org/10.1146/annurev-physiol-021014-071740>
- Davis, R. L. (2005). OLFACTORY MEMORY FORMATION IN DROSOPHILA : From Molecular to Systems Neuroscience . *Annual Review of Neuroscience*, 28(1), 275–302. <https://doi.org/10.1146/annurev.neuro.28.061604.135651>
- Devaud, J.-M., Acebes, A., & Ferrús, A. (2001). Odor Exposure Causes Central Adaptation and Morphological Changes in Selected Olfactory Glomeruli in Drosophila. *The Journal of Neuroscience*, 21(16), 6274–6282. <https://doi.org/>
- Diantonio, A., Petersen, S. A., Heckmann, M., & Goodman, C. S. (1999). Glutamate receptor expression regulates quantal size and quantal content at the Drosophila neuromuscular junction. *Journal of Neuroscience*, 19(8), 3023–3032. <https://doi.org/10.1523/jneurosci.19-08-03023.1999>
- Dickman, D. K., Horne, J. A., Meinertzhagen, I. A., & Schwarz, T. L. (2005). A slowed classical pathway rather than kiss-and-run mediates endocytosis at synapses lacking synaptojanin and endophilin. *Cell*, 123(3), 521–533. <https://doi.org/10.1016/j.cell.2005.09.026>
- Doll, C. A., & Broadie, K. (2014). Impaired activity-dependent neural circuit assembly and refinement in autism spectrum disorder genetic models. *Frontiers in Cellular Neuroscience*, 8. <https://doi.org/10.3389/fncel.2014.00030>
- Dudu, V., Bittig, T., Entchev, E., Kicheva, A., Jülicher, F., & González-Gaitán, M. (2006). Postsynaptic Mad Signaling at the Drosophila Neuromuscular Junction. *Current Biology*, 16(7), 625–635. <https://doi.org/10.1016/j.cub.2006.02.061>

- Durstewitz, D., & Seamans, J. K. (2008). The Dual-State Theory of Prefrontal Cortex Dopamine Function with Relevance to Catechol-O-Methyltransferase Genotypes and Schizophrenia. *Biological Psychiatry*, *64*(9), 739–749. <https://doi.org/10.1016/j.biopsych.2008.05.015>
- Durstewitz, D., Seamans, J. K., & Sejnowski, T. J. (2000). Dopamine-mediated stabilization of delay-period activity in a network model of prefrontal cortex. *Journal of Neurophysiology*, *83*(3), 1733–1750. <https://doi.org/10.1152/jn.2000.83.3.1733>
- Ehmann, N., Van De Linde, S., Alon, A., Ljaschenko, D., Keung, X. Z., Holm, T., Rings, A., DiAntonio, A., Hallermann, S., Ashery, U., Heckmann, M., Sauer, M., & Kittel, R. J. (2014). Quantitative super-resolution imaging of Bruchpilot distinguishes active zone states. *Nature Communications*, *5*. <https://doi.org/10.1038/ncomms5650>
- Eichler, S. A., & Meier, J. C. (2008). E-I balance and human diseases - from molecules to networking. *Frontiers in Molecular Neuroscience*, *1*(MAR), 1–5. <https://doi.org/10.3389/neuro.02.002.2008>
- Elias, G. M., & Nicoll, R. A. (2007). Synaptic trafficking of glutamate receptors by MAGUK scaffolding proteins. *Trends in Cell Biology*, *17*(7), 343–352. <https://doi.org/10.1016/j.tcb.2007.07.005>
- Ellwood, I. T., Patel, T., Wadia, V., Lee, A. T., Liptak, A. T., Bender, K. J., & Sohal, V. S. (2017). Tonic or phasic stimulation of dopaminergic projections to prefrontal cortex causes mice to maintain or deviate from previously learned behavioral strategies. *Journal of Neuroscience*, *37*(35), 8315–8329. <https://doi.org/10.1523/JNEUROSCI.1221-17.2017>
- Featherstone, D. E., Rushton, E., & Brodie, K. (2002). Developmental regulation of glutamate receptor field size by nonvesicular glutamate release. *Nature Neuroscience*, *5*(2), 141–146. <https://doi.org/10.1038/nn789>

- Featherstone, D. E., Rushton, E., Rohrbough, J., Liebl, F., Karr, J., Sheng, Q., Rodesch, C. K., & Broadie, K. (2005). An essential *Drosophila* glutamate receptor subunit that functions in both central neuropil and neuromuscular junction. *Journal of Neuroscience*, *25*(12), 3199–3208. <https://doi.org/10.1523/JNEUROSCI.4201-04.2005>
- Floresco, S. B., Magyar, O., Ghods-Sharifi, S., Vexelman, C., & Tse, M. T. L. (2006). Multiple dopamine receptor subtypes in the medial prefrontal cortex of the rat regulate set-shifting. *Neuropsychopharmacology*, *31*(2), 297–309. <https://doi.org/10.1038/sj.npp.1300825>
- Foeller, E., & Feldman, D. E. (2004). Synaptic basis for developmental plasticity in somatosensory cortex. *Current Opinion in Neurobiology*, *14*(1), 89–95. <https://doi.org/10.1016/j.conb.2004.01.011>
- Frank, C. A. (2014). Neuropharmacology Homeostatic plasticity at the *Drosophila* neuromuscular junction. *Neuropharmacology*, *78*, 63–74. <https://doi.org/10.1016/j.neuropharm.2013.06.015>
- Fritschy, J. M. (2008). Epilepsy, E/I balance and GABAA receptor plasticity. *Frontiers in Molecular Neuroscience*, *1*(MAR). <https://doi.org/10.3389/neuro.02.005.2008>
- Fuentes-Medel, Y., Ashley, J., Barria, R., Maloney, R., Freeman, M., & Budnik, V. (2012). Integration of a retrograde signal during synapse formation by glia-secreted TGF- β ligand. *Current Biology*, *22*(19), 1831–1838. <https://doi.org/10.1016/j.cub.2012.07.063>
- Genç, Ö., & Davis, G. W. (2019). Target-wide Induction and Synapse Type-Specific Robustness of Presynaptic Homeostasis. *Current Biology*, *29*(22), 3863–3873.e2. <https://doi.org/10.1016/j.cub.2019.09.036>
- Giurfa, M. (2013). Cognition with few neurons: Higher-order learning in insects. *Trends in Neurosciences*, *36*(5), 285–294. <https://doi.org/10.1016/j.tins.2012.12.011>

- Gorczyca, D., Ashley, J., Speese, S., Gherbesi, N., Thomas, U., Gundelfinger, E., Gramates, L. S., & Budnik, V. (2007). Postsynaptic membrane addition depends on the discs-large-interacting t-SNARE Gtaxin. *Journal of Neuroscience*, *27*(5), 1033–1044. <https://doi.org/10.1523/JNEUROSCI.3160-06.2007>
- Guan, Z., Saraswati, S., Adolfsen, B., & Littleton, J. T. (2005). Genome-wide transcriptional changes associated with enhanced activity in the Drosophila nervous system. *Neuron*, *48*(1), 91–107. <https://doi.org/10.1016/j.neuron.2005.08.036>
- Harris, K. P., Littleton, J. T., Aberle, H., Haghighi, A. P., Fetter, R. D., McCabe, B. D., Magalhães, T. R., Adolfsen, B., Littleton, J. T., Adolfsen, B., Saraswati, S., Yoshihara, M., Littleton, J. T., Albin, S. D., Davis, G. W., Andlauer, T. F. M., Scholz-Kornehl, S., Tian, R., Kirchner, M., ... Goodman, C. S. (2015). Transmission, Development, and Plasticity of Synapses. *Genetics*, *201*(2), 345–375. <https://doi.org/10.1534/genetics.115.176529>
- Harris, N., Fetter, R. D., Brasier, D. J., Tong, A., & Davis, G. W. (2018). Molecular Interface of Neuronal Innate Immunity, Synaptic Vesicle Stabilization, and Presynaptic Homeostatic Plasticity. *Neuron*, *100*(5), 1163–1179.e4. <https://doi.org/10.1016/j.neuron.2018.09.048>
- He, T., Singh, V., Rumpal, N., & Lnenicka, G. A. (2009). Differences in Ca²⁺ regulation for high-output Is and low-output Ib motor terminals in Drosophila larvae. *Neuroscience*, *159*(4), 1283–1291. <https://doi.org/10.1016/j.neuroscience.2009.01.074>
- Heckscher, E. S., Zarin, A. A., Faumont, S., Clark, M. Q., Manning, L., Fushiki, A., Schneider-Mizell, C. M., Fetter, R. D., Truman, J. W., Zwart, M. F., Landgraf, M., Cardona, A., Lockery, S. R., & Doe, C. Q. (2015). Even-Skipped+ Interneurons Are Core Components of a Sensorimotor Circuit that Maintains Left-Right Symmetric Muscle Contraction Amplitude. *Neuron*, *88*(2), 314–329. <https://doi.org/10.1016/j.neuron.2015.09.009>

- Herculano-Houzel, S. (2009). The human brain in numbers: A linearly scaled-up primate brain. *Frontiers in Human Neuroscience*, 3(NOV), 1–11.
<https://doi.org/10.3389/neuro.09.031.2009>
- Hida, Y., & Ohtsuka, T. (2010). CAST and ELKS proteins: structural and functional determinants of the presynaptic active zone. *J Biochem*, 148(2), 131–137.
<https://doi.org/mvq065> [pii]r10.1093/jb/mvq065
- Hines, R. M., Davies, P. A., Moss, S. J., & Maguire, J. (2012). Functional regulation of GABA A receptors in nervous system pathologies. *Current Opinion in Neurobiology*, 22(3), 552–558.
<https://doi.org/10.1016/j.conb.2011.10.007>
- Hoang, B., & Chiba, A. (2001). Single-Cell Analysis of Drosophila Larval Neuromuscular Synapses. *Developmental Biology*, 229(1), 55–70. <https://doi.org/10.1006/dbio.2000.9983>
- Holtmaat, A., & Svoboda, K. (2009). Experience-dependent structural synaptic plasticity in the mammalian brain. *Nature Reviews Neuroscience*, 10(9), 647–658.
<https://doi.org/10.1038/nrn2699>
- Hubel, D. H., & Wiesel, T. N. (1970). The period of susceptibility to the physiological effects of unilateral eye closure in kittens. *The Journal of Physiology*, 206(2), 419–436.
<http://onlinelibrary.wiley.com/doi/10.1113/jphysiol.1970.sp009022/abstract>
- Hunt, M. J., Kopell, N. J., Traub, R. D., & Whittington, M. A. (2017). Aberrant Network Activity in Schizophrenia. *Trends in Neurosciences*, 40(6), 371–382.
<https://doi.org/10.1016/j.tins.2017.04.003>
- Ikeda, K., Ozawa, S., & Hagiwara, S. (1976). Synaptic transmission reversibly conditioned by single-gene mutation in *Drosophila melanogaster*. *Nature*, 259(5543), 489–491.
<https://doi.org/10.1038/259489a0>

- Ivakhnitskaia, E., Lin, R. W., Hamada, K., & Chang, C. (2018). Timing of neuronal plasticity in development and aging. *Wiley Interdisciplinary Reviews: Developmental Biology*, 7(2).
<https://doi.org/10.1002/wdev.305>
- Jan LY, & Jan YN. (1976). Properties of the larval neuromuscular junction in *Drosophila melanogaster*. *The Journal of Physiology*, 262, 189–214.
- Jia, X. X., Gorczyca, M., & Budnik, V. (1993). Ultrastructure of neuromuscular junctions in *Drosophila*: Comparison of wild type and mutants with increased excitability. *Journal of Neurobiology*, 24(8), 1025–1044. <https://doi.org/10.1002/neu.480250712>
- Jiao, W., Masich, S., Franzén, O., & Shupliakov, O. (2010). Two pools of vesicles associated with the presynaptic cytosolic projection in *Drosophila* neuromuscular junctions. *Journal of Structural Biology*, 172(3), 389–394. <https://doi.org/10.1016/j.jsb.2010.07.007>
- Kaplan, W. D., & Trout, W. E. (1969). The behavior of four neurological mutants of *Drosophila*. *Genetics*, 61(2), 399–409.
- Karunanithi, S., Marin, L., Wong, K., & Atwood, H. L. (2002). Quantal size and variation determined by vesicle size in normal and mutant *Drosophila* glutamatergic synapses. *Journal of Neuroscience*, 22(23), 10267–10276. <https://doi.org/10.1523/jneurosci.22-23-10267.2002>
- Kennedy, B. Y. D., & Takeda, K. (1965). Reflex Control of Abdominal Flexor Muscles in the Crayfish: I. The Twitch System. *Journal of Experimental Biology*, 43(2), 211–227.
- Kerr, K. S., Fuentes-Medel, Y., Brewer, C., Barria, R., Ashley, J., Abruzzi, K. C., Sheehan, A., Tasdemiir-Yilmaz, O. E., Freeman, M. R., & Budnik, V. (2014). Glial wingless/wnt regulates glutamate receptor clustering and synaptic physiology at the *Drosophila* neuromuscular junction. *Journal of Neuroscience*, 34(8), 2910–2920.

<https://doi.org/10.1523/JNEUROSCI.3714-13.2014>

- Korkut, C., Ataman, B., Ramachandran, P., Ashley, J., Barria, R., Gherbesi, N., & Budnik, V. (2009). Trans-Synaptic Transmission of Vesicular Wnt Signals through Evi/Wntless. *Cell*, *139*(2), 393–404. <https://doi.org/10.1016/j.cell.2009.07.051>
- Korkut, C., Li, Y., Koles, K., Brewer, C., Ashley, J., Yoshihara, M., & Budnik, V. (2013). Regulation of Postsynaptic Retrograde Signaling by Presynaptic Exosome Release. *Neuron*, *77*(6), 1039–1046. <https://doi.org/10.1016/j.neuron.2013.01.013>
- Kuffler, S. W., & Williams, E. M. V. (1953). Small-nerve junctional potentials. The distribution of small motor nerves to frog skeletal muscle, and the membrane characteristics of the fibres they innervate. *The Journal of Physiology*, *121*(2), 289–317. <https://doi.org/10.1113/jphysiol.1953.sp004948>
- Kurdyak, P., Atwood, H. L., Stewart, B. A., & Wu, C. (1994). *Differential Physiology and Morphology of Motor Axons to Ventral Longitudinal Muscles in Larval Drosophila*. *472*, 463–472.
- Lamprecht, R., & LeDoux, J. (2004). Structural plasticity and memory. *Nature Reviews Neuroscience*, *5*(1), 45–54. <https://doi.org/10.1038/nrn1301>
- Lee, J., & Wu, C. F. (2010). Orchestration of stepwise synaptic growth by K⁺ and Ca²⁺ channels in *Drosophila*. *Journal of Neuroscience*, *30*(47), 15821–15833. <https://doi.org/10.1523/JNEUROSCI.3448-10.2010>
- Li, J., Ashley, J., Budnik, V., & Bhat, M. A. (2007). Crucial Role of *Drosophila* Neurexin in Proper Active Zone Apposition to Postsynaptic Densities, Synaptic Growth, and Synaptic Transmission. *Neuron*, *55*(5), 741–755. <https://doi.org/10.1016/j.neuron.2007.08.002>
- Li, X., Goel, P., Wondolowski, J., Paluch, J., & Dickman, D. (2018). A Glutamate Homeostat

- Controls the Presynaptic Inhibition of Neurotransmitter Release. *Cell Reports*, 23(6), 1716–1727. <https://doi.org/10.1016/j.celrep.2018.03.130>
- Lnenicka, G. a., & Keshishian, H. (2000). Identified motor terminals in *Drosophila* larvae show distinct differences in morphology and physiology. *Journal of Neurobiology*, 43(2), 186–197. [https://doi.org/10.1002/\(SICI\)1097-4695\(200005\)43:2<186::AID-NEU8>3.0.CO;2-N](https://doi.org/10.1002/(SICI)1097-4695(200005)43:2<186::AID-NEU8>3.0.CO;2-N)
- Lu, Z., Chouhan, A. K., Borycz, J. A., Lu, Z., Rossano, A. J., Brain, K. L., Zhou, Y., Meinertzhagen, I. A., & Macleod, G. T. (2016). High-Probability Neurotransmitter Release Sites Represent an Energy-Efficient Design. *Current Biology*, 1–10. <https://doi.org/10.1016/j.cub.2016.07.032>
- Macdonald, R. L., Kang, J. Q., & Gallagher, M. J. (2010). Mutations in GABAA receptor subunits associated with genetic epilepsies. *Journal of Physiology*, 588(11), 1861–1869. <https://doi.org/10.1113/jphysiol.2010.186999>
- Marie, B., Pym, E., Bergquist, S., & Davis, G. W. (2010). Synaptic homeostasis is consolidated by the cell fate gene *gooseberry*, a *Drosophila* *pax3/7* homolog. *Journal of Neuroscience*, 30(24), 8071–8082. <https://doi.org/10.1523/JNEUROSCI.5467-09.2010>
- Marie, B., Sweeney, S. T., Poskanzer, K. E., Roos, J., Kelly, R. B., & Davis, G. W. (2004). Dap160/Intersectin scaffolds the periaxonal zone to achieve high-fidelity endocytosis and normal synaptic growth. *Neuron*, 43(2), 207–219. <https://doi.org/10.1016/j.neuron.2004.07.001>
- Marqués, G., Bao, H., Haerry, T. E., Shimell, M. J., Duchek, P., Zhang, B., & O'Connor, M. B. (2002). The *Drosophila* BMP type II receptor *wishful thinking* regulates neuromuscular synapse morphology and function. *Neuron*, 33(4), 529–543. [https://doi.org/10.1016/S0896-6273\(02\)00595-0](https://doi.org/10.1016/S0896-6273(02)00595-0)

- Marqués, G., & Zhang, B. (2006). *Retrograde Signaling That Regulates Synaptic Development and Function at the Drosophila Neuromuscular Junction* (Vol. 75, pp. 267–285). Elsevier.
<http://linkinghub.elsevier.com/retrieve/pii/S0074774206750127>
- Marrus, S. B., Portman, S. L., Allen, M. J., Moffat, K. G., & DiAntonio, A. (2004). Differential Localization of Glutamate Receptor Subunits at the Drosophila Neuromuscular Junction. *Journal of Neuroscience*, *24*(6), 1406–1415. <https://doi.org/10.1523/JNEUROSCI.1575-03.2004>
- Mathew, D., Ataman, B., Chen, J., Zhang, Y., Cumberledge, S., & Budnik, V. (2005). Cell signaling: Wingless signaling at synapses is through cleavage and nuclear import of receptor DFrizzled2. *Science*, *310*(5752), 1344–1347.
<https://doi.org/10.1126/science.1117051>
- Mayford, M., Siegelbaum, S. A., & Kandel, E. R. (2012). Synapses and memory storage. *Cold Spring Harbor Perspectives in Biology*, *4*(6), 1–18.
<https://doi.org/10.1101/cshperspect.a005751>
- McCabe, B. D., Hom, S., Aberle, H., Fetter, R. D., Marques, G., Haerry, T. E., Wan, H., O'Connor, M. B., Goodman, C. S., & Haghghi, A. P. (2004). Highwire regulates presynaptic BMP signaling essential for synaptic growth. *Neuron*, *41*(6), 891–905.
[https://doi.org/10.1016/S0896-6273\(04\)00073-X](https://doi.org/10.1016/S0896-6273(04)00073-X)
- McCabe, B. D., Marque, G., Haghghi, A. P., Fetter, R. D., Crotty, M. L., Haerry, T. E., Goodman, C. S., Connor, M. B. O., Francisco, S. S., & Marque, S. (2003). *The BMP Homolog Gbb Provides a Retrograde Signal that Regulates Synaptic Growth at the Drosophila Neuromuscular Junction*. *39*, 241–254.
- McIlroy, G., Foldi, I., Aurikko, J., Wentzell, J. S., Lim, M. A., Fenton, J. C., Gay, N. J., &

- Hidalgo, A. (2013). *Toll-6 and Toll-7 function as neurotrophin receptors in the Drosophila melanogaster CNS*. *16*(9). <https://doi.org/10.1038/nn.3474>
- Melom, J. E., & Littleton, J. T. (2011). Synapse development in health and disease. *Current Opinion in Genetics and Development*, *21*(3), 256–261.
<https://doi.org/10.1016/j.gde.2011.01.002>
- Menon, K. P., Carrillo, R. A., & Zinn, K. (2013). Development and plasticity of the *Drosophila* larval neuromuscular junction: Development and plasticity of the neuromuscular junction. *Wiley Interdisciplinary Reviews: Developmental Biology*, *2*(5), 647–670.
<https://doi.org/10.1002/wdev.108>
- Monastirioti, M., Michael Gorczyca, Rapus, Jü., Eckert, M., White, K., & Budnik, V. (1995). Octopamine Immunoreactivity in the Fruit Fly *Drosophila melanogaster*. *Physiology & Behavior*, *176*(1), 139–148. <https://doi.org/10.1016/j.physbeh.2017.03.040>
- Mosca, T. J., Carrillo, R. a, White, B. H., & Keshishian, H. (2005). Dissection of synaptic excitability phenotypes by using a dominant-negative Shaker K⁺ channel subunit. *Proceedings of the National Academy of Sciences of the United States of America*, *102*(9), 3477–3482. <https://doi.org/10.1073/pnas.0406164102>
- Mosca, T. J., Hong, W., Dani, V. S., Favaloro, V., & Luo, L. (2012). Trans-synaptic Teneurin signalling in neuromuscular synapse organization and target choice. *Nature*, *484*(7393), 237–241. <https://doi.org/10.1038/nature10923>
- Msgghina, M., Govind, C. K., & Atwood, H. L. (1998). Synaptic structure and transmitter release in crustacean phasic and tonic motor neurons. *Journal of Neuroscience*, *18*(4), 1374–1382.
<https://doi.org/10.1523/jneurosci.18-04-01374.1998>
- Msgghina, M., Millar, A. G., Charlton, M. P., Govind, C. K., & Atwood, H. L. (1999). Calcium

entry related to active zones and differences in transmitter release at phasic and tonic synapses. *The Journal of Neuroscience*, 19(19), 8419–8434.

<http://www.jneurosci.org/content/19/19/8419.short>

Nahmani, M., & Turrigiano, G. G. (2014). Adult cortical plasticity following injury:

Recapitulation of critical period mechanisms? *Neuroscience*, 283, 4–16.

<https://doi.org/10.1016/j.neuroscience.2014.04.029>

Newman, Z. L., Hoagland, A., Aghi, K., Worden, K., Levy, S. L., Son, J. H., Lee, L. P., & Isacoff, E. Y. (2017). Input-Specific Plasticity and Homeostasis at the *Drosophila* Larval Neuromuscular Junction. *Neuron*, 93(6), 1388-1404.e10.

<https://doi.org/10.1016/j.neuron.2017.02.028>

Nguyen, C. T., & Stewart, B. A. (2016). The influence of postsynaptic structure on missing quanta at the *Drosophila* neuromuscular junction. *BMC Neuroscience*, 17(1), 53.

<https://doi.org/10.1186/s12868-016-0290-7>

Nguyen, P. V., Marin, L., & Atwood, H. L. (1997). Synaptic physiology and mitochondrial function in crayfish tonic and phasic motor neurons. *Journal of Neurophysiology*, 78(1), 281–294. <https://doi.org/10.1152/jn.1997.78.1.281>

Orr, B. O., Fetter, R. D., & Davis, G. W. (2017). Retrograde semaphorin-plexin signalling drives homeostatic synaptic plasticity. *Nature*, 550(7674), 109–113.

<https://doi.org/10.1038/nature24017>

Osses, N., & Juan, P. (2015). *Bone morphogenetic protein signaling in vertebrate motor neurons and neuromuscular communication*. 8(January), 1–10.

<https://doi.org/10.3389/fncel.2014.00453>

Packard, M., Koo, E. S., Gorczyca, M., Sharpe, J., Cumberledge, S., & Budnik, V. (2002). The

- Drosophila Wnt, wingless, provides an essential signal for pre- and postsynaptic differentiation. *Cell*, *111*(3), 319–330. [https://doi.org/10.1016/S0092-8674\(02\)01047-4](https://doi.org/10.1016/S0092-8674(02)01047-4)
- Petersen, S. a., Fetter, R. D., Noordermeer, J. N., Goodman, C. S., & DiAntonio, A. (1997). Genetic analysis of glutamate receptors in drosophila reveals a retrograde signal regulating presynaptic transmitter release. *Neuron*, *19*(6), 1237–1248. [https://doi.org/10.1016/S0896-6273\(00\)80415-8](https://doi.org/10.1016/S0896-6273(00)80415-8)
- Piccioli, Z. D., & Littleton, J. T. (2014). Retrograde BMP Signaling Modulates Rapid Activity-Dependent Synaptic Growth via Presynaptic LIM Kinase Regulation of Cofilin. *The Journal of Neuroscience*, *34*(12), 4371 LP – 4381. <https://doi.org/10.1523/JNEUROSCI.4943-13.2014>
- Pozo, K., & Goda, Y. (2010). Unraveling mechanisms of homeostatic synaptic plasticity. *Neuron*, *66*(3), 337–351. <https://doi.org/10.1016/j.neuron.2010.04.028>
- Puig, M. V., & Miller, E. K. (2012). The Role of Prefrontal Dopamine D1 Receptors in the Neural Mechanisms of Associative Learning. *Neuron*, *74*(5), 874–886. <https://doi.org/10.1016/j.neuron.2012.04.018>
- Puig, M. V., & Miller, E. K. (2015). Neural substrates of dopamine d2 receptor modulated executive functions in the monkey prefrontal Cortex. *Cerebral Cortex*, *25*(9), 2980–2987. <https://doi.org/10.1093/cercor/bhu096>
- Qin, G., Schwarz, T., Kittel, R. J., Schmid, A., Rasse, T. M., Kappei, D., Ponimaskin, E., Heckmann, M., & Sigrist, S. J. (2005). *Four Different Subunits Are Essential for Expressing the Synaptic Glutamate Receptor at Neuromuscular Junctions of Drosophila This study opens the way for a further characterization of in vivo glutamate receptor assembly and trafficking using the efficien.* *25*(12), 3209–3218.

<https://doi.org/10.1523/JNEUROSCI.4194-04.2005>

Rawson, J. M., Lee, M., Kennedy, E. L., & Selleck, S. B. (2003). Drosophila neuromuscular synapse assembly and function require the TGF- β type I receptor saxophone and the transcription factor Mad. *Journal of Neurobiology*, *55*(2), 134–150.

<https://doi.org/10.1002/neu.10189>

Reiff, D. F., Thiel, P. R., & Schuster, C. M. (2002). Differential regulation of active zone density during long-term strengthening of Drosophila neuromuscular junctions. *Journal of Neuroscience*, *22*(21), 9399–9409. <https://doi.org/10.1523/jneurosci.22-21-09399.2002>

Ruiz-Cañada, C., & Budnik, V. (2006). *Synaptic Cytoskeleton At The Neuromuscular Junction* (Vol. 75, pp. 217–236). Elsevier.

<http://linkinghub.elsevier.com/retrieve/pii/S0074774206750103>

Saitoe, M., Tanaka, S., Takata, K., & Kidokoro, Y. (1997). Neural activity affects distribution of glutamate receptors during neuromuscular junction formation in Drosophila embryos. *Developmental Biology*, *184*(1), 48–60. <https://doi.org/10.1006/dbio.1996.8480>

Saneyoshi, T., Fortin, D. A., & Soderling, T. R. (2010). Regulation of spine and synapse formation by activity-dependent intracellular signaling pathways. *Current Opinion in Neurobiology*, *20*(1), 108–115. <https://doi.org/10.1016/j.conb.2009.09.013>

Sanyal, S., Sandstrom, D. J., Hoeffler, C. A., & Ramaswami, M. (2002). Ap-1 functions upstream of creb to control synaptic plasticity in drosophila. *Nature*, *416*(6883), 870–874.

<https://doi.org/10.1038/416870a>

Schaefer, J. E., Worrell, J. W., & Levine, R. B. (2010). *Role of Intrinsic Properties in Drosophila Motoneuron Recruitment During Fictive Crawling*. 1257–1266.

<https://doi.org/10.1152/jn.00298.2010>

- Schmid, A., Hallermann, S., Kittel, R. J., Khorramshahi, O., Frölich, A. M. J., Quentin, C., Rasse, T. M., Mertel, S., Heckmann, M., & Sigrist, S. J. (2008). Activity-dependent site-specific changes of glutamate receptor composition in vivo. *Nature Neuroscience*, *11*(6), 659–666. <https://doi.org/10.1038/nn.2122>
- Schmid, A., Qin, G., Wichmann, C., Kittel, R. J., Mertel, S., Fouquet, W., Schmidt, M., Heckmann, M., & Sigrist, S. J. (2006). Non-NMDA-type glutamate receptors are essential for maturation but not for initial assembly of synapses at *Drosophila* neuromuscular junctions. *Journal of Neuroscience*, *26*(44), 11267–11277. <https://doi.org/10.1523/JNEUROSCI.2722-06.2006>
- Schuster, C. M. (2006). Experience-Dependent Potentiation of Larval Neuromuscular Synapses. *International Review of Neurobiology*, *75*(06), 307–322. [https://doi.org/10.1016/S0074-7742\(06\)75014-0](https://doi.org/10.1016/S0074-7742(06)75014-0)
- Schuster, C. M., Davis, G. W., & Goodman, C. S. (1996). Genetic dissection of structural and functional components of synaptic plasticity. III. CREB is necessary for presynaptic functional plasticity. *Neuron*, *17*(4), 669–679. [https://doi.org/10.1016/S0896-6273\(00\)80199-3](https://doi.org/10.1016/S0896-6273(00)80199-3)
- Schuster, C. M., Ultsch, A., Schloss, P., Cox, J. A., Schmitt, B., & Betz, H. (1991). Molecular cloning of an invertebrate glutamate receptor subunit expressed in *Drosophila* muscle. *Science*, *254*(5028), 112–114. <https://doi.org/10.1126/science.1681587>
- Seamans, J. K., Floresco, S. B., & Phillips, A. G. (1998). D1 receptor modulation of hippocampal-prefrontal cortical circuits integrating spatial memory with executive functions in the rat. *Journal of Neuroscience*, *18*(4), 1613–1621. <https://doi.org/10.1523/JNEUROSCI.18-04-01613.1998>

- Sigrist, S. J., Reiff, D. F., Thiel, P. R., Steinert, J. R., & Schuster, C. M. (2003). Experience-dependent strengthening of *Drosophila* neuromuscular junctions. *Journal of Neuroscience*, 23(16), 6546–6556. <https://doi.org/10.1523/jneurosci.23-16-06546.2003>
- Sigrist, S. J., Thiel, P. R., Reiff, D. F., Pascal, L. E. D., Lasko, P., & Schuster, C. M. (2000). Postsynaptic translation affects the efficacy and morphology of neuromuscular junctions. *Journal of Neuroscience*, 20(6), 405–413.
- Speese, S. D., Ashley, J., Jokhi, V., Nunnari, J., Barria, R., Li, Y., Ataman, B., Koon, A., Chang, Y. T., Li, Q., Moore, M. J., & Budnik, V. (2012). Nuclear envelope budding enables large ribonucleoprotein particle export during synaptic Wnt signaling. *Cell*, 149(4), 832–846. <https://doi.org/10.1016/j.cell.2012.03.032>
- St. Onge, J. R., Abhari, H., & Floresco, S. B. (2011). Dissociable contributions by prefrontal D1 and D2 receptors to risk-based decision making. *Journal of Neuroscience*, 31(23), 8625–8633. <https://doi.org/10.1523/JNEUROSCI.1020-11.2011>
- Stefani, M. R., & Moghaddam, B. (2006). Rule learning and reward contingency are associated with dissociable patterns of dopamine activation in the rat prefrontal cortex, nucleus accumbens, and dorsal striatum. *Journal of Neuroscience*, 26(34), 8810–8818. <https://doi.org/10.1523/JNEUROSCI.1656-06.2006>
- Stratton, M. M., Chao, L. H., Schulman, H., & Kuriyan, J. (2013). Structural studies on the regulation of Ca²⁺/calmodulin dependent protein kinase II. *Current Opinion in Structural Biology*, 23(2), 292–301. <https://doi.org/10.1016/j.sbi.2013.04.002>
- Styr, B., & Slutsky, I. (2018). Imbalance between firing homeostasis and synaptic plasticity drives early-phase Alzheimer's disease. *Nature Neuroscience*, 21(4), 463–473. <https://doi.org/10.1038/s41593-018-0080-x>

- Sun, M., Xing, G., Yuan, L., Gan, G., Knight, D., With, S. I., He, C., Han, J., Zeng, X., Fang, M., Boulianne, G. L., & Xie, W. (2011). Neuroligin 2 is required for synapse development and function at the *Drosophila* neuromuscular junction. *Journal of Neuroscience*, *31*(2), 687–699. <https://doi.org/10.1523/JNEUROSCI.3854-10.2011>
- Suster, M. L., Martin, J. R., Sung, C., & Robinow, S. (2003). Targeted expression of tetanus toxin reveals sets of neurons involved in larval locomotion in *Drosophila*. *Journal of Neurobiology*, *55*(2), 233–246. <https://doi.org/10.1002/neu.10202>
- Thomas, U., Kim, E., Kuhlendahl, S., Koh, Y. H., Gundelfinger, E. D., Sheng, M., Garner, C. C., & Budnik, V. (1997). Synaptic clustering of the cell adhesion molecule Fasciclin II by discs-large and its role in the regulation of presynaptic structure. *Neuron*, *19*(4), 787–799. [https://doi.org/10.1016/S0896-6273\(00\)80961-7](https://doi.org/10.1016/S0896-6273(00)80961-7)
- Turrigiano, G. (2012). Homeostatic synaptic plasticity: Local and global mechanisms for stabilizing neuronal function. *Cold Spring Harbor Perspectives in Biology*, *4*(1), 1–18. <https://doi.org/10.1101/cshperspect.a005736>
- Verstreken, P., Kjaerulff, O., Lloyd, T. E., Atkinson, R., Zhou, Y., Meinertzhagen, I. A., & Bellen, H. J. (2002). Endophilin mutations block clathrin-mediated endocytosis but not neurotransmitter release. *Cell*, *109*(1), 101–112. [https://doi.org/10.1016/S0092-8674\(02\)00688-8](https://doi.org/10.1016/S0092-8674(02)00688-8)
- Wagh, D. A., Rasse, T. M., Asan, E., Hofbauer, A., Schwenkert, I., Dürrbeck, H., Buchner, S., Dabauvalle, M. C., Schmidt, M., Qin, G., Wichmann, C., Kittel, R., Sigrist, S. J., & Buchner, E. (2006). Bruchpilot, a protein with homology to ELKS/CAST, is required for structural integrity and function of synaptic active zones in *Drosophila*. *Neuron*, *49*(6), 833–844. <https://doi.org/10.1016/j.neuron.2006.02.008>

- Wall, M. J., & Usowicz, M. M. (1997). Development of Action Potential-dependent and Independent Spontaneous GABA A Receptor-mediated Currents in Granule Cells of Postnatal Rat Cerebellum . *European Journal of Neuroscience*, 9(3), 533–548.
<https://doi.org/10.1111/j.1460-9568.1997.tb01630.x>
- Walsh, M. K., & Lichtman, J. W. (2003). In vivo time-lapse imaging of synaptic takeover associated with naturally occurring synapse elimination. *Neuron*, 37(1), 67–73.
[https://doi.org/10.1016/S0896-6273\(02\)01142-X](https://doi.org/10.1016/S0896-6273(02)01142-X)
- Wiesel, T. N., Hubel, D. H., & others. (1963). Effects of visual deprivation on morphology and physiology of cells in the cat's lateral geniculate body. *J Neurophysiol*, 26(978), 6.
<http://hubel.med.harvard.edu/papers/HubelWiesel1963Jneurophysiol3.pdf>
- Xing, G., Gan, G., Chen, D., Sun, M., Yi, J., Lv, H., Han, J., & Xie, W. (2014). Drosophila neuroligin3 regulates neuromuscular junction development and synaptic differentiation. *Journal of Biological Chemistry*, 289(46), 31867–31877.
<https://doi.org/10.1074/jbc.M114.574897>
- Xing, X., & Wu, C. F. (2018). Unraveling synaptic GCaMP signals: Differential excitability and clearance mechanisms underlying distinct Ca²⁺ dynamics in tonic and phasic excitatory, and aminergic modulatory motor terminals in drosophila. *ENeuro*, 5(1).
<https://doi.org/10.1523/ENEURO.0362-17.2018>
- Yoshihara, M., Adolfsen, B., Galle, K. T., & Littleton, J. T. (2005). Retrograde signaling by Syt 4 induces presynaptic release and synapse-specific growth. *Science*, 310(5749), 858–863.
<https://doi.org/10.1126/science.1117541>
- Zheng, C. Y., Seabold, G. K., Horak, M., & Petralia, R. S. (2011). MAGUKs, synaptic development, and synaptic plasticity. *Neuroscientist*, 17(5), 493–512.

<https://doi.org/10.1177/1073858410386384>

Zhong, Y., Budnik, V., & Wu, C. F. (1992). Synaptic plasticity in *Drosophila* memory and hyperexcitable mutants: Role of cAMP cascade. *Journal of Neuroscience*, *12*(2), 644–651.

<https://doi.org/10.1523/jneurosci.12-02-00644.1992>

Zhu, B., Pennack, J. A., McQuilton, P., Forero, M. G., Mizuguchi, K., Sutcliffe, B., Gu, C. J., Fenton, J. C., & Hidalgo, A. (2008). *Drosophila* neurotrophins reveal a common mechanism for nervous system formation. *PLoS Biology*, *6*(11), 2476–2495.

<https://doi.org/10.1371/journal.pbio.0060284>

Zito, K., Fetter, R. D., Goodman, C. S., & Isacoff, E. Y. (1997). Synaptic clustering of Fasciclin II and Shaker: Essential targeting sequences and role of dig. *Neuron*, *19*(5), 1007–1016.

[https://doi.org/10.1016/S0896-6273\(00\)80393-1](https://doi.org/10.1016/S0896-6273(00)80393-1)

Zito, K., Parnas, D., Fetter, R. D., Isacoff, E. Y., & Goodman, C. S. (1999). Watching a synapse grow: noninvasive confocal imaging of synaptic growth in *Drosophila*. *Neuron*, *22*(4), 719–729. <http://www.sciencedirect.com/science/article/pii/S089662730080731X>

Zwart, M. F., Pulver, S. R., Truman, J. W., Fushiki, A., Fetter, R. D., Cardona, A., & Landgraf, M. (2016). Selective Inhibition Mediates the Sequential Recruitment of Motor Pools.

Neuron, *91*(3), 615–628. <https://doi.org/10.1016/j.neuron.2016.06.031>

Chapter 2: Synaptic plasticity induced by differential manipulation of tonic and phasic motoneurons in *Drosophila*

Nicole A. Aponte-Santiago, Kiel G. Ormerod, Yulia Akbergenova, J. Troy Littleton

The Picower Institute for Learning and Memory, Department of Biology and Department of Brain and Cognitive Sciences, Massachusetts Institute of Technology, Cambridge, MA 02139

Kiel G. Ormerod performed electrophysiology and force recording experiments. Yulia Akbergenova performed early 1st instar experiments and experiments with *Gbb* mutants. Nicole A. Aponte-Santiago performed all remaining experiments, created figures, and wrote the text.

Abstract

Structural and functional plasticity induced by neuronal competition is a common feature of developing nervous systems. However, the rules governing how postsynaptic cells differentiate between presynaptic inputs are unclear. In this study we characterized synaptic interactions following manipulations of Ib tonic or Is phasic glutamatergic motoneurons that co-innervate postsynaptic muscles at *Drosophila* neuromuscular junctions (NMJs). After identifying drivers for each neuronal subtype, cell-type specific ablation of Ib or Is motoneurons revealed that only the tonic Ib class was capable of generating functional compensation following loss of the other input. Genetic manipulations of synaptic activity that created an input imbalance demonstrated tonic Ib motoneurons responded with structural changes following reduction in their activity or that of the co-innervating phasic motoneurons. Disruptions of Is or Ib neuronal activity did not cause similar changes at phasic Is terminals, indicating tonic and phasic neuronal inputs respond differently to activity mismatch onto a postsynaptic target.

Introduction

Functional and structural changes in neuronal circuits occur during development and in response to environmental stimuli, learning, and injury (Destexhe and Marder, 2004; Foeller and Feldman, 2004; Holtmaat and Svoboda, 2009; Katz and Shatz, 1996; Lamprecht and LeDoux, 2004). Disruptions of these plasticity pathways can contribute to neurodevelopmental diseases and impair rewiring after brain injury, highlighting the importance of the underlying mechanisms (Doll and Broadie, 2014; Luo and O’Leary, 2005; Melom and Littleton, 2011; Nahmani and Turrigiano, 2014). Both invertebrate and vertebrate nervous systems can display synaptic plasticity in response to changes in neuronal firing patterns or behavioral experiences, suggesting some of the underlying mechanisms emerged early in brain evolution (Cognigni et al., 2018; Davis, 2006; Ghelani and Sigrist, 2018; Giurfa, 2013; Mayford et al., 2012).

In contrast to mammals, invertebrate nervous systems like that of *Drosophila melanogaster* are more stereotypical in their organization. Neuroblasts divide and differentiate in a specific order to generate fixed cellular lineages with genetically hard-wired synaptic targets (Bossing et al., 1996; Harris et al., 2015; Hartenstein and Campos-Ortega, 1984; Hoang and Chiba, 2001; Johansen et al., 1989a; Landgraf et al., 1997; Lee, 2017; Schmid et al., 1999; Shepherd et al., 2019; Thomas et al., 1984; Yu et al., 2010). Although *Drosophila* display stereotypical neuronal connectivity, plasticity can occur throughout development and into adulthood. Structural plasticity is most prominent during metamorphosis, when larval neurons reorganize their processes and synaptic partners to form functional adult circuits (Alyagor et al., 2018; Lee and Luo, 1999; Marin et al., 2005; Maysseless et al., 2018; Schubiger et al., 1998; Technau and Heisenberg, 1982; Truman, 1990; Williams and Truman, 2005). Alterations in connectivity also occur in response to changes in environmental stimuli or following acute or chronic manipulations of neuronal activity

(Berdnik et al., 2006; Cash et al., 1992; Chang and Keshishian, 1996; Davis et al., 1998; Golovin et al., 2019; Hourcade et al., 2010; Lnenicka et al., 2003; Matz et al., 2010; Sigrist et al., 2003).

Although plasticity occurs broadly across neuronal circuits, the motor system has played an important role in defining mechanisms for activity-dependent structural changes in connectivity. Locomotion is an essential behavior in many animals and requires coordinated output from central pattern generators to orchestrate motoneuron firing patterns that activate specific muscles (Marder and Calabrese, 1996; Marder and Rehm, 2005). In vertebrates, individual muscle fibers receive transient innervation from many cholinergic motoneurons during early development (Sanes and Lichtman, 1999). As many as 10 distinct motor axons can innervate a single muscle fiber before an activity-dependent competition results in retention of only a single axon (Tapia et al., 2012). This axonal competition allows a large pool of identical motoneurons to transition from dispersed weak outputs to the muscle field to strong innervation of a smaller subset of muscles (Colman et al., 1997; Turney and Lichtman, 2012; Walsh and Lichtman, 2003).

Unlike vertebrate neuromuscular junctions (NMJs), early promiscuity in synaptic partner choice and subsequent synapse elimination does not occur in *Drosophila*. Instead, the larval motor system is comprised of ~36 motoneurons that are genetically programmed by specific transcription factors and guidance molecules to form stereotypical connections to the 30 muscles in each abdominal hemisegment (Clark et al., 2018; Hoang and Chiba, 2001). Although synaptic partner choice is hardwired, activity-dependent plasticity and homeostatic mechanisms have been characterized that make *Drosophila* an ideal system to study synaptic interactions between well-defined motor neurons (Berke et al., 2013; Böhme et al., 2019; Cho et al., 2015; Davis, 2013; Davis et al., 1998; Davis and Müller, 2015; Frank et al., 2006; Gaviño et al., 2015; Goel et al., 2019; Guan et al., 2005; Harris and Littleton, 2015; Sigrist et al., 2003; Yoshihara et al., 2005).

Four subclasses of motoneurons innervate the abdominal musculature in *Drosophila*, with each class defined by their synaptic partner choice, neurotransmitter or neuromodulator content, and biophysical and synaptic properties (Atwood et al., 1993; Hoang and Chiba, 2001; Jan and Jan, 1976; Johansen et al., 1989a; Lnenicka and Keshishian, 2000). Approximately 30 type Ib glutamatergic motoneurons are found per hemisegment and function as the primary driver of contraction for individual muscles. A single Ib motoneuron individually innervates a muscle fiber, allowing for fine-tuning of specific locomotor programs. The Ib neuronal subclass has big synaptic boutons with tonic release properties, containing active zones (AZs) with low release probability (P_r) that facilitate during high frequency stimulation (Akbergenova et al., 2018; Lnenicka and Keshishian, 2000; Melom et al., 2013; Newman et al., 2017; Peled and Isacoff, 2011). Beyond the Ib neurons, three type Is glutamatergic motoneurons per hemisegment provide input to the ventral, lateral or dorsal muscle groups, respectively. Each Is neuron innervates multiple fibers to coordinate contraction of functionally related muscles. In contrast to Ib, Is motoneurons have smaller synaptic boutons and fewer AZs with phasic release properties, including higher P_r release sites that undergo depression during repetitive stimulation (Figure 1A). The two remaining subclasses, type II and type III, are neuromodulatory. Three type II octopaminergic neurons contain only dense core vesicles (DCVs) and innervate most muscle fibers (Stocker et al., 2018). A single type III peptidergic neuron innervates muscle 13 and releases insulin-like peptide (Gorczyca et al., 1993).

Although individual muscles normally restrict innervation to a single neuron from each subclass, it is unclear if tonic Ib and phasic Is motoneurons display competitive or cooperative interactions during innervation of the same muscle target, or compensatory changes when the output of one motoneuron is altered. To characterize how Ib and Is motoneurons interact at

Drosophila NMJs, we established a system to differentially manipulate the two inputs. After identifying cell-type specific drivers for Ib and Is motoneurons innervating muscle 1 (M1), ablation of each motoneuron class was performed to assay the response from the remaining input. Ablation of either Ib or Is resulted in decreased muscle response, with some functional compensation occurring in the tonic Ib input when Is was missing. In contrast, the phasic Is terminal failed to show functional or structural changes following loss of the co-innervating Ib input. Next, genetic manipulations of synaptic activity were performed to create an input imbalance to the postsynaptic cell. No evidence of synaptic competition was observed following increased activity from either input. However, decreasing activity of the Ib or Is neuron with tetanus toxin light chain caused structural changes in M1 innervation. Decreased Ib synaptic activity resulted in reduced AZ number and decreased postsynaptic subsynaptic reticulum (SSR) volume, with the emergence of filopodial-like protrusions from synaptic boutons of the Ib input. Decreased Is activity did not induce structural changes at its own synapses, but the co-innervating Ib motoneuron increased the number of synaptic boutons and AZs that it formed onto M1. Together, these findings indicate tonic and phasic neurons respond independently to changes in activity, with either functional or structural alterations in the tonic motoneuron occurring following loss or reduced activity of the co-innervating phasic input, respectively.

Results

Screen for Ib and Is motoneuron-specific GAL4 drivers

To preferentially manipulate the Ib and Is subclass of motoneurons, GAL4 lines with subclass-specific expression were identified from the FlyLight Project (Jenett et al., 2012; Manning et al., 2012) and strains provided by Ellie Heckscher (Univ. of Chicago). The FlyLight collection consists of >5000 transgenic *Drosophila* lines with ~3 kb of regulatory genomic DNA from candidate neuronal genes driving GAL4 expression. Images of membrane-tethered UAS-CD8-GFP driven by each GAL4 line in 3rd instar brain lobes and ventral nerve cord (VNC) were provided by Gerry Rubin (Janelia, HHMI). Candidate lines for further analysis were chosen on the basis of two criteria: (1) restricted expression of GFP in a single pair or small subset of segmentally repeated abdominal neurons in the VNC; and (2) GFP expression in axons exiting the VNC as expected for motoneurons innervating peripheral musculature (Figure 1B).

Forty-two GAL4 driver lines were identified as promising candidates in the initial screen and subjected to further immunostaining to identify their synaptic targets. Six of these lines were verified as having restricted expression in a small subset of motoneurons (Table 1), including GAL4 drivers specific for Ib and Is motoneurons (Figure 1C-F). Line GMR94G06 displayed restricted expression in the tonic Ib motoneuron (MN1-Ib) that innervates muscle M1 (Figure 1B-D). GMR94G06 contains regulatory DNA from the *Dpr4* locus, which encodes a member of the cell surface Ig-containing proteins implicated in synaptic target recognition (Carrillo et al., 2015). Line GMR27F01 contained regulatory sequences from the *Fmr1* gene and showed restricted expression in two Is motoneurons and a type II neuromodulatory neuron (Table 1). Line 6-58 displayed restricted expression in the Is motoneurons MNISN-Is and MNSNb/d-Is that innervate the ventral and dorsal muscles, respectively (Figure 1E-F). To determine the gene regulatory

region responsible for Is motoneuron expression in 6-58, which contained an unknown insertion site, plasmid rescue and reverse PCR was performed. The insertion site mapped to the 5' UTR of the *Dip- α* gene. Like DPR4, DIP- α is a member of the Ig domain family of synaptic target recognition proteins and was previously found to be expressed in Is motoneurons (Ashley et al., 2019). The MN1-Ib driver GMR94G06 and an additional Is GAL4 driver line (GMR27E09, containing regulatory sequences from *Fmr1*) were independently identified in a recent study (Pérez-Moreno and O'Kane, 2019). We refer to the restricted GAL4 driver lines as MN1-Ib GAL4 and MNIs GAL4 in the remaining text. Together, they provide a toolkit to genetically manipulate the tonic Ib and phasic Is motoneuron subclasses that co-innervate muscle M1.

Establishment of MN1-Ib and MN-Is synaptic connections during development

MN1-Ib and MNIs drivers were used to fluorescently label the two neuronal subpopulations and establish the timing for M1 innervation, the most peripheral target of the dorsal abdominal musculature. MN1-Ib (formerly referred to as aCC) and MNIs (formerly referred to as RP2) were previously identified as pioneer neurons for the ISN nerve branch, being the first to exit the VNC towards the dorsal muscle field (Jacobs and Goodman, 1989; Johansen et al., 1989b; Lin et al., 1995; Sánchez-Soriano and Prokop, 2005). To co-label MN1-Ib and MNIs in the same animal, a MN1-Ib LexA driver line was generated by subcloning the 2736 bp genomic *Dpr4* fragment from GMR94G06 into pBPLexA::p65Uw. This construct was used to generate transgenic animals containing MN1-Ib LexA, allowing independent LexA and GAL4 transgene expression in MN1-Ib and MNIs motoneurons. Serial intravital imaging through the cuticle of briefly anesthetized animals co-expressing MN1-Ib Lex; LexAop2-CD8-GFP and MNIs GAL4; UAS-DsRed was performed as previously described (Akbergenova et al., 2018). By the beginning of the 1st instar

larval stage, all MN1-Ib motoneurons had correctly targeted M1 during late embryonic development, elaborating a growth-cone like projection over the muscle surface (Figure 2A, B). In contrast, MNIs had a more variable time-course of innervation, with the Is growth cone trailing behind MN1-Ib, often without targeting M1 in early 1st instars. By the end of the 1st instar larval stage, only 28% of MNIs motoneurons had innervated the muscle. MNIs innervation of M1 continued over the rest of larval development, with 72% of Is motoneurons innervating M1 by the 3rd instar stage (abdominal segments 2-4, n=7 larvae, Figure 2C). The remaining M1 muscles lacked Is innervation. These data indicate the tonic Ib motoneuron innervates M1 prior to the arrival of Is, with the phasic motoneuron forming synaptic contacts with the muscle later in development or failing to innervate the target completely.

Since phasic Is motoneurons have stronger synapses with higher P_r active zones than their Ib counterparts at the 3rd instar stage (Genç and Davis, 2019; Karunanithi et al., 2020; Kurdyak et al., 1994; Lnenicka and Keshishian, 2000; Lu et al., 2016; Newman et al., 2017), we examined Is synaptic maturation given their shorter developmental time window compared to the pre-existing Ib input. Presynaptic bouton and AZ number at motoneuron NMJs rapidly increase throughout larval development, accompanied by expansion in the size of the postsynaptic density (PSD) and glutamate receptor fields (Akbergenova et al., 2018; Zito et al., 1999). To examine glutamate receptor field formation and maturation at developing tonic and phasic synapses, we followed muscle 4 (M4) innervation during early larval development (Figure 2D). The Ib and Is inputs arrive at distinct positions on M4, allowing unambiguous identification of neuronal subclass without having to genetically label the motoneurons as required for M1. Live imaging was performed in developing larvae expressing RFP-tagged GluRIIA and GFP-tagged GluRIIB under the control of their endogenous promoters (Rasse et al., 2005). Glutamate receptors at the NMJ are tetramers,

with three essential subunits and a 4th subunit of either GluRIIA or GluRIIB (Featherstone et al., 2005; Marrus et al., 2004; Petersen et al., 1997; Qin et al., 2005; Schuster et al., 1991). As observed at M1, Ib innervation preceded Is arrival at M4, with 18% of M4 fibers completely lacking Is innervation at the 3rd instar stage (abdominal segments A2-A4, n=9 larvae). Although Is innervation of M4 was delayed compared to Ib, the rate of synapse formation, quantified by appearance of new GluRIIA/GluRIIB positive PSDs, was increased at Is terminals during consecutive days of imaging (MN4-Ib: 1.46-fold increase; MNIs: 1.86-fold increase, n=11, p<0.001, Figure 2E, F). Overall, the delayed innervation by Is resulted in reduced PSD number at M4 compared to Ib (day 1: MN4-Ib, 31.9 ± 3.3 AZs; MNIs, 16.5 ± 2.6 AZs, n=11, p<0.0001; day 2: MN4-Ib, 46.5 ± 4.9 AZs; MNIs, 29.9 ± 4.5 AZs, n=11, p<0.0001, Figure 2F). Although the Is motoneuron formed fewer synapses than Ib, the average PSD size defined by GluRIIB area in 1st instar larvae was 69% larger than those of the corresponding Ib input (MN4-Ib: 0.215 ± 0.004 μm², n=1006 PSDs; MNIs: 0.363 ± 0.013 μm², n=399 PSDs, p<0.0001, Figure 2G, H). Given PSD maturation is activity-dependent at NMJs (Akbergenova et al., 2018; Petzoldt et al., 2014; Schmid et al., 2008), these data suggest PSDs may develop faster at the stronger Is AZs than PSDs apposed to the weaker Ib AZs. Alternatively, the postsynaptic muscle may compartmentalize delivery of PSD material to Is versus Ib synapses such that Is sites are favored.

A central pathway regulating synaptic maturation at *Drosophila* NMJs is mediated through muscle secretion of Glass Bottom Boat (Gbb), a BMP ligand that acts on presynaptic BMP receptors to activate a SMAD-dependent transcriptional synaptic growth program (Aberle et al., 2002; Ball et al., 2010; Berke et al., 2013; Marqués et al., 2002; McCabe et al., 2003; Rodal et al., 2011). To determine if tonic Ib and phasic Is motoneurons were equally sensitive to Gbb signaling given their different innervation time course, we assayed synapse formation and growth of MN4-

Ib and MNIs at M4 in *Gbb* mutants (Figure 3A). As previously observed, loss of *Gbb* reduced synaptic growth of Ib motoneurons innervating M4 compared to controls (control MN4-Ib NMJ area: $182.8 \pm 21.6 \mu\text{m}^2$, n=11 NMJs from 5 larvae; *Gbb* MN4-Ib NMJ area: $56.2 \pm 5.8 \mu\text{m}^2$, n=21 NMJs from 8 larvae, $p < 0.0001$, Figure 3B). Although synaptic growth was reduced, 100% of M4 muscles displayed Ib synaptic innervation. In contrast, synaptic innervation from the phasic Is motoneuron was reduced in *Gbb* mutants, with only 48% of M4 muscles containing Is innervation compared to 82% in controls (Figure 3C). In cases where the Is motoneuron innervated M4 in *Gbb*, similar reductions in synaptic growth compared to Ib were observed (control Is NMJ area: $102.2 \pm 11.3 \mu\text{m}^2$, n=7 NMJs from 5 larvae; *Gbb* Is NMJ area: $33.8 \pm 4.0 \mu\text{m}^2$, n=16 NMJs from 8 larvae, $p < 0.0006$, Figure 3B). These data indicate the *Gbb* pathway promotes synaptic growth in tonic Ib motoneurons but is not required for target innervation. In contrast, loss of *Gbb* signaling in phasic Is motoneurons decreases synaptic growth and also reduces the percent of muscles with Is innervation.

Role of MN1-Ib and MNIs in muscle excitability and contraction

To determine the relative contribution of Ib and Is motoneurons in muscle excitability, simultaneous electrophysiological recordings were performed at 3rd instar larval muscles M1 and M2 in HL3.1 saline containing 0.3 mM extracellular Ca^{2+} . A minimal stimulation protocol was used to isolate MN1-Ib or MNIs, as MNIs innervates both muscles compared to MN1-Ib (Figure 4A). By increasing current applied to the larval nerve through the stimulating electrode, responses following activation of one or both motor axons could be isolated in cases where dual innervation was present. The average excitatory junctional potential (EJP) amplitude recorded at M1 when both Ib and Is inputs were active was $24.2 \pm 1.7 \text{ mV}$ (n=22, Figure 4B, C). When Ib or Is were

individually recruited during minimal stimulation, reduced responses of similar amplitude at M1 were observed (MN1-Ib: 11.8 ± 1.6 mV, n=22; MNIs: 12.4 ± 1.4 mV, n=22), indicating each neuron provides similar drive to M1 following single action potentials (Figure 4B, C). Given MN1-Ib has more AZs compared to MNIs at M1 (Figure 2F), these results are consistent with MNIs motoneurons having higher P_r per AZ as previously described (Genç and Davis, 2019; Lu et al., 2016; Newman et al., 2017).

To examine the contribution of MN1-Ib and MNIs for muscle contractility, nerve-evoked bodywall contraction force was recorded with a force transducer attached to the head of dissected larvae (Figure 4D). To isolate contraction force mediated predominantly by the dorsal muscle group (M1, M2, M3, M9, M10), 3rd instar larvae were dissected along the ventral midline. Severed abdominal nerves were placed in a suction electrode and the nerve bundle was stimulated at increasing frequencies in HL3.1 saline containing 1.5 mM extracellular Ca^{2+} as previously described (Ormerod et al., 2016). Control MN1-Ib and MNIs GAL4 larval preparations showed increasing contraction force when a 0.1 msec simulation was ramped from 1 Hz to 150 Hz for 600 ms (Figure 4E). To determine the contribution of each motoneuron subclass for contractile force, MN1-Ib or MNIs was ablated by expressing the cell death gene *reaper* (UAS-RPR) to induce apoptosis (Goyal et al., 2000; White et al., 1996, 1994). Expression of UAS-RPR with MN1-Ib or MNIs GAL4 resulted in elimination of the corresponding motoneuron class. Ablation of MNIs removed phasic input to all dorsal and ventral muscles and resulted in a robust reduction in contractile force over the entire frequency distribution, including a 53% decrease in maximum force following 150 Hz stimulation (MNIs GAL4: 5.4 ± 0.2 mN, n=7; MNIs>UAS-RPR: 2.5 ± 0.1 mN, n=8, $p < 0.005$, Figure 4F) and a 65% decrease in minimal contractile force following a single action potential (MNIs GAL4: 0.2 ± 0.02 mN, n=7; MNIs>RPR: 0.07 ± 0.02 mN, n=7, $p < 0.05$,

Figure 4G). Ablation of MN1-Ib eliminated tonic input only to M1, leaving innervation of the other dorsal muscles by their respective Ib and Is neurons intact. Loss of MN1-Ib caused a significant though less severe defect, resulting in a 25% decrease in contractile force at 150 Hz (MN1-Ib GAL4: 5.5 ± 0.2 mN, n=7; MN1-Ib>UAS-RPR: 4.1 ± 0.2 mN, n=7, $p < 0.05$, Figure 4F) and a 33% decrease at 1 Hz (MN1-Ib GAL4: 0.21 ± 0.02 mN, n=7; MN1-Ib>UAS-RPR: 0.14 ± 0.01 mN, n=7, $p < 0.05$, Figure 4G). These results indicate both motoneuron subclasses contribute to muscle contraction force, with the phasic Is input providing major drive for both excitability and contraction.

Lack of Ib and Is synaptic competition during NMJ development

Given the role of tonic and phasic motoneuron inputs in driving muscle excitability, we examined whether interactions between the inputs occurred during larval development that shaped their axonal arbor expansion and AZ number when they co-innervated M1 or M4. If Ib and Is neurons competed for synaptic growth signals emanating from the muscle, or suppressed growth of the co-innervating input, competitive interactions should generate a negative correlation between Ib and Is synapse number. If the two inputs display cooperative interactions during growth, for example by co-activating the muscle to release more synaptogenic factors, one would expect a positive correlation. Similarly, if both inputs were independent and growing only in response to muscle size, a positive correlation would be expected. Ib and Is synaptic terminals were identified following anti-Discs large (DLG) immunostaining. DLG is a component of the postsynaptic muscle SSR and prominent around presynaptic Ib boutons compared to Is (Lahey et al., 1994). Synapse number was quantified for wandering 3rd instar larvae by immunolabeling for the core AZ T-bar component Bruchpilot (BRP) (Fouquet et al., 2009; Wagh et al., 2006). Synaptic

bouton number was determined using anti-HRP immunostaining, which provides a neuron-specific membrane label. No correlation was observed between Ib and Is AZ number per NMJ at M1 ($r = -0.11$, $n=29$, $p=0.57$, Figure 5A) or between Ib and Is inputs at M4 ($r = -0.10$, $n=19$, $p=0.69$, Figure 5B). Similarly, no correlation for Ib versus Is bouton number at M1 ($r = 0.15$, $n=29$, $p=0.44$, Figure 5C) or M4 ($r = 0.13$, $n=19$, $p=0.60$) was found (Figure 5D). These observations are consistent with Ib and Is motoneurons forming synapses on the muscle without obvious competitive or cooperative interactions that shape their connectivity during development.

As described above, ~30% of larval M1 muscles lack Is innervation. This natural variation provided an opportunity to examine if growth of the co-innervating MN1-Ib motoneuron was altered at mature 3rd instar NMJs when MNIs innervation was absent. Lack of Is innervation did not result in any change in M1 muscle surface area (co-innervation: $46661 \pm 1457 \mu\text{m}^2$, $n=16$; Ib only: $48206 \pm 1170 \mu\text{m}^2$, $n=8$, $p=0.66$). Although total AZ number was reduced at M1 in the absence of Is innervation (Ib only: 285.8 ± 29.7 AZs, $n=10$; co-innervation: 389.7 ± 17.3 AZs, $n=13$, $p<0.004$), AZ number contributed solely by the MN1-Ib input was not significantly altered whether Is was absent (285.8 ± 29.7 Ib AZs, $n=10$, $p=0.61$) or present (329.1 ± 15.8 Ib AZs, $n=13$, Figure 6A). Similarly, no change in synaptic bouton number in MN1-Ib motoneurons was observed whether MNIs was absent (18.0 ± 4.3 Ib boutons, $n=8$, $p=0.99$) or present (19.1 ± 4.4 Ib boutons, $n=16$, Figure 6B). We conclude that synaptic growth of MN1-Ib is not altered when muscle M1 lacks Is innervation.

Ablation of MNIs triggers increased evoked release from the remaining MN1-Ib input

Although no structural compensation was observed in MN1-Ib when MNIs was absent, functional changes in neurotransmitter release could occur in the absence of increased release sites.

In addition, a mismatch in neuronal activity between inputs during development could result in unique forms of plasticity compared to when a motoneuron was missing. To generate an input imbalance, MN1-Ib or MNIs GAL4 drivers were used to express several well-characterized UAS-transgenes that alter neuronal activity (Pauls et al., 2015; Simpson, 2009; Venken et al., 2011; Yoshihara and Ito, 2012). To decrease neurotransmitter release and synaptic output, a transgene encoding tetanus toxin light chain (UAS-TeTXLC) was expressed to cleave the v-SNARE n-Synaptobrevin and eliminate evoked synaptic transmission (Sweeney et al., 1995). A transgene encoding a bacterial voltage-gated Na⁺ channel (UAS-NaChBac) that enhances depolarization was used to constitutively increase neuronal excitability (Nitabach et al., 2006). To compare the effects of reduced or enhanced activity with the complete absence of each input, Reaper expression (UAS-RPR) was used to ablate MN1-Ib or MNIs. None of the manipulations altered M1 muscle surface area, indicating muscle growth is not affected by ablation or activity changes in MN1-Ib or MNIs motoneurons (Figure 7 – supplemental figure 1). For all experimental manipulations, the Ib motoneuron was labeled with MN1-Ib LexA, LexAop-GFP in the background for unambiguous identification of the two inputs following immunostaining with the pan-neuronal marker anti-HRP (Ib and Is) and anti-GFP (Ib only). Synaptic development, synaptic function and muscle contraction force were analyzed in controls and compared to Ib and Is motoneurons expressing the transgenes with their respective GAL4 driver.

We first examined if ablation of each motoneuron subclass altered synaptic structure of the remaining input. Expression of UAS-RPR with either MN1-Ib GAL4 or MNIs GAL4 resulted in elimination of the respective motoneuron compared to controls (Figure 7A-E). Membrane fragments immuno-positive for GFP from the MN1-Ib LexA, LexAop-GFP labeling were often observed near M1 in MN1-Ib GAL4>UAS-RPR larvae (Figure 7D), suggesting cell death and

membrane fragmentation occurred after the initial stages of axonal pathfinding. Genetic ablation of the phasic Is motoneuron in MNIs GAL4>UAS-RPR larvae caused a mild decrease in total AZ and synaptic bouton number due to loss of the Is input (Figure 8A, B). However, there was no change in MN1-Ib AZ (Figure 9A) or bouton number (Figure 9B) following MNIs ablation, similar to conditions where MNIs naturally failed to innervate M1 in control larvae.

To determine if MN1-Ib altered its functional properties without changes in the number of release sites, electrophysiology was performed at 3rd instar M1 muscles to measure Ib evoked release when Is innervation was present in control versus when Is was ablated with UAS-RPR. Although no structural changes were identified at MN1-Ib NMJs, a functional change in the output of the tonic motoneuron was observed. The evoked EJP response triggered by MN1-Ib activation was increased 24% at M1 muscles when the MNIs input was ablated (15.4 ± 1.0 mV, n=11) versus when MNIs was present (11.8 ± 1.6 mV, n=22 p=0.05, Figure 10). This compensation did not result in complete recovery of the evoked output observed when both inputs were present (controls: Is-GAL4: 25.9 ± 1.5 mV, n=10; UAS-RPR: 25.1 ± 1.1 mV, n=11). In addition, contractile force was still decreased following MNIs ablation as previously noted (Figure 4E-G, Figure 10 – supplemental figure 1A, C). These data suggest the muscle is capable of detecting loss of the Is input and increasing synaptic output from the remaining Ib motoneuron, resulting in a partial rescue of muscle excitability.

To examine if phasic motoneurons displayed similar functional compensation, genetic ablation of the tonic Ib motoneuron was performed using MN1-Ib GAL4; UAS-RPR. As previously described, M1 occasionally lacked MNIs input due to natural variation in controls. As such, MN1-Ib ablation resulted in M1 having no synaptic innervation (42%) or only MNIs innervation (58%). Larvae with Is innervation at M1 following ablation of the Ib motoneuron displayed a dramatic

decrease in the number of total AZs (control: 332.1 ± 13.5 AZs, $n=25$; Ib>RPR: 67.7 ± 8.4 AZs, $n=11$, $p<0.0001$, Figure 8A) and synaptic boutons (control: 28.8 ± 1.4 , $n=25$; Ib>RPR: 11.0 ± 2.1 , $n=11$, $p<0.0001$, Figure 8B), given the larger number of synapses normally contributed by the MN1-Ib input. However, loss of MN1-Ib did not trigger changes in the number of Is AZs (Figure 9C) or Is synaptic boutons (Figure 9D) compared to Is innervation when MN1-Ib was present. In contrast to the functional increase in evoked release in tonic Ib neurons following ablation of Is, loss of MN1-Ib did not trigger a compensatory increase in evoked output from the remaining Is motoneuron (Figure 10). We conclude that compensatory structural or functional changes do not occur in the phasic Is input following loss of the tonic Ib motoneuron at M1. In contrast, loss of Is results in functional changes in the co-innervating Ib input that partially compensate for the reduced evoked response.

Imbalances in MN1-Ib or MNIs neuronal activity reveal structural plasticity of tonic Ib inputs

To examine the consequences of activity perturbations between Ib and Is motoneurons at M1 NMJs during development, manipulations were performed to increase or decrease synaptic output of one of the two neurons. Expression of UAS-TeTXLC in either the Ib or Is input blocked synaptic transmission from the affected motoneuron, reducing the evoked response recorded physiologically to the level observed when only the Ib or Is motoneuron were recruited during minimal stimulation (Figure 10). Silencing the Is motoneuron in MNIs GAL4; UAS-TeTXLC larvae resulted in structural changes at the NMJ, with an increase in the total number of AZs (control: 396.3 ± 14.6 AZs, $n=15$; Is>TeTXLC: 465.0 ± 14.7 AZs, $n=18$, $p<0.02$, Figure 8A) and synaptic boutons (control: 41.2 ± 2.7 , $n=15$; Is>TeTXLC: 50.9 ± 2.7 , $n=18$, $p<0.03$, Figure 8B).

This enhanced synaptic growth was due to increases occurring in the co-innervating MN1-Ib input (Figure 9A, B), with no changes observed in the affected MNIs (Figure 9C, D). In particular, MN1-Ib displayed a large increase in AZ number when Is was silenced compared to when Is was present or ablated (Is present: 314 ± 12.9 , n=15; Is ablated: 326.6 ± 14.4 , n=14; Is silenced: 402.7 ± 13.0 , n=18, $p < 0.0001$). Although the number of release sites increased in MN1-Ib following silencing of MNIs (MNIs>TeTXLC), electrophysiology (Figure 10) and contraction assays (Figure 10 – supplemental figure 1A, C) indicated these structural changes were insufficient to induce increased excitability or contractility of the muscle. We conclude that the complete absence of the phasic Is input leads to a functional increase in release from the co-innervating tonic Ib input without a change in the number of release sites. When Is is present but functionally silent, the tonic Ib input displays a distinct response with a structural change that includes more release sites, but the overall functional output of the motoneuron remains unaltered.

We next examined the consequences of silencing MN1-Ib activity with TeTXLC. Similar to when MN1-Ib was ablated, the co-innervating MNIs did not display structural (Figure 9C, D) or functional compensation (Figure 10, Figure 10 – figure supplement 1A, B), indicating the phasic motoneuron is less capable of compensatory synaptic plasticity when the co-innervating tonic motoneuron is ablated or silenced. In contrast to the lack of change in the phasic Is input, silencing MN1-Ib (Ib>TeTXLC) triggered several structural changes to its own morphology. First, a striking reduction in AZ number was found, with a 30% decrease in release sites in MN1-Ib motoneurons lacking evoked transmission (UAS-TeTXLC: 333.6 ± 21.2 AZs, n=14; MN1-Ib GAL4: 281.6 ± 11.9 AZs, n=25; Ib>TeTXLC: 215.3 ± 13.6 AZs, n=15, $p < 0.001$, Figure 9A). Second, there was a change in the anatomy of the MN1-Ib axon at the NMJ, with the appearance of synaptic filopodial-like protrusions (Figure 11A-C). This phenotype was never observed in controls (average

protrusions per MN1-Ib NMJ: UAS-TeTXLC: 0, n=14; MN1-Ib GAL4: 0, n=25; MN1-Ib>TeTXLC: 7.2 ± 2.4 , n=16, $p<0.0001$, Figure 11D). Similar filopodial-like protrusions were described previously at early 1st instar NMJs during the initial stages of synapse formation in wildtype animals, but never at mature 3rd instar NMJs (Akbergenova et al., 2018). Such protrusions were not observed in silenced Is motoneurons or in Ib motoneurons following Is silencing (Figure 11A-D), indicating MN1-Ib and MNIs react differently to changes in their own activity.

A final morphological change at silenced MN1-Ib NMJs was a decrease in postsynaptic SSR membrane revealed by anti-DLG staining (Figure 12A-D). SSR volume compared to presynaptic NMJ volume (anti-HRP staining) was reduced by 50% on average at MN1-Ib>TeTXLC NMJs compared to controls ($p<0.0001$, Figure 12D). Together, the reduced AZ number, decreased muscle SSR volume and increased synaptic filopodial-like protrusions suggest silenced MN1-Ib motoneurons maintain an immature state with reduced AZ formation and a failure to properly induce normal postsynaptic specializations. These defects are not observed at silenced Is phasic synapses, indicating the phasic Is motoneuron class is less sensitive to activity changes and any potential compensatory responses triggered from the muscle.

To determine if enhanced activity of either of the two motoneuron subclasses would induce structural or functional changes, the NaChBac depolarizing Na⁺ channel was expressed in either MN1-Ib or MNIs (Figure 13A-C). NaChBaC expression has been previously demonstrated to enhance membrane depolarization by increasing Na⁺ conductance (Pauls et al., 2015). Consistent with enhanced excitability and increased burst spiking in affected motoneurons, trains of EJPs in response to a single stimulus were often recorded from M1 in larvae expressing NaChBac (Figure 13D). Although expression of the channel enhanced excitability, it did not result in structural (Figure 8, Figure 9) or functional (Figure 13E, Figure 10 – supplemental figure 1) changes in

synaptic properties of MN1-Ib>NaChBac or MNIs>NaChBac larvae. No alterations of the Ib or Is input were observed in either condition. Similarly, increased activity in either motoneuron class did not trigger any obvious structural competition between the inputs. We conclude that NMJ plasticity is more sensitive to manipulations that reduce presynaptic release versus those that enhance membrane excitability, and that these changes preferentially manifest within the tonic Ib subclass of motoneurons.

Discussion

To characterize how changes in the presence or activity of tonic versus phasic motoneurons alter NMJ development and function in *Drosophila*, we identified GAL4 drivers specific for the Ib and Is neuronal subclasses that innervate M1 and used them to alter the balance of input to the muscle. Our data indicate Ib and Is glutamatergic motoneurons largely form independent inputs that make similar contributions to muscle excitability and contractile force. The tonic Ib subclass was capable of structural or functional changes following manipulations that altered their output or that of the co-innervating phasic Is motoneuron (Figure 14A-D). These changes were only observed during conditions when neuronal activity was decreased or when the Is input was ablated. Functional increases in evoked release without enhanced synapse number were observed in Ib motoneurons following ablation of Is (Figure 14B). In contrast, morphological changes that increased AZ number without enhancing evoked release occurred when Is synaptic output was blocked with tetanus toxin (Figure 14C). While Ib motoneurons were capable of several forms of plastic change following reduced input to the muscle, the phasic Is motoneurons were insensitive to manipulations of their own activity or that of the tonic Ib input. Unlike plasticity observed in Ib neurons following reduction in synaptic drive to the muscle, enhancing excitability of either the Ib or Is input was ineffective at triggering changes in either motoneuron class. These data indicate reductions in activity from either input trigger a structural or functional change primarily from the tonic Ib motoneuron subclass.

Plasticity of target choice by motoneurons at Drosophila NMJs

The stereotypical connectivity found in the abdominal musculature of *Drosophila* larvae suggest individual muscles normally allow synaptic innervation from only a single motoneuron of

each subclass (Hoang and Chiba, 2001). However, expanded postsynaptic target choice has been observed following muscle loss induced by laser ablation or genetic mutation, with the affected Ib motoneuron targeting inappropriate nearby muscles without altering the innervation pattern of the correctly-targeted Ib neuron (Chang and Keshishian, 1996; Keshishian et al., 1994; Sink and Whittington, 1991). Similarly, ablation of some motoneurons can result in axonal sprouting from neighboring connections that target the de-innervated muscle (Chang and Keshishian, 1996). Mis-expression of synaptic cell surface proteins can also alter target choice for some Ib and Is motoneurons (Ashley et al., 2019; Kose et al., 1997; Lin and Goodman, 1994; Shishido et al., 1998). Finally, silencing neuronal activity during development has been demonstrated to induce ectopic NMJs formed primarily by type II neuromodulatory neurons (Carrillo et al., 2010; Jarecki and Keshishian, 1995; Keshishian et al., 1994; Lnenicka et al., 2003; Mosca et al., 2005; Vonhoff and Keshishian, 2017; White et al., 2001). These cases of poly-innervation suggest the *Drosophila* motor system differs from that found in vertebrates, with each motoneuron displaying an autonomous role in target selection.

Although motoneuron innervation is normally hard-wired, the examples described above indicate plasticity can occur when a postsynaptic target is eliminated, or the activity or cell-surface proteome of the motoneuron is altered. We did not observe any axonal sprouting onto M1 from other motoneurons that resulted in altered target choice when MN1-Ib or MNIs was ablated or silenced in our experiments. Given M1 is the most dorsal muscle of the abdominal musculature, axons from other motoneurons are not present in the direct vicinity, so any signals released from M1 might be insufficient to attract additional innervation. However, we did find evidence that M1 may attempt to promote more synaptic innervation when MN1-Ib was silenced with tetanus toxin. Under these conditions, the MN1-Ib axon terminal maintained an immature-like state with the

presence of filopodial-like extensions that may represent attempts to increase innervation of the muscle (Figure 14D). This effect was only observed in Ib motoneurons, highlighting differences in how phasic Is terminals interact with or respond to signals from the muscle. We and others have previously observed similar filopodial-like extensions at newly forming NMJ connections in late embryos and early 1st instar larvae (Akbergenova et al., 2018; Broadie and Bate, 1993; Halpern et al., 1991; Kohsaka and Nose, 2009; Ritzenthaler et al., 2000; Ritzenthaler and Chiba, 2003). These presynaptic filopodial processes contain elevated levels of the Cacophony (Cac) N-type Ca²⁺ channel and interact with GluRIIA-rich myopodia, with some progressing to form new synapses during early development (Akbergenova et al., 2018). These protrusions are not found after the initial stages of target selection and synapse formation, disappearing by the end of the 1st instar period. Due to the lack of reinforcement signals caused by absence of synaptic activity in silenced MN1-Ib motoneurons, we hypothesize these filopodial-like extensions fail to properly drive AZ assembly and new synapse formation. The lack of BRP-positive AZ puncta in these structures and the reduction in total AZ number in silenced Ib motoneurons are consistent with this model. In addition, the observation that these structures are still found at mature 3rd instar NMJs suggest the muscle is continuing to provide a synaptogenic signal due to decreased synaptic drive that would normally be restricted to the early window of synapse formation. Indeed, a role for neuronal activity in regulating synaptogenic filopodial stabilization as a precursor to AZ seeding and synapse formation has been recently characterized in the developing *Drosophila* visual system (Özel et al., 2019; Sheng et al., 2018). In addition, changes in neuronal activity levels can decrease or increase PSD maturation and AZ seeding during development (Akbergenova et al., 2018), consistent with synaptic activity shaping NMJ maturation at Ib terminals.

In future studies it will be interesting to explore whether distinct forms of plasticity can be observed when a muscle is targeted by two motoneurons of the same class, similar to the situation found at mammalian NMJs (Tapia et al., 2012). Based on our data, we would hypothesize that two phasic Is motoneurons innervating the same muscle would not show interactions given their lack of response to manipulations of Ib activity. In contrast, dual innervation by two independent Ib motoneurons would be more likely to generate competition, given their exaggerated potential for plasticity compared to the Is subclass. In this regard, manipulation of transcription factors required for neuroblast differentiation of several dorsal Ib motoneurons have been found to trigger poly-innervation of the same muscle from duplicated motoneurons (Meng et al., 2019). The increased Ib innervation does not result in synapse elimination of motor axons as observed at mammalian NMJs, but whether the multiple presynaptic inputs compete, cooperate or function independently is unclear.

Different plasticity rules for tonic versus phasic motoneurons

Many forms of plasticity, including synapse elimination at mammalian NMJs, ocular dominance plasticity, and cerebellar climbing fiber pruning, require Hebbian-like input imbalances to trigger synaptic interactions (Colman et al., 1997; Hashimoto and Kano, 2013; Sanes and Lichtman, 1999; Sherman and Spear, 1982; Tomàs et al., 2017; Turney and Lichtman, 2012; Walsh and Lichtman, 2003; Wiesel and Hubel, 1965, 1963; Wilson et al., 2019). As such, we were interested to see if changes in the activity of Ib or Is motoneurons that created an imbalance between the output of the two neurons could drive unique changes compared to when one input was missing. In the case of the tonic Ib neuron this was indeed observed. In the absence of Is input, either due to natural variation in innervation in control animals or following ablation with UAS-

RPR, there was no structural response in terms of adding additional release sites. However, loss of Is triggered a functional increase in evoked release from the Ib neuron (Figure 14B). In contrast, when an activity imbalance was created by expressing tetanus toxin in the Is neuron, a different change in Ib was elicited. When Is was present but functionally silent, the Ib neuron displayed structural plasticity that increased the number of release sites, but failed to increase its functional output in terms of the amount of evoked release (Figure 14C). A similar observation using optical quantal imaging was made following Is expression of tetanus toxin (Newman et al., 2017). Although the underlying molecular pathways that mediate the two distinct responses are unknown, the results suggest the physical presence of Is likely alters the signaling system(s) responsible for triggering compensation in Ib motoneurons in response to reduced muscle drive.

Another key finding from our manipulations was the differential plasticity responses observed in tonic versus phasic motoneurons. For every manipulation we made beyond increasing excitability of the neurons, a response from the tonic Ib class was detected, while the phasic Is motoneuron displayed less plasticity. Since each muscle is innervated by only a single Ib motoneuron, plasticity within the tonic subclass may allow more robust and local regulation of muscle function. Although the Is did not show plastic change in response to manipulation of its activity or the co-innervating Ib in our experiments, we cannot rule out that Is neurons are capable of such plasticity but display less sensitivity to putative muscle-derived retrograde signals. In addition, given Is neurons innervate multiple muscles compared to Ib, it is also possible that small plastic changes occurring in Is are not synapse-specific and are subsequently distributed over a much larger population of AZs onto multiple muscles, resulting in little observed effect at any single postsynaptic target.

Similar differences in homeostatic plasticity induction potential in Ib versus Is motoneurons have been previously described following reduced postsynaptic muscle glutamate receptor function, with the Ib motoneuron showing a more robust upregulation of presynaptic release compared to Is (Cunningham and Littleton, 2019a, 2019b; Genç and Davis, 2019; Li et al., 2018; Newman et al., 2017). One contributing mechanism is due to changes in phosphorylated CAMKII levels at PSDs apposed to Ib versus Is AZs (Li et al., 2018; Newman et al., 2017). In addition, changes in Is output appear to be limited to low extracellular Ca^{2+} conditions, as the high P_r AZs found at Is terminals provides a smaller window for potentiation (Genç and Davis, 2019). Together, these results imply tonic Ib motoneurons express distinct plasticity mechanisms that can be triggered by reduced muscle function that are less robust or lacking in the Is phasic subclass.

Molecular pathways underlying structural and functional plasticity in motoneurons

An important question moving forward is what distinct presynaptic and postsynaptic mechanisms control structural and functional plasticity in tonic Ib motoneurons following manipulations of the co-innervating phasic Is input. Similarly, defining why the Is fails to respond to many of the same manipulations is poorly understood. Undoubtedly, there are key differences in molecular signaling components and surface receptors expressed by Is and Ib motoneurons that contribute to many of these differences. Indeed, the classic synaptic growth regulator Gbb appears to have both shared and distinct roles in the two neuronal populations. In Ib motoneurons, the pathway is not required for target innervation, but controls subsequent synaptic growth. Although the pathway regulates synaptic growth in Is motoneurons, a large decrease in target innervation is also observed. Using these GAL4-specific Ib and Is drivers, we are now in a position to characterize the distinct transcriptional profiles of each neuronal subclass to identify candidate

mechanisms that mediate differences in synaptic targeting, biophysical and synaptic properties, and differential plasticity responses.

Whether homeostatic plasticity mechanisms triggered in response to acute or chronic reduction in glutamate receptor function are also activated following the absence or functional silencing of presynaptic inputs as described here is unknown. Several molecular pathways contributing to homeostatic plasticity have been described at the NMJ (Bergquist et al., 2010; Böhme et al., 2019; Davis, 2013, 2006; Davis and Müller, 2015; Frank, 2014; Frank et al., 2020; Gaviño et al., 2015; Goel et al., 2019; Gratz et al., 2019; Kiragasi et al., 2017; Li et al., 2018; Müller et al., 2012, 2011; Müller and Davis, 2012; Ortega et al., 2018; Wang et al., 2016, 2014; Younger et al., 2013). Functional increases in presynaptic output have been attributed to increased synaptic vesicle pools, increased presynaptic Ca²⁺ influx, and enhanced membrane excitability. Recently, reorganization of the AZ proteome with increased levels of BRP and other AZ components at single release sites has been suggested to also contribute to enhanced release in chronic forms of homeostatic plasticity (Böhme et al., 2019; Gratz et al., 2019; Li et al., 2018). There are also numerous pathways that control structural plasticity and regulation of AZ number at *Drosophila* NMJs, including Neurexin/Neurologin, Teneurins, Neurotrophins, Synaptotagmin 4-mediated retrograde signaling, BMPs, Wingless, and regulated proteolysis (Aberle et al., 2002; Ataman et al., 2008, 2006; Banerjee et al., 2017; Banovic et al., 2010; Berke et al., 2013; Collins et al., 2006; Collins and DiAntonio, 2007; DiAntonio and Hicke, 2004; Harris et al., 2016; Harris and Littleton, 2015; Johnson et al., 2009; Korkut et al., 2013; Li et al., 2007; Marqués et al., 2002; Miller et al., 2012; Mosca et al., 2012; Muhammad et al., 2015; Oswald et al., 2012; Piccioli and Littleton, 2014; Sun et al., 2011; Ulian-Benitez et al., 2017; Wairkar et al., 2009; Wan et al., 2000; Yoshihara et al., 2005). Future work will elucidate which of these molecular systems are at play for the forms of

plasticity described here, as well as how similar they are to those that underlie homeostatic control of synaptic output.

Beyond *Drosophila*, studies in crustacean motor systems have shown that long-term alterations in activity can induce cell-type specific changes in tonic or phasic motoneuron structure or release properties (Atwood and Wojtowicz, 1986; Govind and Walrond, 1989; Hong and Lnenicka, 1993; Lnenicka et al., 1991, 1986; Lnenicka and Atwood, 1989; Wojtowicz et al., 1994). Although muscles can differentiate between tonic and phasic inputs in both *Drosophila* and crustaceans, it is unclear how the postsynaptic cell detects the two synaptic populations and differentially regulates their properties. Given tonic and phasic neurons are abundant in the nervous systems of both invertebrates and vertebrates (Atwood and Karunanithi, 2002; Millar and Atwood, 2004; Schultz, 2001; Ventimiglia and Bargmann, 2017; Zucker and Regehr, 2002), it will be important to define how these two classes interact when innervating a common postsynaptic target in other systems as well.

Materials and Methods

Drosophila stocks

Drosophila melanogaster were cultured on standard medium at 25°C. Genotypes used in this study include: *w¹¹¹⁸* (BDSC 3605); 13X LexAop2-mCD8-GFP (Bloomington Drosophila Stock Center (BDSC) 32204); UAS-DsRed (BDSC 6282); UAS-CD8-GFP (BDSC 32185); UAS-Reaper (BDSC 5823); UAS-TeTXLC (BDSC 28837); UAS-NaChBac (BDSC 9469); GMR27E09-GAL4 (BDSC 49227); MN1-Ib-GAL4 (BDSC 40701); 6-58 Is-GAL4 (Ellie Heckscher, U. Chicago). Animals of either sex were used depending upon genetic scheme.

Transgenic constructs

To create the MN1-Ib LexA driver line, a 2736 base pair fragment from the intronic region of the *Dpr4* locus that was used to generate the GMR94G06 MN1-Ib-GAL4 driver line (BDSC stock #40701) was PCR amplified and cloned into pCR8/GW/TOPO® (Invitrogen). This was followed by an LR cloning step into the pBPLexA::p65Uw plasmid (Addgene 26231). The resulting construct was sent for injection into an attP40 donor site strain by BestGene (Chino Hills, CA, USA).

Immunocytochemistry

3rd instar wandering larvae were reared at 25°C and dissected in hemolymph-like HL3.1 solution (in mM: 70 NaCl, 5 KCl, 1.5 CaCl₂, 4 MgCl₂, 10 NaHCO₃, 5 trehalose, 115 sucrose, 5 HEPES, pH 7.2). Larvae were fixed for ten minutes in HL3.1 buffer with 4% formaldehyde and washed three times for ten minutes with PBT (PBS containing 0.1% Triton X-100), followed by a thirty-

minute incubation in block solution (5% NGS in PBT). Fresh block solution and primary antibodies were added. Samples were incubated overnight at 4°C and washed with two short washes and three extended 20 minutes washed in PBT. Secondary antibodies were added to block solution and incubated at room temperature for two hours or at 4°C overnight. Finally, larvae were rewashed and mounted in 80% Glycerol. Antibodies used for this study include: mouse anti-BRP, 1:500 (NC82, Developmental Studies Hybridoma Bank (DSHB) NC82, Iowa City, IA)); mouse anti-DLG, 1:1000 (DSHB stock #4F3); chicken anti-DLG, 1:500; DyLight 649 conjugated anti-HRP, 1:500 (#123-605-021; Jackson Immuno Research, West Grove, PA, USA); rabbit anti-GFP Alexa Fluor 488, 1:500 ((#G10362, ThermoFisher Scientific, Waltham, MA, USA); goat anti-mouse Alexa Fluor 546, 1:500 (A-11030; ThermoFisher); Phalloidin-conjugated Alexa Fluor 555 or 657, 1:500 (ThermoFisher). Immunoreactive proteins were imaged on a Zeiss Pascal confocal microscope (Carl Zeiss Microscopy, Jena, GERMANY) using either a 40X 1.3 NA, 63X 1.3 NA or a 100X 1.3 NA oil-immersion objective (Carl Zeiss Microscopy). Images were processed using Zen (Zeiss) software.

Motoneuron GAL4 driver screen

The FlyLight Project image database of larval brain and VNC GFP expression provided by Gerry Rubin (Janelia, HHMI) was searched for GAL4 lines displaying restricted expression in small subsets of segmentally repeated neurons with GFP-labeled axons projecting from the VNC. Candidate lines meeting these criteria were obtained and crossed to UAS-CD8::GFP (BDSC 32185) for immunostaining with DyLight 649 conjugated anti-HRP (Jackson ImmunoResearch), Alexa Fluor 555 Phalloidin (ThermoFisher) and rabbit anti-GFP Alexa Fluor 488 (ThermoFisher).

Confocal imaging was performed to classify labeled neurons based on their synaptic connectivity within the abdominal musculature.

Quantification of confocal images

Imaris 9.2 software (Oxford Instruments, Zurich, Switzerland) was used to identify BRP puncta to quantify AZ number and HRP labeling to quantify synaptic bouton number from 3D image stacks through the NMJ. For DLG/HRP measurements, the 3D mask feature was used and the software determined bouton volume within HRP staining and muscle SSR volume from DLG staining. Quantification was conducted at muscle M1 in abdominal segment A3. The n value refers to the number of NMJs analyzed, with no more than two NMJs analyzed per larvae. Animals used in each analysis were derived from at least three independent experimental crosses. All analysis was performed blind to genotype.

Live imaging of Ib and Is innervation and synaptic growth

Live imaging was done under desflurane anesthesia at muscles M1 and M4 at abdominal segments A2-A4 as previously described (Akbergenova et al., 2018). Selected larvae were covered with halocarbon oil and a cover glass and imaged. After imaging, larvae were placed in numbered chambers with food in a 25°C incubator. Larvae were imaged at the beginning of the 1st instar larval stage and during the subsequent 24 hr interval with the same data acquisition settings. Confocal images were obtained on a Zeiss Axio Imager 2 equipped with a spinning-disk confocal head (CSU-X1; Yokagawa, Tokyo, JAPAN) and ImagEM X2 EM-CCD camera (Hamamatsu, Hamamatsu City, Japan). A pan-APOCHROMAT 63X objective with 1.40 NA from Zeiss (Carl Zeiss Microscopy) was used for imaging.

Electrophysiology

Wandering 3rd instar larvae were dissected in modified HL3.1 saline (in mM: 70 NaCl, 5 KCl, 0.3 CaCl₂, 4 MgCl₂, 10 NaHCO₃, 5 Trehalose, 115 Sucrose, 5 HEPES, pH 7.18). For electrophysiology and force recordings, larvae were pinned medial side up at the anterior and posterior ends, an incision was made along the midline, and the visceral organs were removed. All nerves emerging from the CNS were severed at the ventral nerve cord, and the CNS and ventral nerve cord was removed. EJPs were elicited by stimulating severed abdominal nerves. A Master 8 A.M.P.I. stimulator (A-M Systems, Sequim, WA) was used for stimulation via a suction electrode. EJPs were recorded using sharp glass microelectrodes containing a 2:1 mixture of 3M potassium chloride:3M potassium acetate with electrode resistances of 40-80 megaohms. An Axoclamp 2B amplifier (Molecular Devices, San Jose, CA) was used for signal detection and digitized via Axon Instruments Digidata 1550 (Molecular Devices). Signals were acquired at 10 kHz using Clampex and analyzed with Clampfit, MiniAnalysis, and Microsoft Excel. All analysis was performed blind to genotype.

Muscle force contraction measurements

Force recordings were obtained using an Aurora Scientific 403A force transducer system (Aurora Scientific, Aurora, ON, CA) with a force transducer headstage, amplifier and digitizer. Larvae were dissected ventral side up in HL3.1 saline containing 1.5 mM Ca²⁺. Nerve-evoked contractions were generated using stimulation bursts from a Master 8 stimulator (A.M.P.I.). The duration of single impulses was 5 ms and interburst duration was kept constant at 15 s. Burst frequency were altered during each individual experiment. Digitized data was acquired using Dynamic Muscle

Acquisition Software (DMCv5.5, Aurora Scientific) and imported and processed in Matlab using custom code. All analysis was performed blind to genotype.

Statistical analysis

Prism software (v. 8.1.1, GraphPad Software, La Jolla, CA, USA) and FIJI /ImageJ was used for statistical analysis. Statistical significance in two-way comparisons was determined by a Student's t-test, while one-way ANOVA parametric analysis was used when comparing more than two datasets. Statistical comparisons are with control unless noted. Appropriate sample size was determined using a normality test. Data is presented as mean \pm SEM; * = $p < 0.05$, ** = $p < 0.01$, *** = $p < 0.001$, n.s. = not significant.

Acknowledgements

This work was supported by NIH grants NS40296 and MH104536 to J.T.L. N.A.S. was supported in part by NIH pre-doctoral training grant T32GM007287. We thank Ellie Heckscher and Gerry Rubin for sharing fly lines. We thank the Bloomington Drosophila Stock Center (Indiana University, Bloomington, IN; NIH P40OD018537), the Drosophila Genome Resource Center (Indiana University, Bloomington, IN; NIH 2P40OD010949-10A1), the TRiP Center at Harvard Medical School (Boston, MA; NIH/NIGMS R01-GM084947), the Developmental Studies Hybridoma Bank (University of Iowa, Iowa City, IA) and the Vienna Drosophila Resource Center (Austria) for providing materials used in this study. We also thank the staff and students in the Cold Spring Harbor Laboratory Drosophila Neurobiology course and members of the Littleton lab for sharing resources and advice.

Table 1



Genotype	GAL4 driver sequences	Protein role	Expression pattern
<i>w¹¹¹⁸</i> ;; GMR79H07-GAL4	CG3964	Tubulin tyrosine ligase-like	M6 Ib (A2 only)
<i>w¹¹¹⁸</i> ;; GMR94G06-GAL4	<i>Dpr4</i>	Synaptic specificity	MN1-Ib
<i>w¹¹¹⁸</i> ;; GMR54H01-GAL4	CG13532	Immunoglobulin-like domain superfamily	MN1SN-Is M1,2,3,4,9,10, 18,19,20 and/ or MN1SN-II MN12-Ib MN13-Ib
<i>w¹¹¹⁸</i> ;; GMR27F01-GAL4	<i>Fmr1</i>	RNA binding protein	MNSNb/d-Is, MN1SN-Is, MN1SN-II,
<i>w¹¹¹⁸</i> ;; GMR25H08-GAL4	<i>Milt</i>	Kinesin-associated protein	Type III
<i>w¹¹¹⁸</i> , 6-58-GAL4	<i>Dip-α</i>	Synaptic specificity	MNSNb/d-Is, MN1SN-Is

Table 1

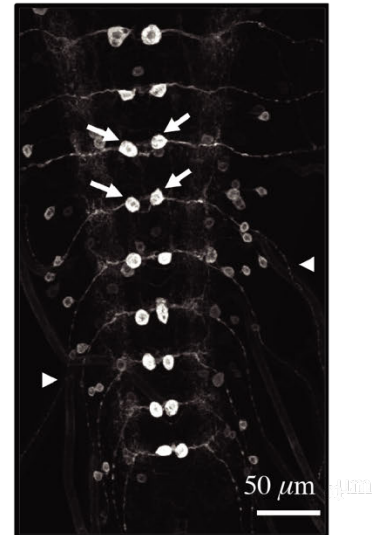
The genotype, GAL4 driver enhancer sequence or site of insertion, predicted protein role and expression pattern revealed by crossing to UAS-CD8-GFP for 3rd instar larvae is shown for the six lines identified with motoneuron-restricted expression. GMR94G06 and 6-58 are referred to as MN1-Ib GAL4 and MNIs GAL4, respectively, throughout the manuscript.

Figure 1

A

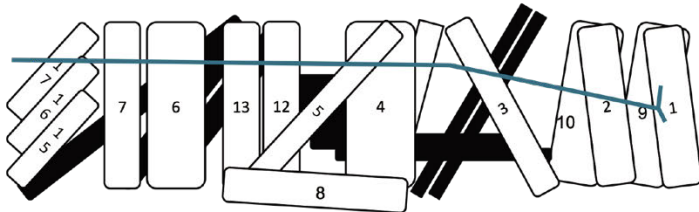
	Ib	Is
Morphology		
Properties	Tonic	Phasic
Probability of release	Low P_r	High P_r
Short-term plasticity	Facilitation	Depression
Synaptic area and SSR	Larger	Smaller
Active zone number	Higher	Lower
Homeostatic plasticity	Chronic	Acute
Spiking Threshold	Lower	Higher
Postsynaptic Target Innervation	Single muscle	Multiple muscles

B

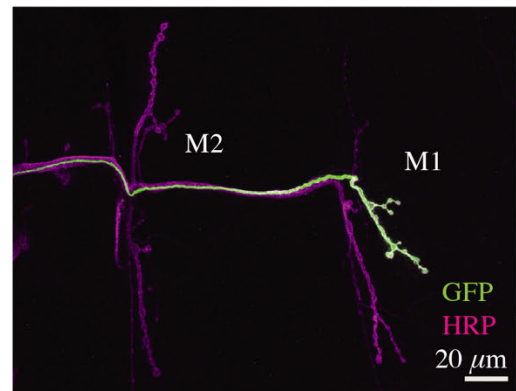


C

MN1-Ib GAL4 Expression

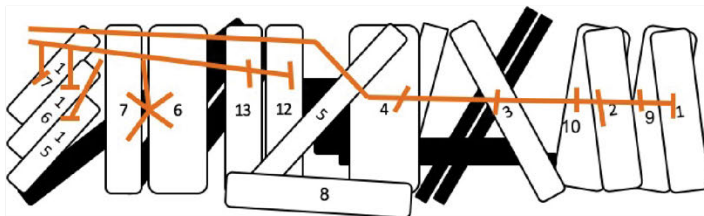


D



E

MNIs GAL4 Expression



F

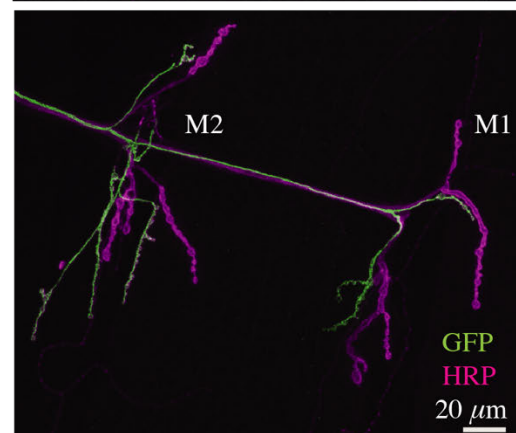


Figure 1. Identification of tonic Ib and phasic Is motoneuron GAL4 drivers. **(A)** Comparison of synaptic and biophysical properties of Ib and Is motoneurons in *Drosophila* larvae. **(B)** Confocal image of UAS-CD8-GFP driven by MN1-Ib GAL4 (GMR94G06) in the 3rd instar larval VNC from the FlyLight Project GAL4 collection. Arrows denote the paired MN1-Ib cell bodies in each abdominal segment, arrowheads denote GFP expression in axons exiting the VNC. Scale bar = 50 μm . **(C)** Diagram of MN1-Ib innervation in a larval abdominal hemisegment. **(D)** Immunostaining for anti-GFP (green) to label MN1-Ib and HRP (magenta) to label all axons in a MN1-Ib GAL4; UAS-CD8-GFP 3rd instar larva. Muscles M1 and M2 are indicated. Scale bar = 20 μm . **(E)** Diagram of MNISN-Is and MNSNb/d-Is innervation in a larval abdominal hemisegment. **(F)** Immunostaining for anti-GFP (green) to label MNIs and HRP (magenta) to label all axons in a MNIs GAL4 (6-58); UAS-CD8-GFP 3rd instar larva. Muscles M1 and M2 are indicated. Scale bar = 20 μm .

Figure 2

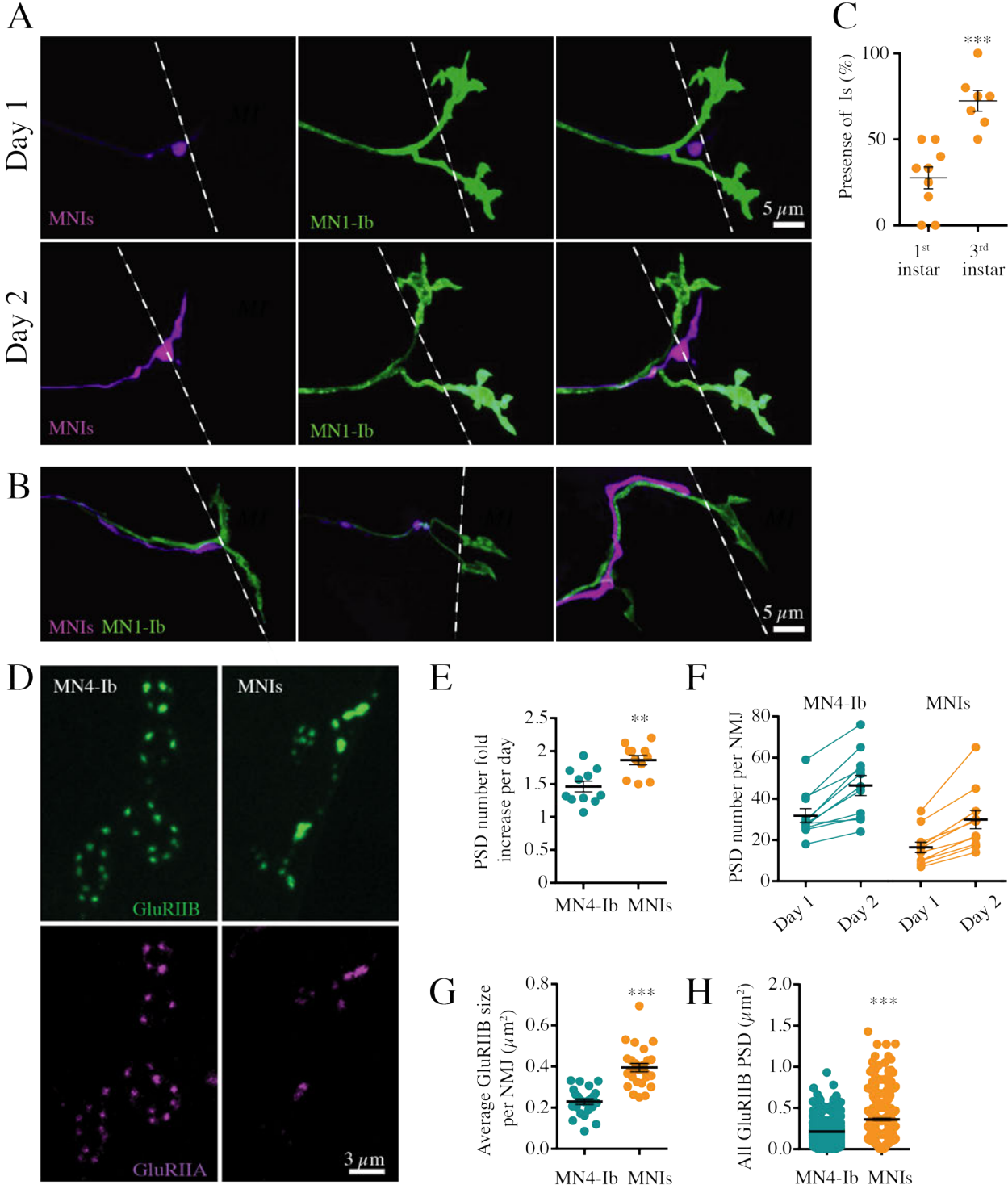


Figure 2. Quantification of MN1-Ib and MNIs target innervation and synapse formation with serial intravital imaging across development. **(A)** Sequential confocal images of muscle M1 innervation by MN1-Ib (green) and MNIs (magenta) at day 1 (top panels) and day 2 (bottom panels) of larval development in dual-labeled animals (MN1-Ib *LexA>LexAop2-CD8-GFP*; MNIs *GAL4>UAS-DsRed*). Dashed line indicates M1 muscle boundary. MNIs has delayed innervation compared to MN1-Ib. Scale bar = 5 μ m. **(B)** Representative confocal images of three M1 muscles on day 1 showing delayed innervation by MNIs (magenta) compared to MN1-Ib (green). MNIs axons in the left and middle panels proceeded to innervate M1 later in development, while the MNIs axon on the right failed to innervate M1. Dashed line indicates M1 muscle boundary. Scale bar = 5 μ m. **(C)** Quantification of Is motoneuron innervation of M1 in 1st instar ($27.6 \pm 6.3\%$, n=9 larvae) versus 3rd instar ($72.4 \pm 6.1\%$, n=7 larvae, $p<0.0002$). Each point represents the average percent of M1 innervation in segments A2-A4 from a single larva. **(D)** Confocal imaging of PSDs formed at MN4-Ib and MNIs NMJs on M4 in larvae expressing RFP-tagged GluRIIA (magenta) and GFP-tagged GluRIIB (green). Note the Is terminal has fewer synapses but larger PSDs. Scale bar = 3 μ m. **(E)** Increase in GluRIIB-positive PSDs over 24 hrs starting at the 1st instar larval stage. The increase in PSD number is plotted as fold-increase of day 2 PSDs over the initial day 1 PSDs for MN4-Ib and MNIs. Each point represents the average increase at M4 from segments A2-A4 for a single larva. **(F)** Increase in PSD number at M4 during serial imaging of MN4-Ib and MNIs over 24 hrs beginning at the 1st instar stage. Each point represents the average PSD number at M4 from segments A2-A4 for a single larva on day 1 and day 2. **(G)** Quantification of GluRIIB-positive PSD area for MN4-Ib and MNIs synapses at M4 in 1st instar larvae. Each point represents the average PSD area at M4 from segments A2-A4 for a single larva. **(H)** Distribution of individual PSD sizes at M4 from segments A2-A4 for MN4-Ib and MNIs NMJs for all 1st instar larvae imaged

(n=9 larvae each). Statistical significance was determined using Student's t-test. Data is shown as mean \pm SEM; ** = $p < 0.01$, *** = $p < 0.001$.

Figure 3

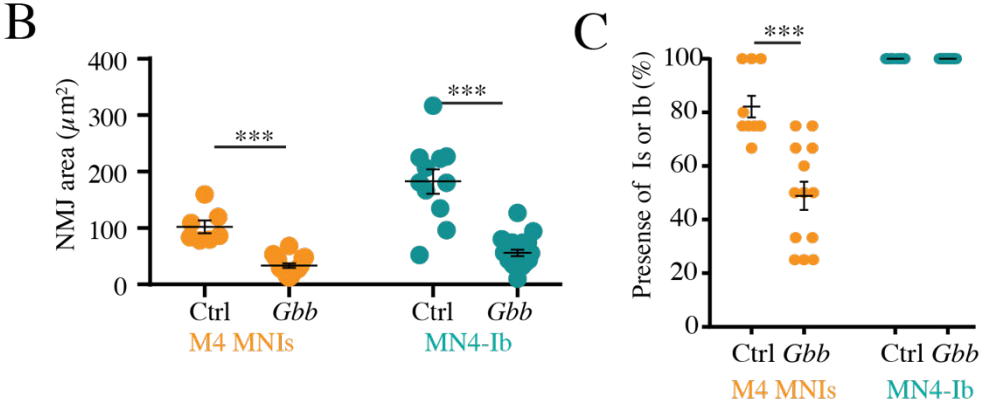
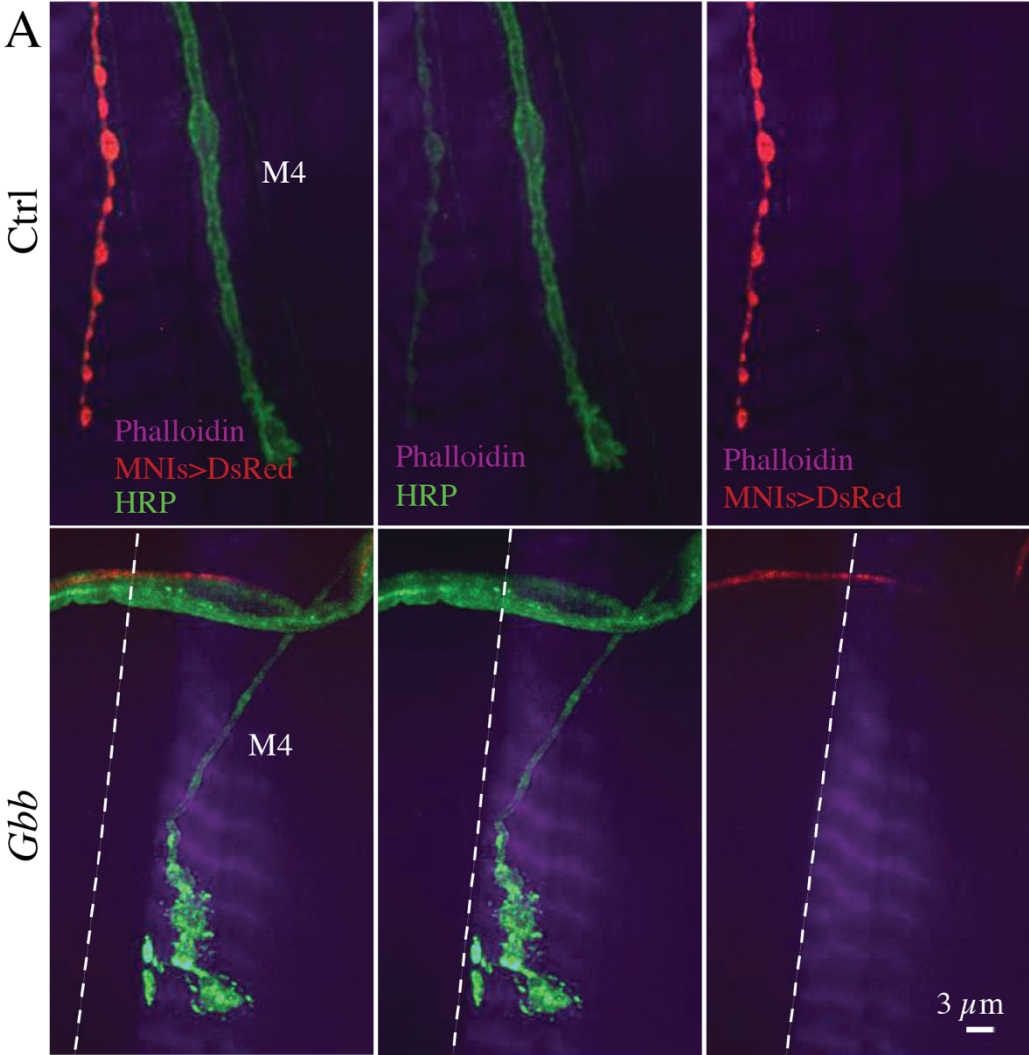


Figure 3. Reduction in synaptic growth and muscle innervation by Is motoneurons in *Gbb* mutants. **(A)** Confocal images of 3rd instar muscle M4 innervation by MN4-Ib (green, anti-HRP staining) and MNIs (magenta, MNIs GAL4>UAS-DsRed) in controls (top panels) or *Gbb* mutants (*gbb¹/gbb²*). Muscles were labeled with Phalloidin-conjugated Alexa Fluor 647. Dashed line indicates M4 muscle boundary. Scale bar = 3 μ m. **(B)** Quantification of NMJ area for MNIs and MN4-Ib at 3rd instar M4 defined by anti-HRP staining for controls and *Gbb* mutants. Each point represents the average NMJ area at M4 from segments A2-A4 for a single larva. **(C)** Quantification of the percent of M4 muscles innervated by MNIs or MN4-Ib at the 3rd instar stage. Each point represents the average percent of M4 innervation in segments A2-A4 from a single larva. Statistical significance was determined using Student's t-test. Data is shown as mean \pm SEM; *** = $p < 0.001$.

Figure 4

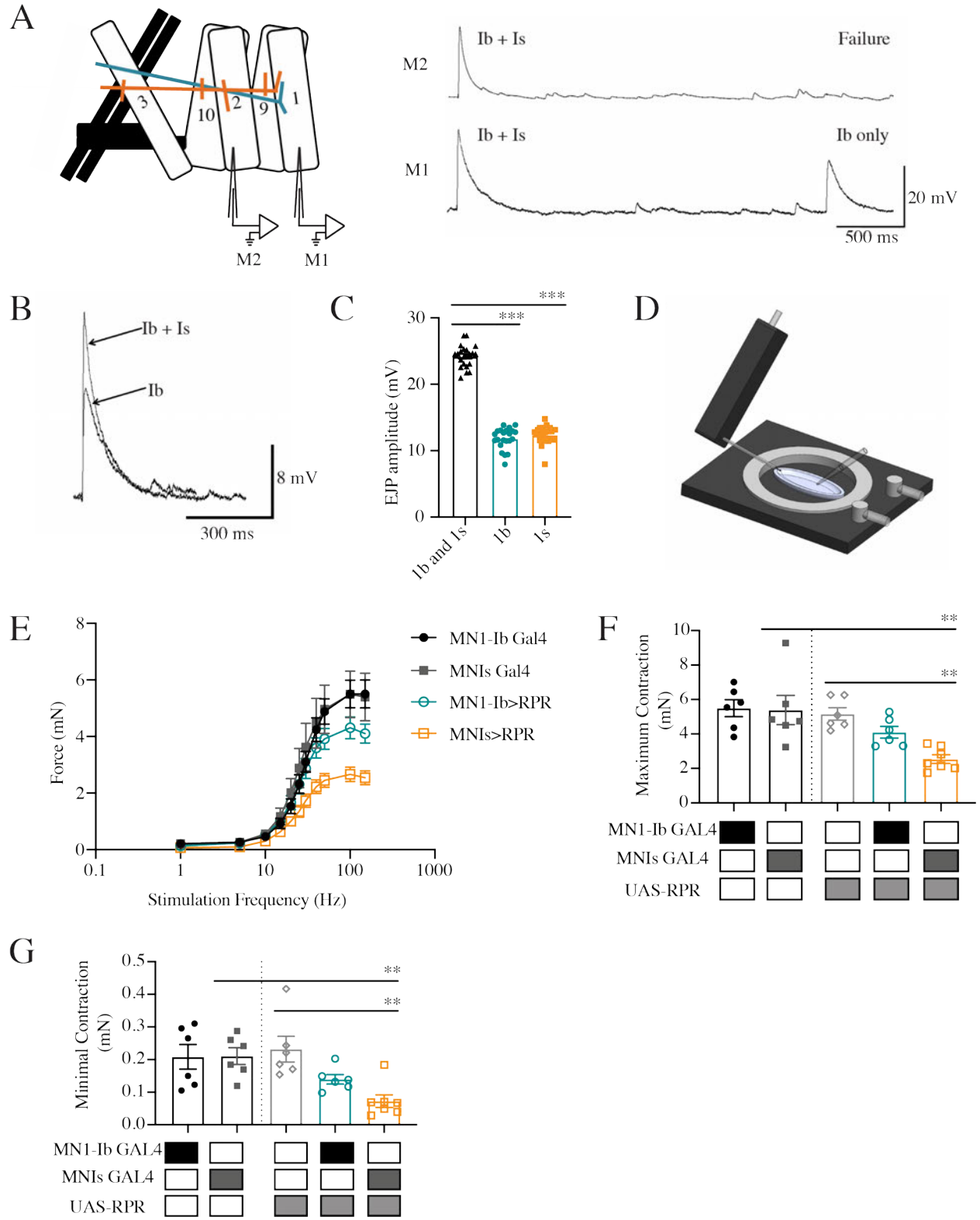


Figure 4. Contributions of MN1-Ib and MNIs to muscle excitability and contractile force. **(A)** Depiction of dual intracellular electrode paradigm for performing simultaneous voltage recordings from muscles M1 and M2 in control *w¹¹⁸* 3rd instar larvae, with MN1-Ib (teal) and MNIs (orange) labeled. Representative recordings from M1 and M2 are shown on the right. Ib + Is shows the compound EJP generated when both motoneurons are activated. Lowering stimulation intensity results in recruitment of only MN1-Ib or MNIs. Stimulation of only MNIs triggers responses in both muscles given it innervates M1 and M2. Stimulation of MN1-Ib, as shown in the Ib-only trace, results in responses only from M1. **(B)** Representative traces of simple or compound EJPs at M1 showing recruitment of MN1-Ib only or both MN1-Ib and MNIs. **(C)** Average EJP amplitude at M1 following recruitment of both motoneurons or MN1-Ib or MNIs only (n=22 larvae). **(D)** Schematic of force transducer setup used to measure larval muscle contractile force. **(E)** Force-frequency curves for 1 Hz to 150 Hz nerve stimulation in MN1-Ib and MNIs GAL4 controls and MN1-Ib GAL4>RPR and MNIs GAL4>RPR ablated 3rd instar larvae. Six replicate contractions were generated at each stimulation frequency for each recording and averaged across 7 larvae per genotype. **(F)** Maximal contraction force elicited at 150 Hz is shown. Shaded boxes under each bar indicate the genotypes for each experimental group. **(G)** Minimal contraction force elicited by a single action potential for the indicated genotypes. Statistical significance was determined using ANOVA. Data is shown as mean \pm SEM; * = p<0.01, *** = p<0.001.

Figure 5

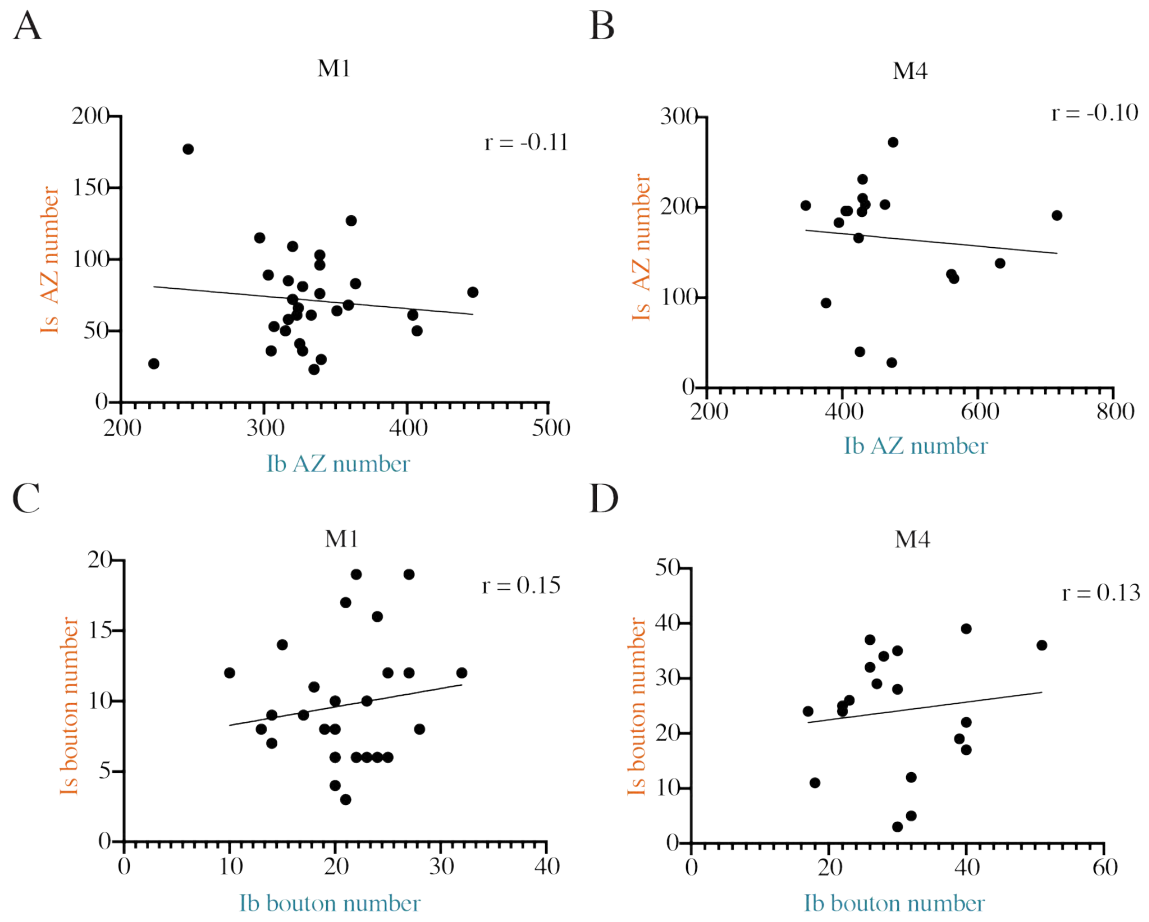


Figure 5. Lack of correlation between Ib and Is synaptic innervation at M1 and M4. **(A)** Correlation of MN1-Ib and MNIs AZ number at M1 quantified following immunolabeling for BRP in control *w¹¹⁸* 3rd instar larvae ($r=-0.11$, $n=29$, $p=0.57$). **(B)** Correlation of MN4-Ib and MNIs AZ number at M4 quantified following immunolabeling for BRP in *w¹¹⁸* 3rd instar larvae ($r=-0.10$, $n=19$, $p=0.69$). **(C)** Correlation of MN1-Ib and MNIs synaptic bouton number at M1 quantified following immunolabeling for HRP in *w¹¹⁸* 3rd instar larvae ($r=0.15$, $n=29$, $p=0.44$). **(D)** Correlation of MN4-Ib and MNIs synaptic bouton number at M4 quantified following immunolabeling for HRP in *w¹¹⁸* 3rd instar larvae ($r=0.13$, $n=19$, $p=0.60$). The Pearson correlation coefficient (r) is shown on the upper right for each analysis. Each data point corresponds to Ib and Is AZ or bouton number from a single larva at the indicated muscle of segment A3.

Figure 6

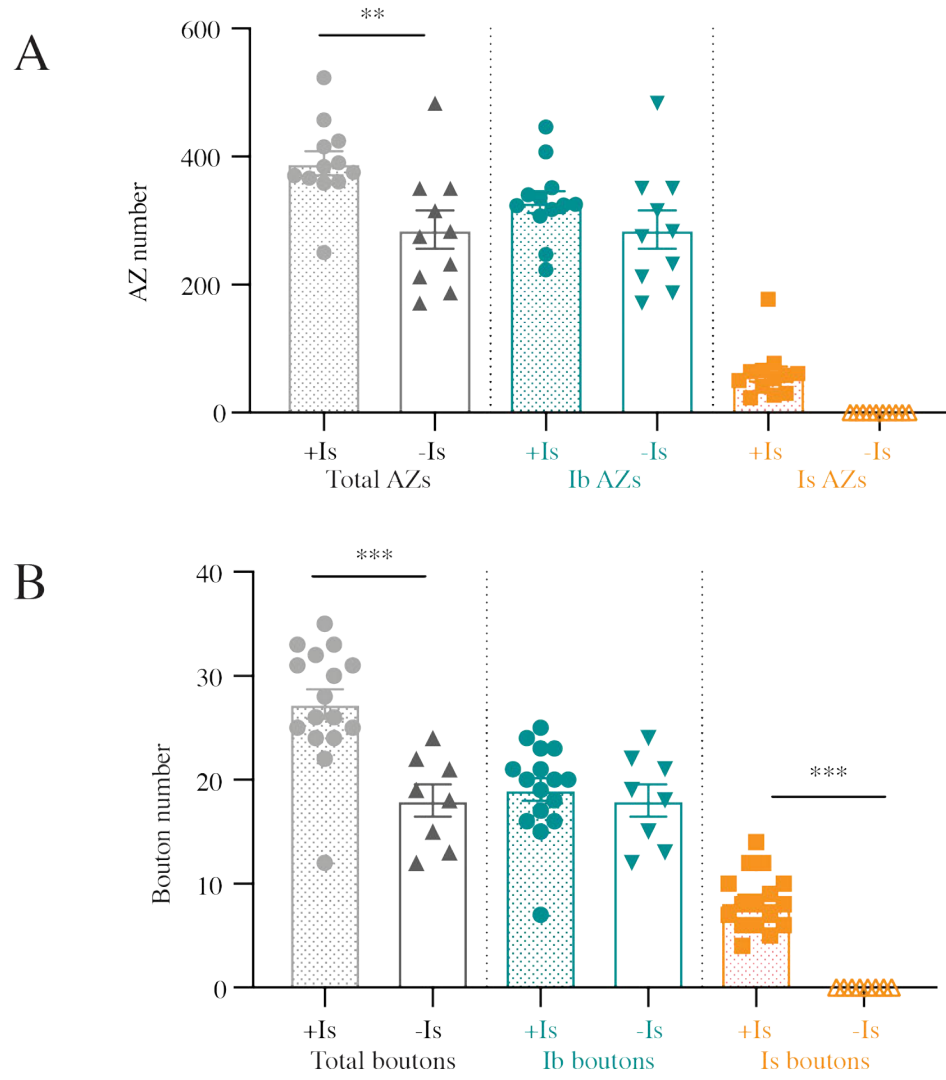


Figure 6. Lack of structural synaptic changes in MN1-Ib when Is innervation is absent. **(A)** Quantification of MN1-Ib and MNIs AZ number following immunolabeling for BRP in control *w¹¹⁸* 3rd instar larval M1 muscles in segment A3. Total AZ number when both inputs are present (+Is) or when Is innervation is absent (-Is) is shown. AZ number specifically for MN1-Ib (teal) or MNIs (orange) is also shown when both inputs are present (+Is) or when Is innervation is absent (-Is). **(B)** Quantification of MN1-Ib and MNIs synaptic bouton number following immunolabeling for HRP in *w¹¹⁸* 3rd instar larval M1 muscles in segment A3. Total bouton number when both inputs are present (+Is) or when Is innervation is absent (-Is) is shown. Bouton number specifically for MN1-Ib (teal) or MNIs (orange) is also shown when both inputs are present (+Is) or when Is innervation is absent (-Is). Each data point represents quantification from a single larva. Statistical significance was determined using ANOVA. Data is shown as mean \pm SEM; ** = $p < 0.01$.

Figure 7

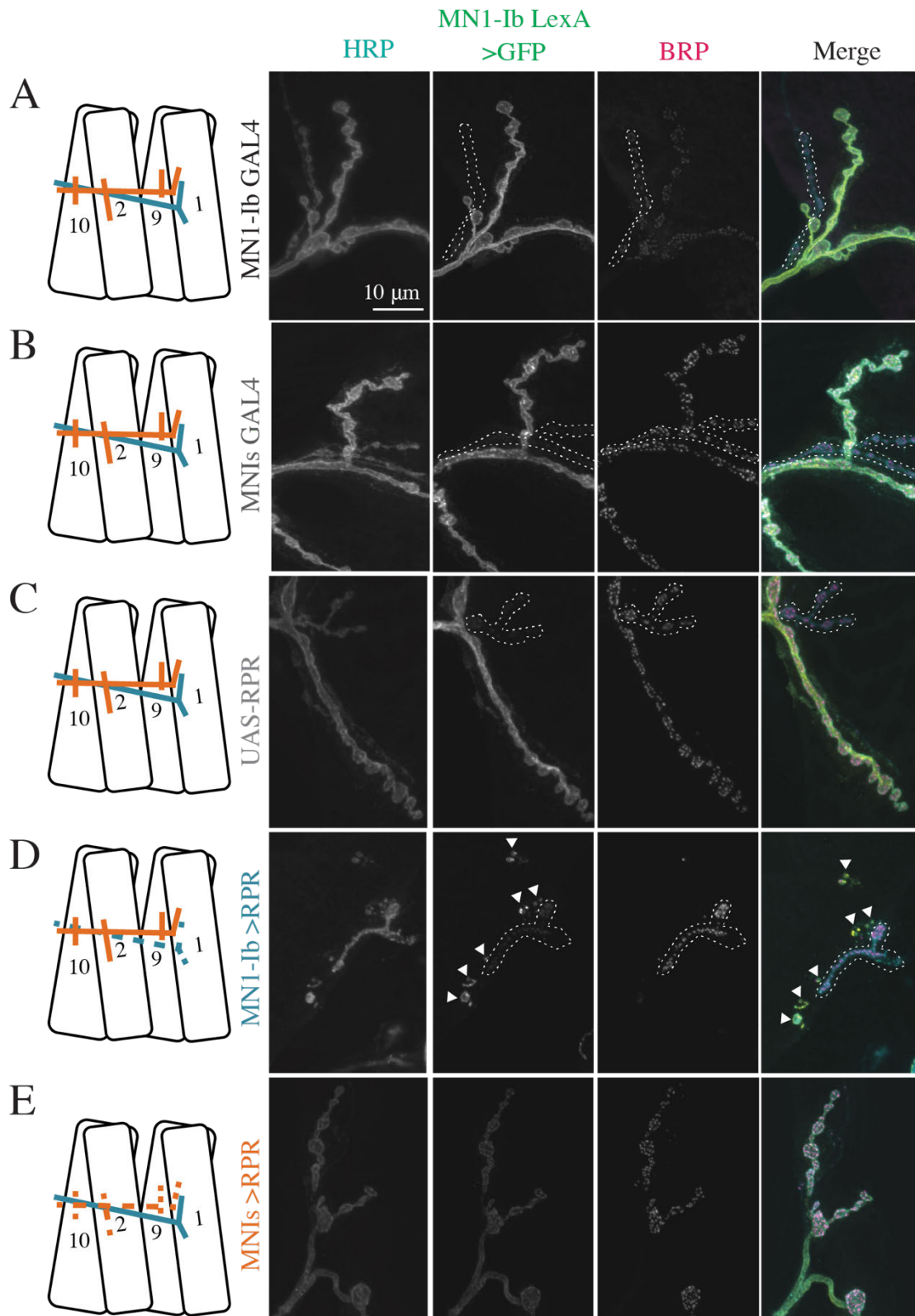


Figure 7. Morphological consequences of ablation of MN1-Ib or MNIs. Representative confocal images of 3rd instar larval M1 NMJs at segment A3 following immunolabeling with anti-HRP, anti-GFP and anti-BRP in the following genotypes: **(A)** MN1-Ib GAL4 control; **(B)** MNIs GAL4 control; **(C)** UAS-RPR control; **(D)** MN1-Ib GAL4>UAS-RPR; **(E)** MNIs GAL4>UAS-RPR. MN1-Ib LexA>LexAop2-CD8-GFP was present in each genetic background to allow unambiguous identification of the Ib terminal. Diagrams of the experimental manipulation is shown on the left, with MN1-Ib (teal) and MNIs (orange) labeled. The merged image is shown on the right. The white dashed line highlights the MNIs terminal in the final 3 panels for each manipulation except for **(E)**, where Is is absent following ablation. Arrowheads in **(D)** depict GFP-positive debris near M1 secondary to death and fragmentation of MN1-Ib following Reaper expression. Scale bar = 10 μ m for all panels.

Figure 7 - figure supplement 1

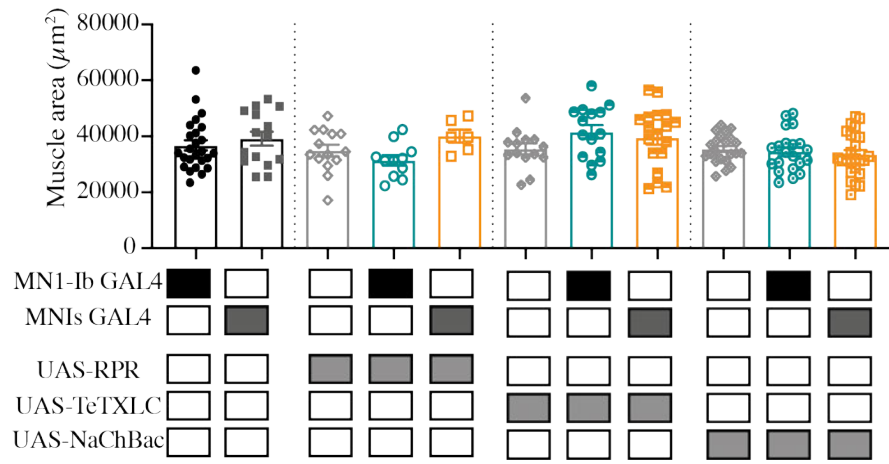


Figure 7 – figure supplement 1. M1 muscle size is not altered by ablation or activity changes of MN1-Ib or MNIs motoneurons. Shaded boxes under each bar indicate the genotypes for each group, with control GAL4 driver lines alone (MN1-Ib, MNIs), control UAS transgenes alone (UAS-RPR, UAS-TeTXLC, UAS-NaChBac) and experimental crosses of MN1-Ib GAL4 (teal) or MNIs GAL4 (orange) to each transgene. Each data point represents quantification of segment A3 M1 surface area from a single 3rd instar larvae. Statistical significance was determined using ANOVA. No statistical difference was found across genotypes. Data is shown as mean \pm SEM.

Figure 8

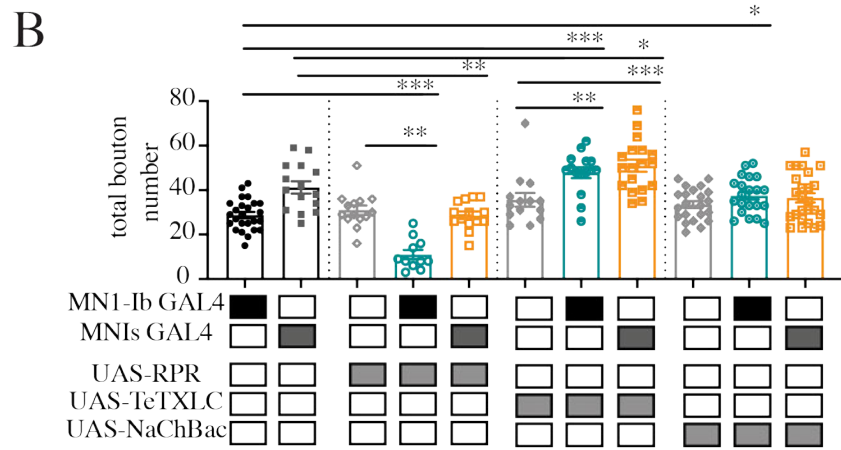
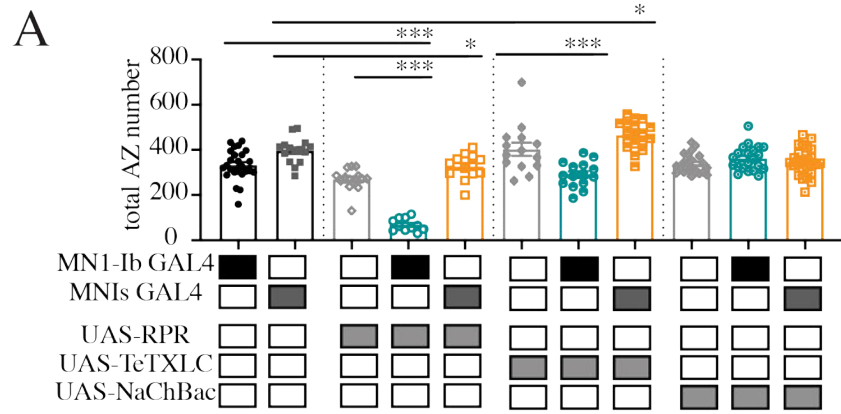


Figure 8. Quantification of total AZ and bouton number follow ablation or activity changes of MN1-Ib or MNIs. **(A)** Quantification of combined MN1-Ib and MNIs AZ number following immunolabeling for BRP in 3rd instar larval M1 muscles in segment A3 of the indicated genotypes. **(B)** Quantification of combined MN1-Ib and MNIs synaptic bouton number following immunolabeling for HRP in 3rd instar larval M1 muscles in segment A3 of the indicated genotypes. Shaded boxes under each bar indicate the genotypes for each group, with control GAL4 driver lines alone (MN1-Ib, MNIs), control UAS transgenes alone (UAS-RPR, UAS-TeTXLC, UAS-NaChBac) and experimental crosses of MN1-Ib GAL4 (teal) or MNIs GAL4 (orange) to each transgene. Each data point represents quantification from segment A3 M1 from a single 3rd instar larvae. Statistical significance was determined using ANOVA. Data is shown as mean \pm SEM; * = $p < 0.05$, ** = $p < 0.01$, *** = $p < 0.001$.

Figure 9

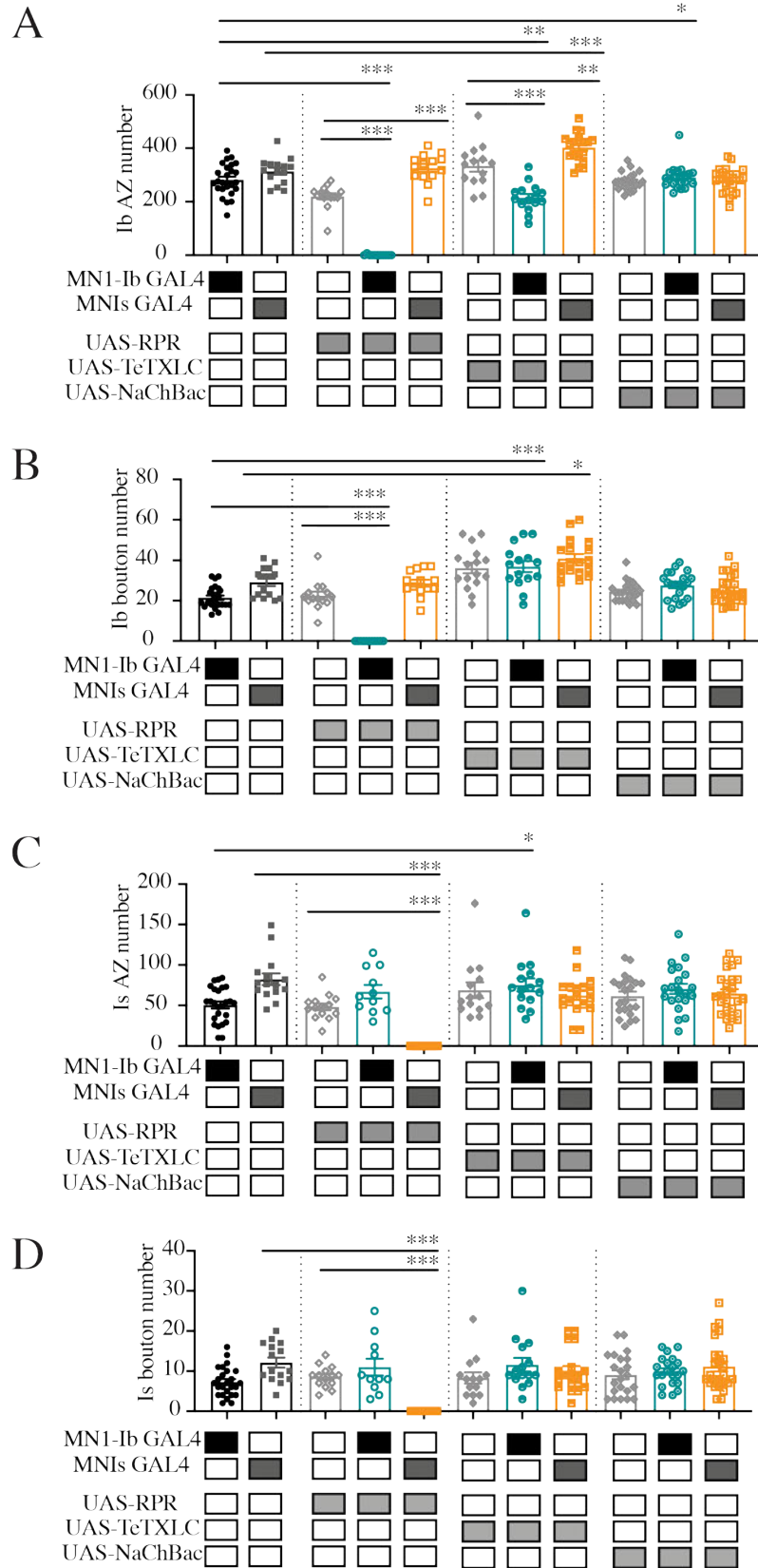


Figure 9. Quantification of MN1-Ib or MNIs AZ and bouton number follow ablation or activity changes. **(A)** Quantification of MN1-Ib AZ number following immunolabeling for BRP in 3rd instar larval M1 muscles in segment A3 of the indicated genotypes. **(B)** Quantification of combined MN1-Ib synaptic bouton number following immunolabeling for HRP in 3rd instar larval M1 muscles in segment A3 of the indicated genotypes. **(C)** Quantification of MNIs AZ number following immunolabeling for BRP in 3rd instar larval M1 muscles in segment A3 of the indicated genotypes. **(D)** Quantification of MNIs synaptic bouton number following immunolabeling for HRP in 3rd instar larval M1 muscles in segment A3 of the indicated genotypes. Shaded boxes under each bar indicate the genotypes for each group, with control GAL4 driver lines alone (MN1-Ib, MNIs), control UAS transgenes alone (UAS-RPR, UAS-TeTXLC, UAS-NaChBac) and experimental crosses of MN1-Ib GAL4 (teal) or MNIs GAL4 (orange) to each transgene. Each data point represents quantification from segment A3 M1 from a single 3rd instar larva. Statistical significance was determined using ANOVA. Data is shown as mean \pm SEM; * = $p < 0.05$, ** = $p < 0.01$, *** = $p < 0.001$.

Figure 10

A

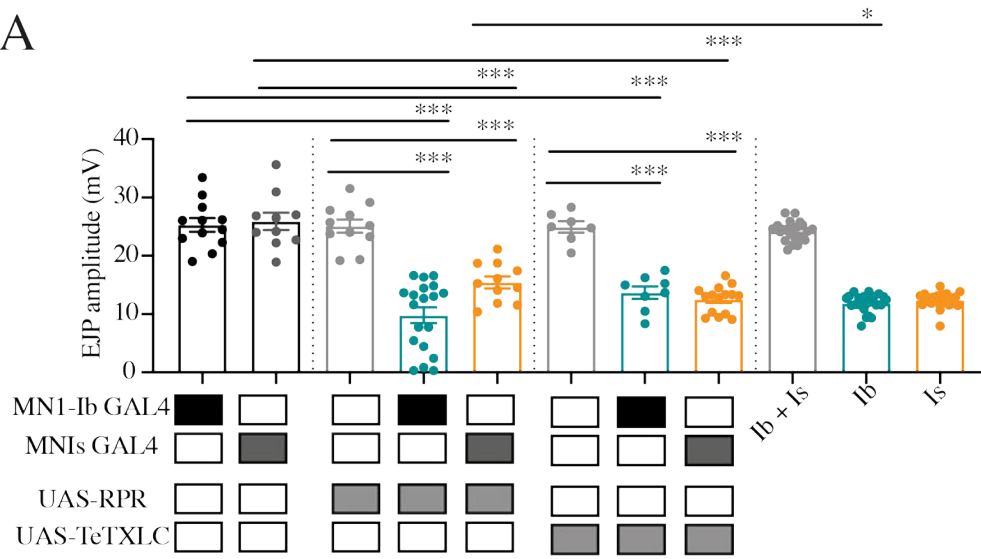


Figure 10. Electrophysiological analysis of synaptic function at M1 following ablation or silencing of MN1-Ib or MNIs. (A) EJP amplitudes recorded from 3rd instar larval M1 muscles in segment A3 of the indicated genotypes. Each data point is the average of at least 20 EJPs recorded from each larva. Shaded boxes under each bar indicate the genotypes for each group, with control GAL4 driver lines alone (MN1-Ib, MNIs), control UAS transgenes alone (UAS-RPR, UAS-TeTXLC) and experimental crosses of MN1-Ib GAL4 (teal) or MNIs GAL4 (orange) to each transgene. The final 3 bars on the right show results from dual intracellular recordings in controls using the minimal stimulation protocol where both MN1-Ib or MNIs motoneurons were active (Ib+Is), or MN1-Ib (Ib) or MNIs (Is) were independently isolated. Statistical significance was determined using ANOVA. Data is shown as mean \pm SEM; * = $p < 0.05$, *** = $p < 0.001$.

Figure 10- figure supplement 1

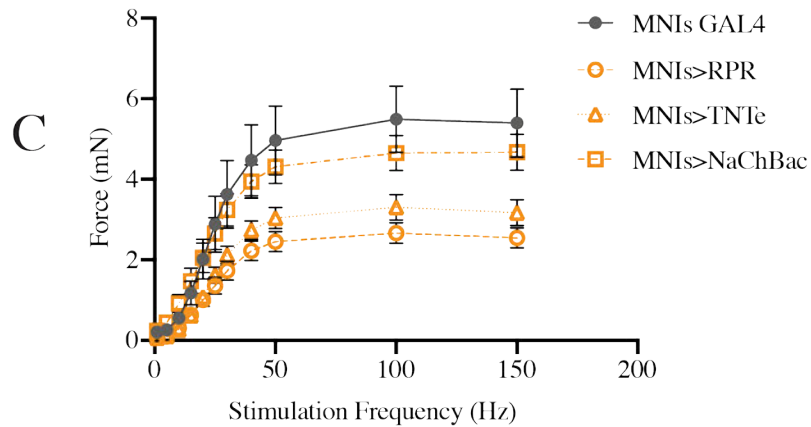
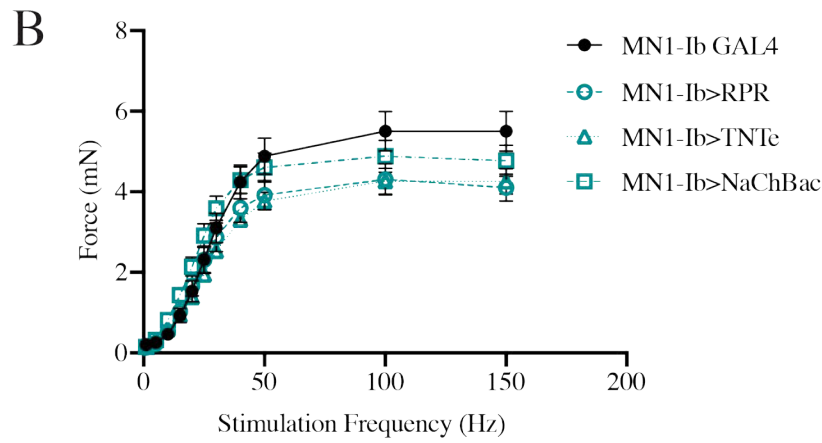
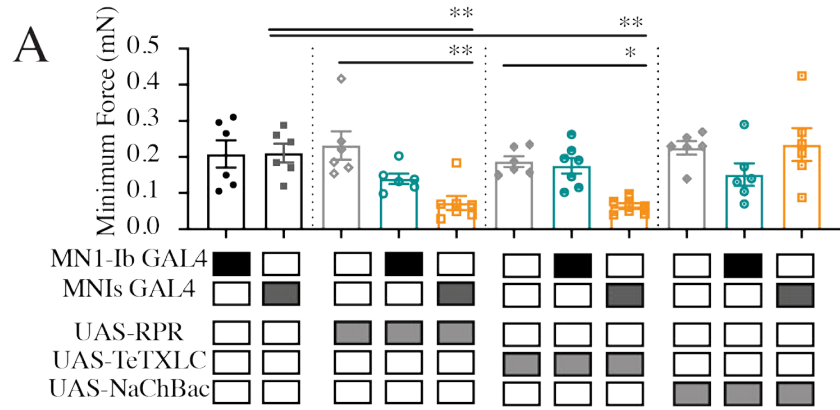


Figure 10 – figure supplement 1. Force recordings from muscles following ablation or activity changes of MN1-Ib or MNIs. **(A)** Maximal contraction force elicited by 150 Hz stimulation in 3rd instar larvae of the indicated genotypes. Six replicate contractions per genotype were generated at each stimulation frequency per recording. Shaded boxes under each bar indicate the genotypes for each group, with control GAL4 driver lines alone (MN1-Ib, MNIs), control UAS transgenes alone (UAS-RPR, UAS-TeTXLC, UAS-NaChBac) and experimental crosses of MN1-Ib GAL4 (teal) or MNIs GAL4 (orange) to each transgene. Statistical significance was determined using ANOVA. Data is shown as mean \pm SEM; * = $p < 0.05$, ** = $p < 0.01$. **(B)** Force-frequency curves for MN1-Ib GAL4 controls and the indicated experimental genotypes. Data points represent 6 replicate contractions elicited at each frequency from 6-7 3rd instar larvae. **(C)** Force-frequency curves for MN1-Is GAL4 controls and the indicated experimental genotypes. Data points represent 6 replicate contractions elicited at each frequency from 6-7 3rd instar larvae.

Figure 11

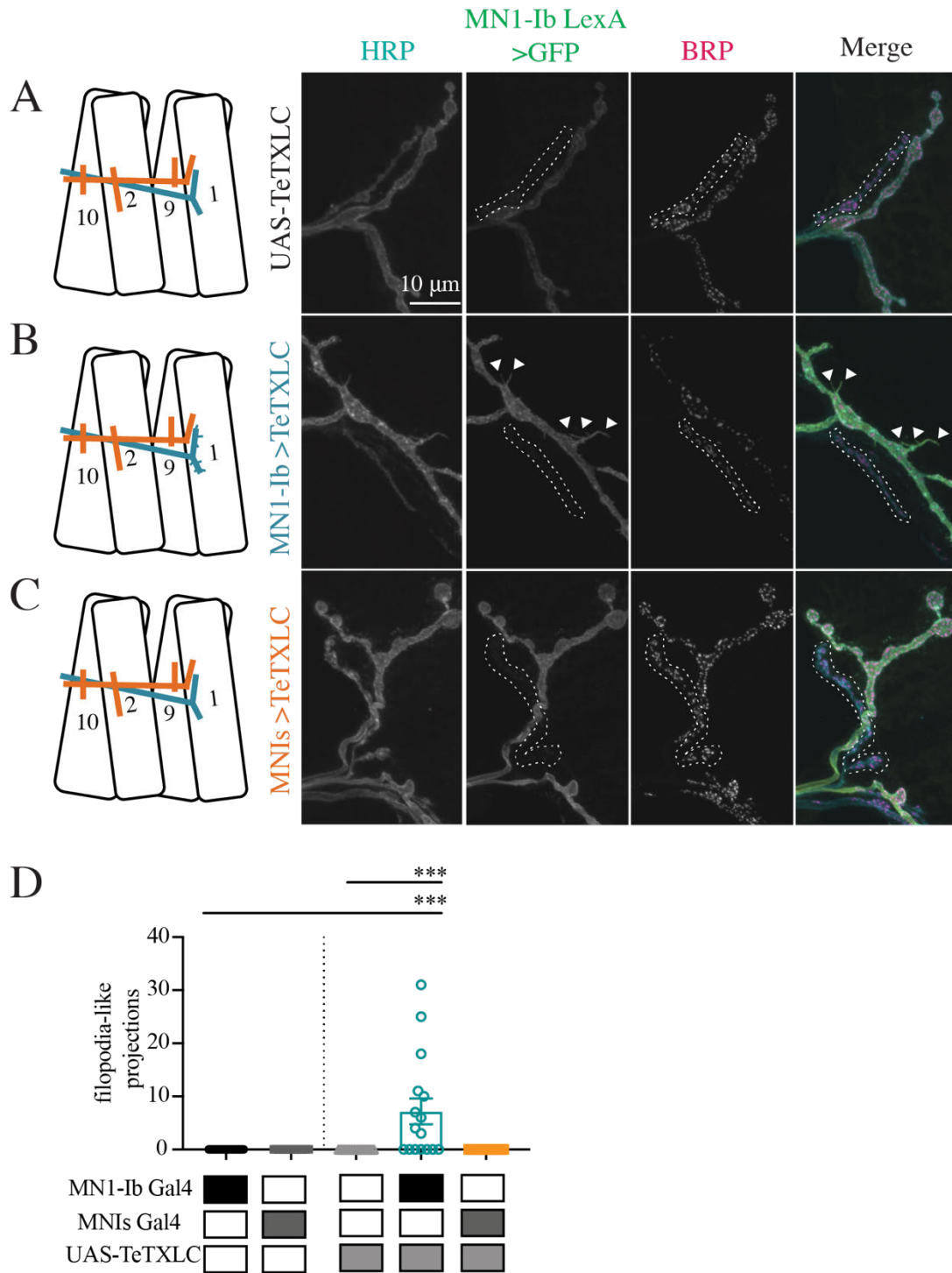


Figure 11. Morphological consequences of silencing of MN1-Ib or MNIs. Representative confocal images of 3rd instar larval M1 NMJs at segment A3 following immunolabeling with anti-HRP, anti-GFP and anti-BRP in the following genotypes: **(A)** UAS-TeTXLC control; **(B)** MN1-Ib GAL4>UAS-TeTXLC; **(C)** MNIs GAL4>UAS-TeTXLC. MN1-Ib LexA>LexAop2-CD8-GFP was present in each genetic background to allow unambiguous identification of the Ib terminal. Diagrams of the experimental manipulation is shown on the left, with MN1-Ib (teal) and MNIs (orange) labeled. The merged image is shown on the right. The white dashed line highlights the MNIs terminal in the final 3 panels for each manipulation. Arrowheads in **(B)** depict GFP-positive filopodial-like projections from MN1-Ib following tetanus toxin expression. Scale bar = 10 μ m for all panels. **(D)** Quantification of filopodial-like projections in controls and following UAS-TeTXLC expression with MN1-Ib or MNIs GAL4. Each data point represents quantification from segment A3 M1 from a single 3rd instar larvae. Statistical significance was determined using ANOVA. Data is shown as mean \pm SEM; *** = $p < 0.001$.

Figure 12

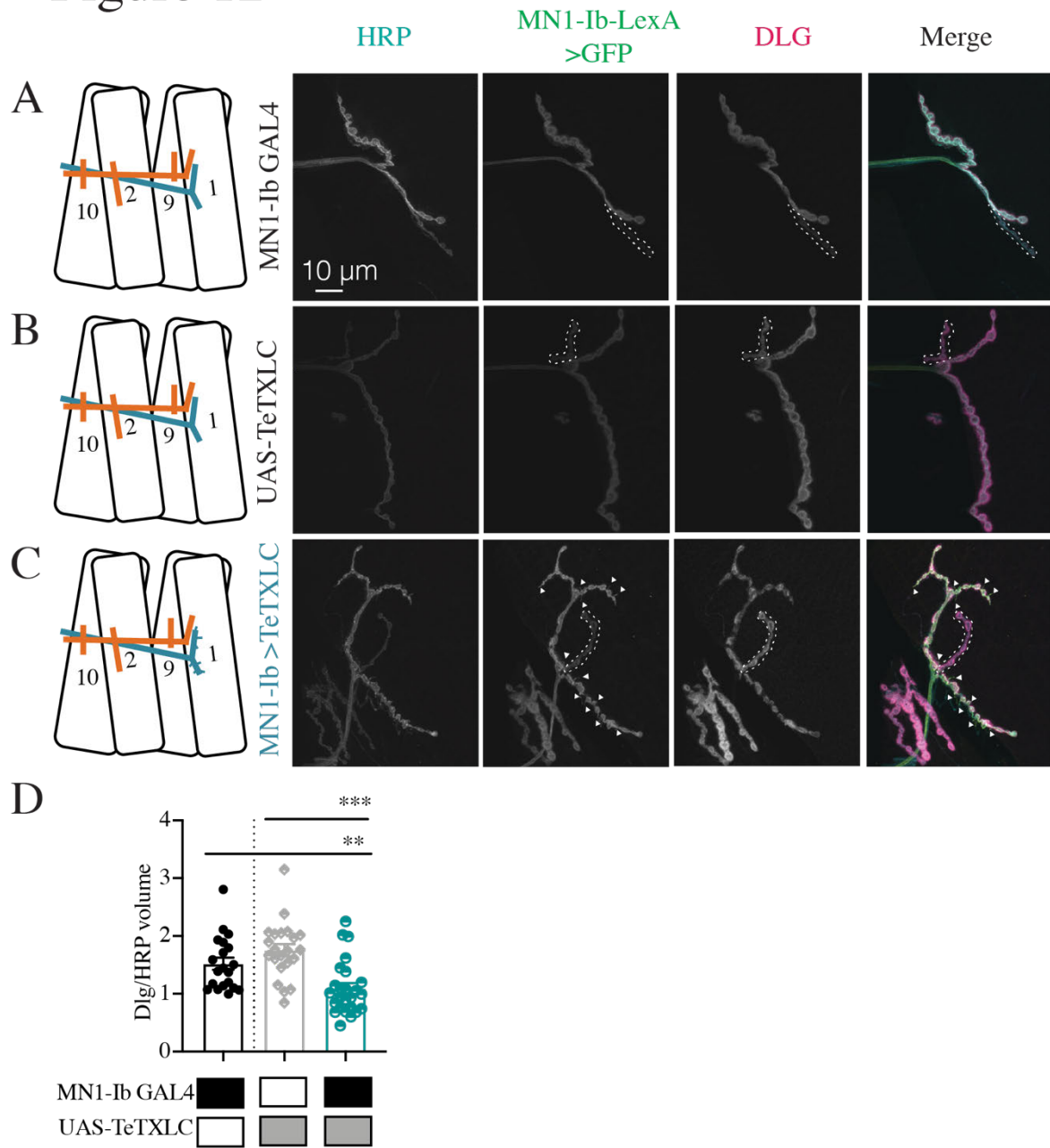


Figure 12. Reduced postsynaptic SSR volume following silencing of MN1-Ib. Representative confocal images of 3rd instar larval M1 NMJs at segment A3 following immunolabeling with anti-HRP, anti-GFP and anti-DLG in the following genotypes: (A) MN1-Ib GAL4 control; (B) UAS-TeTXLC control; (C) MN1-Ib GAL4>UAS-TeTXLC. MN1-Ib LexA>LexAop2-CD8-GFP was present in each genetic background to allow unambiguous identification of the Ib terminal. Diagrams of the experimental manipulation is shown on the left, with MN1-Ib (teal) and MNIs (orange) labeled. The merged image is shown on the right. The white dashed line highlights the MNIs terminal in the final 3 panels for each manipulation. Arrowheads in (C) depict GFP-positive filopodial-like projections from MN1-Ib following tetanus toxin expression. Scale bar = 10 μ m for all panels. (D) Quantification of DLG to HRP volume in MN1-Ib in controls and following UAS-TeTXLC expression with MN1-Ib GAL4. Each data point represents quantification from segment A3 M1 from a single 3rd instar larvae. Statistical significance was determined using ANOVA. Data is shown as mean \pm SEM; ** = $p < 0.01$, *** = $p < 0.001$.

Figure 13

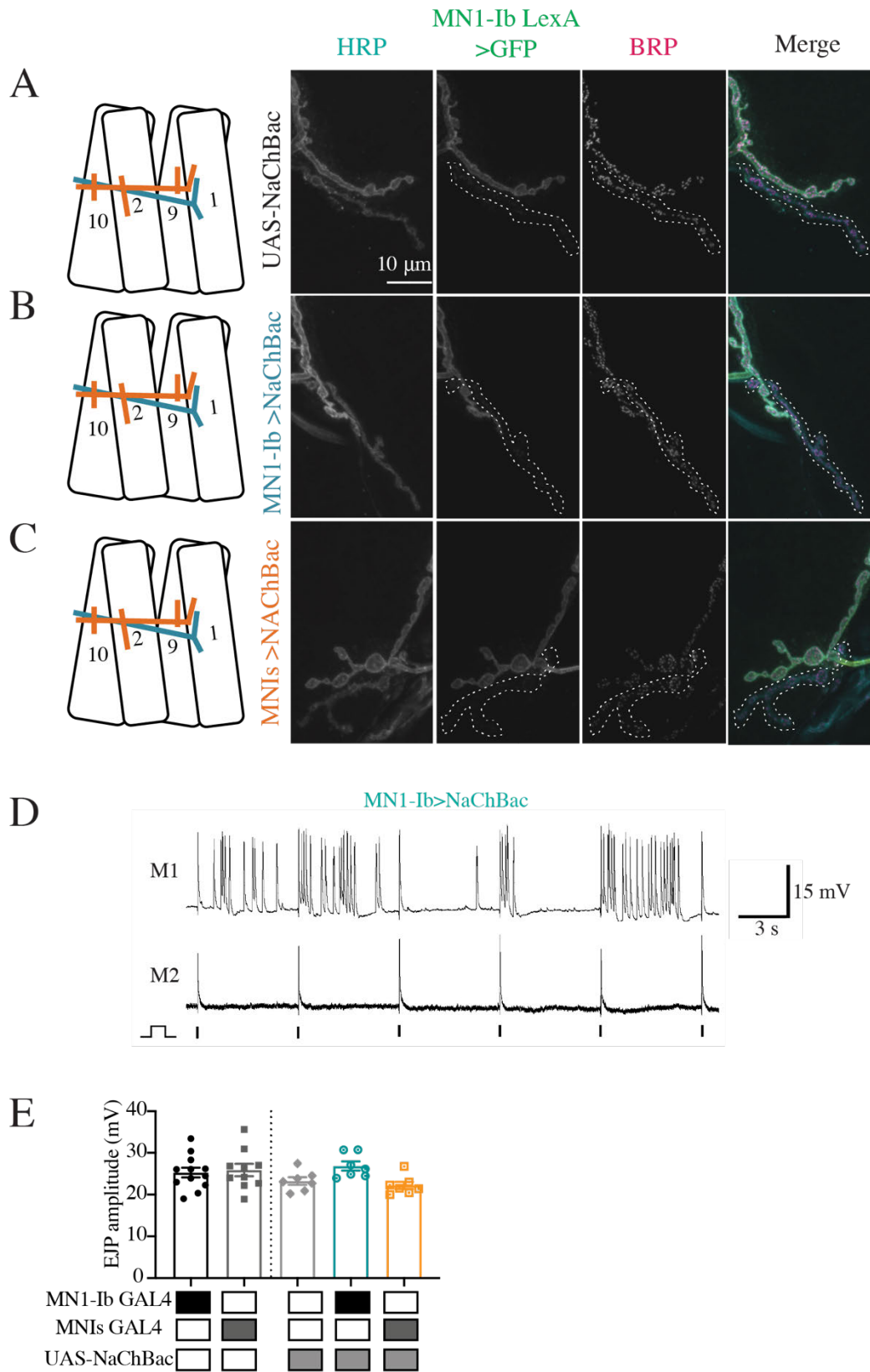
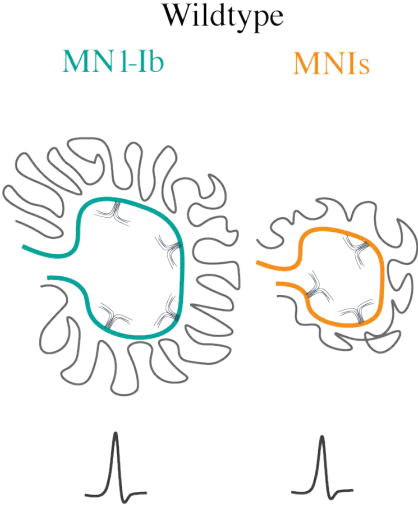


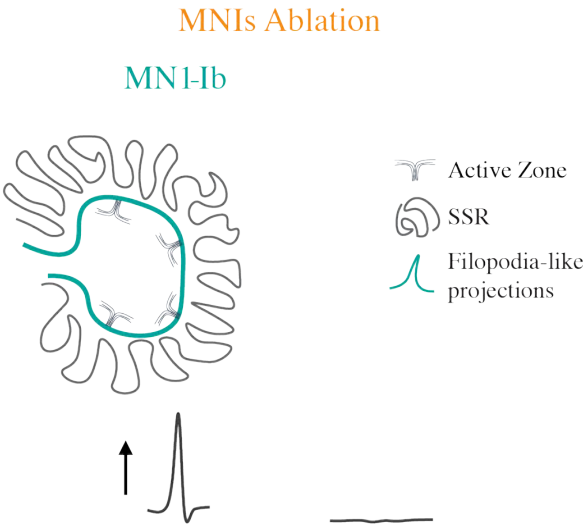
Figure 13. Chronic increases in MN1-Ib or MNIs activity do not impact NMJ morphology or synaptic release. Representative confocal images of 3rd instar larval M1 NMJs at segment A3 following immunolabeling with anti-HRP, anti-GFP and anti-BRP in the following genotypes: (A) UAS-NaChBac control; (B) MN1-Ib GAL4>UAS-NaChBac; (C) MNIs GAL4>UAS-NaChBac. MN1-Ib LexA>LexAop2-CD8-GFP was present in each genetic background to allow unambiguous identification of the Ib terminal. Diagrams of the experimental manipulation is shown on the left, with MN1-Ib (teal) and MNIs (orange) labeled. The merged image is shown on the right. The white dashed line highlights the MNIs terminal in the final 3 panels for each manipulation. Scale bar = 10 μ m for all panels. (D) Representative dual intracellular recordings from M1 and M2 in MN1-Ib>NaChBac 3rd instar larvae during 0.2 Hz stimulation. Note the train of EJPs following a single stimulus at M1 compared to M2. Vertical lines below the M2 recordings indicate timing of nerve stimulation. (E) EJP amplitudes recorded from 3rd instar larval M1 muscles in segment A3 of the indicated genotypes. Each data point is the average of at least 20 EJPs recorded from each larva. Statistical significance was determined using ANOVA. No statistical difference was found across genotypes. Data is shown as mean \pm SEM.

Figure 14

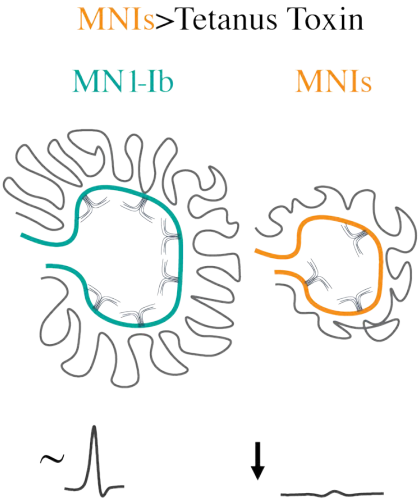
A



B



C



D

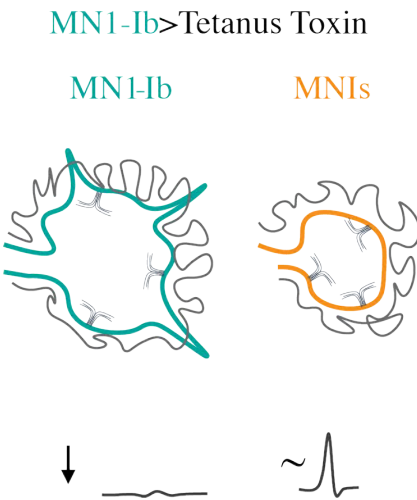


Figure 14. Summary of observed MN1-Ib plasticity. **(A)** In wildtype, MN1-Ib and MNIs provide similar drive to muscle M1. MN1-Ib forms more synaptic boutons and AZs onto M1 compared to MNIs. **(B)** Ablation of MNIs results in increased output from MN1-Ib as evidenced by larger EJPs, but does not trigger increases in bouton or AZ number. **(C)** Silencing of MNIs with tetanus toxin triggers increased bouton and AZ number in the co-innervating MN1-Ib. These changes do not increase presynaptic output from MN1-Ib, with EJP amplitude (~) at M1 unchanged compared to controls. No structural changes are observed in the silenced MNIs. **(D)** Silencing of MN1-Ib with tetanus toxin results in decreased bouton and AZ number at MN1-Ib terminals. Postsynaptic SSR development is also reduced. Presynaptic filopodia-like projections normally restricted to early 1st instar stage are observed at mature MN1-Ib silenced terminals. No structural or functional (~) changes occur in the co-innervating MNIs.

References

- Aberle, H., Haghghi, A.P., Fetter, R.D., McCabe, B.D., Magalhães, T.R., Goodman, C.S., 2002. wishful thinking encodes a BMP type II receptor that regulates synaptic growth in *Drosophila*. *Neuron* 33, 545–558.
- Akbergenova, Y., Cunningham, K.L., Zhang, Y.V., Weiss, S., Littleton, J.T., 2018. Characterization of developmental and molecular factors underlying release heterogeneity at *Drosophila* synapses. *Elife* 7. doi:10.7554/eLife.38268
- Alyagor, I., Berkun, V., Keren-Shaul, H., Marmor-Kollet, N., David, E., Mayseless, O., Issman-Zecharya, N., Amit, I., Schuldiner, O., 2018. Combining Developmental and Perturbation-Seq Uncovers Transcriptional Modules Orchestrating Neuronal Remodeling. *Dev. Cell* 47, 38–52.
- Ashley, J., Sorrentino, V., Lobb-Rabe, M., Nagarkar-Jaiswal, S., Tan, L., Xu, S., Xiao, Q., Zinn, K., Carrillo, R.A., 2019. Transsynaptic interactions between IgSF proteins DIP- α and Dpr10 are required for motor neuron targeting specificity. *Elife* 8. doi:10.7554/eLife.42690
- Ataman, B., Ashley, J., Gorczyca, D., Gorczyca, M., Mathew, D., Wichmann, C., Sigrist, S.J., Budnik, V., 2006. Nuclear trafficking of *Drosophila* Frizzled-2 during synapse development requires the PDZ protein dGRIP. *Proc. Natl. Acad. Sci. USA* 103, 7841–7846.
- Ataman, B., Ashley, J., Gorczyca, M., Ramachandran, P., Fouquet, W., Sigrist, S.J., Budnik, V., 2008. Rapid activity-dependent modifications in synaptic structure and function require bidirectional Wnt signaling. *Neuron* 57, 705–718.
- Atwood, H.L., Govind, C.K., Wu, C.F., 1993. Differential ultrastructure of synaptic terminals on ventral longitudinal abdominal muscles in *Drosophila* larvae. *J. Neurobiol.* 24, 1008–1024.
- Atwood, H.L., Karunanithi, S., 2002. Diversification of synaptic strength: presynaptic elements.

Nat. Rev. Neurosci. 3, 497–516.

Atwood, H.L., Wojtowicz, J.M., 1986. Short-term and long-term plasticity and physiological differentiation of crustacean motor synapses. *Int Rev Neurobiol* 28, 275–362.

Ball, R.W., Warren-Paquin, M., Tsurudome, K., Liao, E.H., Elazzouzi, F., Cavanagh, C., An, B.-S., Wang, T.-T., White, J.H., Haghghi, A.P., 2010. Retrograde BMP signaling controls synaptic growth at the NMJ by regulating trio expression in motor neurons. *Neuron* 66, 536–549.

Banerjee, S., Venkatesan, A., Bhat, M.A., 2017. Neurexin, Neuroligin and Wishful Thinking coordinate synaptic cytoarchitecture and growth at neuromuscular junctions. *Mol. Cell. Neurosci.* 78, 9–24.

Banovic, D., Khorramshahi, O., Oswald, D., Wichmann, C., Riedt, T., Fouquet, W., Tian, R., Sigrist, S.J., Aberle, H., 2010. *Drosophila* neuroligin 1 promotes growth and postsynaptic differentiation at glutamatergic neuromuscular junctions. *Neuron* 66, 724–738.

Berdnik, D., Chihara, T., Couto, A., Luo, L., 2006. Wiring stability of the adult *Drosophila* olfactory circuit after lesion. *J. Neurosci.* 26, 3367–3376. Bergquist, S., Dickman, D.K., Davis, G.W., 2010. A hierarchy of cell intrinsic and target-derived homeostatic signaling. *Neuron* 66, 220–234. Berke, B., Wittnam, J., McNeill, E., Van Vactor, D.L., Keshishian, H., 2013. Retrograde BMP signaling at the synapse: a permissive signal for synapse maturation and activity-dependent plasticity. *J. Neurosci.* 33, 17937–17950.

Bergquist, S., Dickman, D.K., Davis, G.W., 2010. A hierarchy of cell intrinsic and target-derived homeostatic signaling. *Neuron* 66, 220–234.

Berke, B., Wittnam, J., McNeill, E., Van Vactor, D.L., Keshishian, H., 2013. Retrograde BMP signaling at the synapse: a permissive signal for synapse maturation and activity-dependent plasticity. *J. Neurosci.* 33, 17937–17950.

Böhme, M.A., McCarthy, A.W., Grasskamp, A.T., Beuschel, C.B., Goel, P., Jusyte, M., Laber, D., Huang, S., Rey, U., Petzoldt, A.G., Lehmann, M., Göttfert, F., Haghghi, P., Hell, S.W., Oswald, D., Dickman, D., Sigrist, S.J., Walter, A.M., 2019. Rapid active zone remodeling consolidates presynaptic potentiation. *Nat. Commun.* 10, 1085.

Bossing, T., Udolph, G., Doe, C.Q., Technau, G.M., 1996. The embryonic central nervous system lineages of *Drosophila melanogaster*. I. Neuroblast lineages derived from the ventral half of the neuroectoderm. *Dev. Biol.* 179, 41–64.

Broadie, K.S., Bate, M., 1993. Development of the embryonic neuromuscular synapse of *Drosophila melanogaster*. *J. Neurosci.* 13, 144–166.

Carrillo, R.A., Olsen, D.P., Yoon, K.S., Keshishian, H., 2010. Presynaptic activity and CaMKII modulate retrograde semaphorin signaling and synaptic refinement. *Neuron* 68, 32–44.

Carrillo, R.A., Özkan, E., Menon, K.P., Nagarkar-Jaiswal, S., Lee, P.-T., Jeon, M., Birnbaum, M.E., Bellen, H.J., Garcia, K.C., Zinn, K., 2015. Control of synaptic connectivity by a network of *drosophila* IgSF cell surface proteins. *Cell* 163, 1770–1782.

Cash, S., Chiba, A., Keshishian, H., 1992. Alternate neuromuscular target selection following the loss of single muscle fibers in *Drosophila*. *J. Neurosci.* 12, 2051–2064.

Chang, T.N., Keshishian, H., 1996. Laser ablation of *Drosophila* embryonic motoneurons causes ectopic innervation of target muscle fibers. *J. Neurosci.* 16, 5715–5726.

Cho, R.W., Buhl, L.K., Volfson, D., Tran, A., Li, F., Akbergenova, Y., Littleton, J.T., 2015. Phosphorylation of Complexin by PKA Regulates Activity-Dependent Spontaneous Neurotransmitter Release and Structural Synaptic Plasticity. *Neuron* 88, 749–761.

Clark, M.Q., Zarin, A.A., Carreira-Rosario, A., Doe, C.Q., 2018. Neural circuits driving larval locomotion in *Drosophila*. *Neural Dev.* 13, 6.

Cognigni, P., Felsenberg, J., Waddell, S., 2018. Do the right thing: neural network mechanisms of memory formation, expression and update in *Drosophila*. *Curr. Opin. Neurobiol.* 49, 51–58.

Collins, C.A., DiAntonio, A., 2007. Synaptic development: insights from *Drosophila*. *Curr. Opin. Neurobiol.* 17, 35–42.

Collins, C.A., Wairkar, Y.P., Johnson, S.L., DiAntonio, A., 2006. Highwire restrains synaptic growth by attenuating a MAP kinase signal. *Neuron* 51, 57–69.

Colman, H., Nabekura, J., Lichtman, J.W., 1997. Alterations in synaptic strength preceding axon withdrawal. *Science* 275, 356–361.

Cunningham, K.L., Littleton, J.T., 2019a. Neurons regulate synaptic strength through homeostatic scaling of active zones. *J. Cell Biol.* 218, 1434–1435.

Cunningham, K.L., Littleton, J.T., 2019b. Synaptic plasticity: close encounters of the tonic and phasic kind. *Curr. Biol.* 29, R1196–R1198.

Davis, G.W., 2006. Homeostatic control of neural activity: from phenomenology to molecular design. *Annu. Rev. Neurosci.* 29, 307–323.

Davis, G.W., 2013. Homeostatic signaling and the stabilization of neural function. *Neuron* 80, 718–728.

Davis, G.W., DiAntonio, A., Petersen, S.A., Goodman, C.S., 1998. Postsynaptic PKA controls quantal size and reveals a retrograde signal that regulates presynaptic transmitter release in *Drosophila*. *Neuron* 20, 305–315.

Davis, G.W., Müller, M., 2015. Homeostatic control of presynaptic neurotransmitter release. *Annu. Rev. Physiol.* 77, 251–270. doi:10.1146/annurev-physiol-021014-071740

Destexhe, A., Marder, E., 2004. Plasticity in single neuron and circuit computations. *Nature* 431, 789–795.

DiAntonio, A., Hicke, L., 2004. Ubiquitin-dependent regulation of the synapse. *Annu. Rev. Neurosci.* 27, 223–246.

Doll, C.A., Broadie, K., 2014. Impaired activity-dependent neural circuit assembly and refinement in autism spectrum disorder genetic models. *Front. Cell Neurosci.* 8, 30.

Featherstone, D.E., Rushton, E., Rohrbough, J., Liebl, F., Karr, J., Sheng, Q., Rodesch, C.K., Broadie, K., 2005. An essential *Drosophila* glutamate receptor subunit that functions in both central neuropil and neuromuscular junction. *J. Neurosci.* 25, 3199–3208.

Foeller, E., Feldman, D.E., 2004. Synaptic basis for developmental plasticity in somatosensory cortex. *Curr. Opin. Neurobiol.* 14, 89–95

Fouquet, W., Oswald, D., Wichmann, C., Mertel, S., Depner, H., Dyba, M., Hallermann, S., Kittel, R.J., Eimer, S., Sigrist, S.J., 2009. Maturation of active zone assembly by *Drosophila* Bruchpilot. *J. Cell Biol.* 186, 129–145.

Frank, C.A., 2014. Homeostatic plasticity at the *Drosophila* neuromuscular junction. *Neuropharmacology* 78, 63–74.

Frank, C.A., James, T.D., Müller, M., 2020. Homeostatic control of *Drosophila* neuromuscular junction function. *Synapse* 74, e22133.

Frank, C.A., Kennedy, M.J., Goold, C.P., Marek, K.W., Davis, G.W., 2006. Mechanisms underlying the rapid induction and sustained expression of synaptic homeostasis. *Neuron* 52, 663–677.

Gaviño, M.A., Ford, K.J., Archila, S., Davis, G.W., 2015. Homeostatic synaptic depression is achieved through a regulated decrease in presynaptic calcium channel abundance. *Elife* 4. doi:10.7554/eLife.05473

Genç, Ö., Davis, G.W., 2019. Target-wide Induction and Synapse Type-Specific Robustness of

Presynaptic Homeostasis. *Curr. Biol.* 29, 3863–3873.

Ghelani, T., Sigrist, S.J., 2018. Coupling the structural and functional assembly of synaptic release sites. *Front. Neuroanat.* 12, 81.

Giurfa, M., 2013. Cognition with few neurons: higher-order learning in insects. *Trends Neurosci.* 36, 285–294.

Goel, P., Dufour Bergeron, D., Böhme, M.A., Nunnally, L., Lehmann, M., Buser, C., Walter, A.M., Sigrist, S.J., Dickman, D., 2019. Homeostatic scaling of active zone scaffolds maintains global synaptic strength. *J. Cell Biol.* 218, 1706–1724.

Golovin, R.M., Vest, J., Vita, D.J., Broadie, K., 2019. Activity-Dependent Remodeling of *Drosophila* Olfactory Sensory Neuron Brain Innervation during an Early-Life Critical Period. *J. Neurosci.* 39, 2995–3012.

Gorczyca, M., Augart, C., Budnik, V., 1993. Insulin-like receptor and insulin-like peptide are localized at neuromuscular junctions in *Drosophila*. *J. Neurosci.* 13, 3692–3704.

Govind, C.K., Walrond, J.P., 1989. Structural plasticity at crustacean neuromuscular synapses. *J. Neurobiol.* 20, 409–421.

Goyal, L., McCall, K., Agapite, J., Hartweg, E., Steller, H., 2000. Induction of apoptosis by *Drosophila* reaper, hid and grim through inhibition of IAP function. *EMBO J.* 19, 589–597.

Gratz, S.J., Goel, P., Bruckner, J.J., Hernandez, R.X., Khateeb, K., Macleod, G.T., Dickman, D., O'Connor-Giles, K.M., 2019. Endogenous Tagging Reveals Differential Regulation of Ca²⁺ Channels at Single Active Zones during Presynaptic Homeostatic Potentiation and Depression. *J. Neurosci.* 39, 2416–2429.

Guan, Z., Saraswati, S., Adolfsen, B., Littleton, J.T., 2005. Genome-wide transcriptional changes associated with enhanced activity in the *Drosophila* nervous system. *Neuron* 48, 91–107.

Halpern, M.E., Chiba, A., Johansen, J., Keshishian, H., 1991. Growth cone behavior underlying the development of stereotypic synaptic connections in *Drosophila* embryos. *J. Neurosci.* 11, 3227–3238.

Harris, K.P., Littleton, J.T., 2015. Transmission, development, and plasticity of synapses. *Genetics* 201, 345–375.

Harris, K.P., Zhang, Y.V., Piccioli, Z.D., Perrimon, N., Littleton, J.T., 2016. The postsynaptic t-SNARE Syntaxin 4 controls traffic of Neuroligin 1 and Synaptotagmin 4 to regulate retrograde signaling. *Elife* 5. doi:10.7554/eLife.13881

Harris, R.M., Pfeiffer, B.D., Rubin, G.M., Truman, J.W., 2015. Neuron hemilineages provide the functional ground plan for the *Drosophila* ventral nervous system. *Elife* 4. doi:10.7554/eLife.04493

Hartenstein, V., Campos-Ortega, J.A., 1984. Early neurogenesis in wild-type *Drosophila melanogaster*. *Wilhelm Roux' Archiv.* 193, 308–325.

Hashimoto, K., Kano, M., 2013. Synapse elimination in the developing cerebellum. *Cell Mol. Life Sci.* 70, 4667–4680.

Hoang, B., Chiba, A., 2001. Single-cell analysis of *Drosophila* larval neuromuscular synapses. *Dev. Biol.* 229, 55–70.

Holtmaat, A., Svoboda, K., 2009. Experience-dependent structural synaptic plasticity in the mammalian brain. *Nat. Rev. Neurosci.* 10, 647–658.

Hong, S.J., Lnenicka, G.A., 1993. Long-term changes in the neuromuscular synapses of a crayfish motoneuron produced by calcium influx. *Brain Res.* 605, 121–127.

Hourcade, B., Muenz, T.S., Sandoz, J.-C., Rössler, W., Devaud, J.-M., 2010. Long-term memory leads to synaptic reorganization in the mushroom bodies: a memory trace in the insect brain? *J.*

Neurosci. 30, 6461--6465.

Jacobs, J.R., Goodman, C.S., 1989. Embryonic development of axon pathways in the *Drosophila* CNS. II. Behavior of pioneer growth cones. *J. Neurosci.* 9, 2412–2422.

Jan, L.Y., Jan, Y.N., 1976. Properties of the larval neuromuscular junction in *Drosophila melanogaster*. *J. Physiol. (Lond.)* 262, 189–214.

Jarecki, J., Keshishian, H., 1995. Role of neural activity during synaptogenesis in *Drosophila*. *J. Neurosci.* 15, 8177–8190.

Jenett, A., Rubin, G.M., Ngo, T.-T.B., Shepherd, D., Murphy, C., Dionne, H., Pfeiffer, B.D., Cavallaro, A., Hall, D., Jeter, J., Iyer, N., Fetter, D., Hausenfluck, J.H., Peng, H., Trautman, E.T., Svirskas, R.R., Myers, E.W., Iwinski, Z.R., Aso, Y., DePasquale, G.M., Enos, A., Hulamm, P., Lam, S.C.B., Li, H.-H., Lavery, T.R., Long, F., Qu, L., Murphy, S.D., Rokicki, K., Safford, T., Shaw, K., Simpson, J.H., Sowell, A., Tae, S., Yu, Y., Zugates, C.T., 2012. A GAL4-driver line resource for *Drosophila* neurobiology. *Cell Rep.* 2, 991–1001.

Johansen, J., Halpern, M.E., Johansen, K.M., Keshishian, H., 1989a. Stereotypic morphology of glutamatergic synapses on identified muscle cells of *Drosophila* larvae. *J. Neurosci.* 9, 710–725.

Johansen, J., Halpern, M.E., Keshishian, H., 1989b. Axonal guidance and the development of muscle fiber-specific innervation in *Drosophila* embryos. *J. Neurosci.* 9, 4318–4332.

Johnson, E.L., Fetter, R.D., Davis, G.W., 2009. Negative regulation of active zone assembly by a newly identified SR protein kinase. *PLoS Biol.* 7, e1000193. doi:10.1371/journal.pbio.1000193

Karunanithi, S., Cylinder, D., Ertekin, D., Zalucki, O.H., Marin, L., Lavidis, N.A., Atwood, H.L., van Swinderen, B., 2020. Proportional downscaling of glutamatergic release sites by the general anesthetic propofol at *Drosophila* motor nerve terminals. *Eneuro*. doi:10.1523/ENEURO.0422-19.2020

Katz, L.C., Shatz, C.J., 1996. Synaptic activity and the construction of cortical circuits. *Science* 274, 1133–1138.

Keshishian, H., Chang, T.N., Jarecki, J., 1994. Precision and plasticity during *Drosophila* neuromuscular development. *FASEB J.* 8, 731–737.

Kiragasi, B., Wondolowski, J., Li, Y., Dickman, D.K., 2017. A presynaptic glutamate receptor subunit confers robustness to neurotransmission and homeostatic potentiation. *Cell Rep.* 19, 2694–2706.

Kohsaka, H., Nose, A., 2009. Target recognition at the tips of postsynaptic filopodia: accumulation and function of Capricious. *Development* 136, 1127–1135.

Korkut, C., Li, Y., Koles, K., Brewer, C., Ashley, J., Yoshihara, M., Budnik, V., 2013. Regulation of postsynaptic retrograde signaling by presynaptic exosome release. *Neuron* 77, 1039–1046.

Kose, H., Rose, D., Zhu, X., Chiba, A., 1997. Homophilic synaptic target recognition mediated by immunoglobulin-like cell adhesion molecule Fasciclin III. *Development* 124, 4143–4152.

Kurdyak, P., Atwood, H.L., Stewart, B.A., Wu, C.F., 1994. Differential physiology and morphology of motor axons to ventral longitudinal muscles in larval *Drosophila*. *J. Comp. Neurol.* 350, 463–472.

Lahey, T., Gorczyca, M., Jia, X.X., Budnik, V., 1994. The *Drosophila* tumor suppressor gene *dlg* is required for normal synaptic bouton structure. *Neuron* 13, 823–835.

Lamprecht, R., LeDoux, J., 2004. Structural plasticity and memory. *Nat. Rev. Neurosci.* 5, 45–54.

Landgraf, M., Bossing, T., Technau, G.M., Bate, M., 1997. The origin, location, and projections of the embryonic abdominal motoneurons of *Drosophila*. *J. Neurosci.* 17, 9642–9655.

Lee, T., 2017. Wiring the *Drosophila* Brain with Individually Tailored Neural Lineages. *Curr. Biol.* 27, R77–R82.

Lee, T., Luo, L., 1999. Mosaic analysis with a repressible cell marker for studies of gene function in neuronal morphogenesis. *Neuron* 22, 451–461.

Li, J., Ashley, J., Budnik, V., Bhat, M.A., 2007. Crucial role of *Drosophila* neurexin in proper active zone apposition to postsynaptic densities, synaptic growth, and synaptic transmission. *Neuron* 55, 741–755.

Li, X., Goel, P., Chen, C., Angajala, V., Chen, X., Dickman, D.K., 2018. Synapse-specific and compartmentalized expression of presynaptic homeostatic potentiation. *Elife* 7. doi:10.7554/eLife.34338

Lin, D.M., Auld, V.J., Goodman, C.S., 1995. Targeted neuronal cell ablation in the *Drosophila* embryo: pathfinding by follower growth cones in the absence of pioneers. *Neuron* 14, 707–715.

Lin, D.M., Goodman, C.S., 1994. Ectopic and increased expression of Fasciclin II alters motoneuron growth cone guidance. *Neuron* 13, 507–523.

Lnenicka, G.A., Atwood, H.L., 1989. Impulse activity of a crayfish motoneuron regulated its neuromuscular synaptic properties. *J. Neurophysiol.* 61, 91–96.

Lnenicka, G.A., Atwood, H.L., Marin, L., 1986. Morphological transformation of synaptic terminals of a phasic motoneuron by long-term tonic stimulation. *J. Neurosci.* 6, 2252–2258.

Lnenicka, G.A., Hong, S.J., Combatti, M., LePage, S., 1991. Activity-dependent development of synaptic varicosities at crayfish motor terminals. *J. Neurosci.* 11, 1040–1048.

Lnenicka, G.A., Keshishian, H., 2000. Identified motor terminals in *Drosophila* larvae show distinct differences in morphology and physiology. *J. Neurobiol.* 43, 186–197.

Lnenicka, G.A., Spencer, G.M., Keshishian, H., 2003. Effect of reduced impulse activity on the development of identified motor terminals in *Drosophila* larvae. *J. Neurobiol.* 54, 337–345.

Lu, Zhongmin, Chouhan, A.K., Borycz, J.A., Lu, Zhiyuan, Rossano, A.J., Brain, K.L., Zhou, Y.,

Meinertzhagen, I.A., Macleod, G.T., 2016. High-Probability Neurotransmitter Release Sites Represent an Energy-Efficient Design. *Curr. Biol.* 26, 2562–2571.

Luo, L., O’Leary, D.D.M., 2005. Axon retraction and degeneration in development and disease. *Annu. Rev. Neurosci.* 28, 127–156.

Manning, L., Heckscher, E.S., Purice, M.D., Roberts, J., Bennett, A.L., Kroll, J.R., Pollard, J.L., Strader, M.E., Lupton, J.R., Dyukareva, A.V., Doan, P.N., Bauer, D.M., Wilbur, A.N., Tanner, S., Kelly, J.J., Lai, S.-L., Tran, K.D., Kohwi, M., Lavery, T.R., Pearson, J.C., Crews, S.T., Rubin, G.M., Doe, C.Q., 2012. A resource for manipulating gene expression and analyzing cis-regulatory modules in the *Drosophila* CNS. *Cell Rep.* 2, 1002–1013.

Marder, E., Calabrese, R.L., 1996. Principles of rhythmic motor pattern generation. *Physiol. Rev.* 76, 687–717.

Marder, E., Rehm, K.J., 2005. Development of central pattern generating circuits. *Curr. Opin. Neurobiol.* 15, 86–93.

Marin, E.C., Watts, R.J., Tanaka, N.K., Ito, K., Luo, L., 2005. Developmentally programmed remodeling of the *Drosophila* olfactory circuit. *Development* 132, 725–737.

Marqués, G., Bao, H., Haerry, T.E., Shimell, M.J., Duchek, P., Zhang, B., O’Connor, M.B., 2002. The *Drosophila* BMP type II receptor *Wishful Thinking* regulates neuromuscular synapse morphology and function. *Neuron* 33, 529–543.

Marrus, S.B., Portman, S.L., Allen, M.J., Moffat, K.G., Diantonio, A., 2004. Differential localization of glutamate receptor subunits at the *Drosophila* neuromuscular junction. *J. Neurosci.* 24, 1406–1415.

Matz, J., Gilyan, A., Kolar, A., McCarvill, T., Krueger, S.R., 2010. Rapid structural alterations of the active zone lead to sustained changes in neurotransmitter release. *Proc. Natl. Acad. Sci. USA*

107, 8836–8841.

Mayford, M., Siegelbaum, S.A., Kandel, E.R., 2012. Synapses and memory storage. *Cold Spring Harb. Perspect. Biol.* 4. doi:10.1101/cshperspect.a005751

Mayseless, O., Berns, D.S., Yu, X.M., Riemensperger, T., Fiala, A., Schuldiner, O., 2018. Developmental Coordination during Olfactory Circuit Remodeling in *Drosophila*. *Neuron* 99, 1204–1215.e5.

McCabe, B.D., Marqués, G., Haghighi, A.P., Fetter, R.D., Crotty, M.L., Haerry, T.E., Goodman, C.S., O'Connor, M.B., 2003. The BMP homolog *Gbb* provides a retrograde signal that regulates synaptic growth at the *Drosophila* neuromuscular junction. *Neuron* 39, 241–254.

Melom, J.E., Akbergenova, Y., Gavornik, J.P., Littleton, J.T., 2013. Spontaneous and evoked release are independently regulated at individual active zones. *J. Neurosci.* 33, 17253–17263.

Melom, J.E., Littleton, J.T., 2011. Synapse development in health and disease. *Curr. Opin. Genet. Dev.* 21, 256–261.

Meng, J.L., Marshall, Z.D., Lobb-Rabe, M., Heckscher, E.S., 2019. How prolonged expression of *Hunchback*, a temporal transcription factor, re-wires locomotor circuits. *Elife* 8. doi:10.7554/eLife.46089

Millar, A.G., Atwood, H.L., 2004. Crustacean phasic and tonic motor neurons. *Integr. Comp. Biol.* 44, 4–13.

Miller, D.L., Ballard, S.L., Ganetzky, B., 2012. Analysis of synaptic growth and function in *Drosophila* with an extended larval stage. *J. Neurosci.* 32, 13776–13786.

Mosca, T.J., Carrillo, R.A., White, B.H., Keshishian, H., 2005. Dissection of synaptic excitability phenotypes by using a dominant-negative *Shaker* K⁺ channel subunit. *Proc. Natl. Acad. Sci. USA* 102, 3477–3482.

Mosca, T.J., Hong, W., Dani, V.S., Favaloro, V., Luo, L., 2012. Trans-synaptic Teneurin signalling in neuromuscular synapse organization and target choice. *Nature* 484, 237–241.

Muhammad, K., Reddy-Alla, S., Driller, J.H., Schreiner, D., Rey, U., Böhme, M.A., Hollmann, C., Ramesh, N., Depner, H., Lützkendorf, J., Matkovic, T., Götz, T., Bergeron, D.D., Schmoranzler, J., Goettfert, F., Holt, M., Wahl, M.C., Hell, S.W., Scheiffele, P., Walter, A.M., Loll, B., Sigrist, S.J., 2015. Presynaptic spinophilin tunes neurexin signalling to control active zone architecture and function. *Nat. Commun.* 6, 8362.

Müller, M., Davis, G.W., 2012. Transsynaptic control of presynaptic Ca²⁺ influx achieves homeostatic potentiation of neurotransmitter release. *Curr. Biol.* 22, 1102–1108.

Müller, M., Liu, K.S.Y., Sigrist, S.J., Davis, G.W., 2012. RIM controls homeostatic plasticity through modulation of the readily-releasable vesicle pool. *J. Neurosci.* 32, 16574–16585.

Müller, M., Pym, E.C.G., Tong, A., Davis, G.W., 2011. Rab3-GAP controls the progression of synaptic homeostasis at a late stage of vesicle release. *Neuron* 69, 749–762.

Nahmani, M., Turrigiano, G.G., 2014. Adult cortical plasticity following injury: Recapitulation of critical period mechanisms? *Neuroscience* 283, 4–16.

Newman, Z.L., Hoagland, A., Aghi, K., Worden, K., Levy, S.L., Son, J.H., Lee, L.P., Isacoff, E.Y., 2017. Input-Specific Plasticity and Homeostasis at the *Drosophila* Larval Neuromuscular Junction. *Neuron* 93, 1388–1404.e10.

Nitabach, M.N., Wu, Y., Sheeba, V., Lemon, W.C., Strumbos, J., Zelensky, P.K., White, B.H., Holmes, T.C., 2006. Electrical hyperexcitation of lateral ventral pacemaker neurons desynchronizes downstream circadian oscillators in the fly circadian circuit and induces multiple behavioral periods. *J. Neurosci.* 26, 479–489.

Ormerod, K.G., LePine, O.K., Bhutta, M.S., Jung, J., Tattersall, G.J., Mercier, A.J., 2016.

Characterizing the physiological and behavioral roles of proctolin in *Drosophila melanogaster*. *J. Neurophysiol.* 115, 568–580.

Ortega, J.M., Genç, Ö., Davis, G.W., 2018. Molecular mechanisms that stabilize short term synaptic plasticity during presynaptic homeostatic plasticity. *Elife* 7. doi:10.7554/eLife.40385

Owald, D., Khorramshahi, O., Gupta, V.K., Banovic, D., Depner, H., Fouquet, W., Wichmann, C., Mertel, S., Eimer, S., Reynolds, E., Holt, M., Aberle, H., Sigrist, S.J., 2012. Cooperation of Syd-1 with Neurexin synchronizes pre- with postsynaptic assembly. *Nat. Neurosci.* 15, 1219–1226.

Özel, M.N., Kulkarni, A., Hasan, A., Brummer, J., Moldenhauer, M., Daumann, I.-M., Wolfenberg, H., Dercksen, V.J., Kiral, F.R., Weiser, M., Prohaska, S., von Kleist, M., Hiesinger, P.R., 2019. Serial Synapse Formation through Filopodial Competition for Synaptic Seeding Factors. *Dev. Cell* 50, 447–461.

Pauls, D., von Essen, A., Lyutova, R., van Giesen, L., Rosner, R., Wegener, C., Sprecher, S.G., 2015. Potency of transgenic effectors for neurogenetic manipulation in *Drosophila* larvae. *Genetics* 199, 25–37.

Peled, E.S., Isacoff, E.Y., 2011. Optical quantal analysis of synaptic transmission in wild-type and *rab3*-mutant *Drosophila* motor axons. *Nat. Neurosci.* 14, 519–526.

Pérez-Moreno, J.J., O’Kane, C.J., 2019. GAL4 drivers specific for type *ib* and type *is* motor neurons in *drosophila*. *G3 (Bethesda)* 9, 453–462.

Petersen, S.A., Fetter, R.D., Noordermeer, J.N., Goodman, C.S., DiAntonio, A., 1997. Genetic analysis of glutamate receptors in *Drosophila* reveals a retrograde signal regulating presynaptic transmitter release. *Neuron* 19, 1237–1248.

Petzoldt, A.G., Lee, Y.-H., Khorramshahi, O., Reynolds, E., Plested, A.J.R., Herzog, H., Sigrist, S.J., 2014. Gating characteristics control glutamate receptor distribution and trafficking in vivo.

Curr. Biol. 24, 2059–2065.

Piccioli, Z.D., Littleton, J.T., 2014. Retrograde BMP signaling modulates rapid activity-dependent synaptic growth via presynaptic LIM kinase regulation of cofilin. *J. Neurosci.* 34, 4371–4381.

Qin, G., Schwarz, T., Kittel, R.J., Schmid, A., Rasse, T.M., Kappei, D., Ponimaskin, E., Heckmann, M., Sigrist, S.J., 2005. Four different subunits are essential for expressing the synaptic glutamate receptor at neuromuscular junctions of *Drosophila*. *J. Neurosci.* 25, 3209–3218.

Rasse, T.M., Fouquet, W., Schmid, A., Kittel, R.J., Mertel, S., Sigrist, C.B., Schmidt, M., Guzman, A., Merino, C., Qin, G., Quentin, C., Madeo, F.F., Heckmann, M., Sigrist, S.J., 2005. Glutamate receptor dynamics organizing synapse formation in vivo. *Nat. Neurosci.* 8, 898–905.

Ritzenthaler, S., Chiba, A., 2003. Myopodia (postsynaptic filopodia) participate in synaptic target recognition. *J. Neurobiol.* 55, 31–40.

Ritzenthaler, S., Suzuki, E., Chiba, A., 2000. Postsynaptic filopodia in muscle cells interact with innervating motoneuron axons. *Nat. Neurosci.* 3, 1012–1017.

Rodal, A.A., Blunk, A.D., Akbergenova, Y., Jorquera, R.A., Buhl, L.K., Littleton, J.T., 2011. A presynaptic endosomal trafficking pathway controls synaptic growth signaling. *J. Cell Biol.* 193, 201–217.

Sánchez-Soriano, N., Prokop, A., 2005. The influence of pioneer neurons on a growing motor nerve in *Drosophila* requires the neural cell adhesion molecule homolog FasciclinII. *J. Neurosci.* 25, 78–87.

Sanes, J.R., Lichtman, J.W., 1999. Development of the vertebrate neuromuscular junction. *Annu. Rev. Neurosci.* 22, 389–442.

Schmid, A., Chiba, A., Doe, C.Q., 1999. Clonal analysis of *Drosophila* embryonic neuroblasts: neural cell types, axon projections and muscle targets. *Development* 126, 4653–4689.

Schmid, A., Hallermann, S., Kittel, R.J., Khorramshahi, O., Frölich, A.M.J., Quentin, C., Rasse, T.M., Mertel, S., Heckmann, M., Sigrist, S.J., 2008. Activity-dependent site-specific changes of glutamate receptor composition in vivo. *Nat. Neurosci.* 11, 659–666.

Schubiger, M., Wade, A.A., Carney, G.E., Truman, J.W., Bender, M., 1998. *Drosophila* EcR-B ecdysone receptor isoforms are required for larval molting and for neuron remodeling during metamorphosis. *Development* 125, 2053–2062.

Schultz, W., 2001. Reward signaling by dopamine neurons. *Neuroscientist* 7, 293–302.

Schuster, C.M., Ultsch, A., Schloss, P., Cox, J.A., Schmitt, B., Betz, H., 1991. Molecular cloning of an invertebrate glutamate receptor subunit expressed in *Drosophila* muscle. *Science* 254, 112–114.

Sheng, C., Javed, U., Gibbs, M., Long, C., Yin, J., Qin, B., Yuan, Q., 2018. Experience-dependent structural plasticity targets dynamic filopodia in regulating dendrite maturation and synaptogenesis. *Nat. Commun.* 9, 3362.

Shepherd, D., Sahota, V., Court, R., Williams, D.W., Truman, J.W., 2019. Developmental organization of central neurons in the adult *Drosophila* ventral nervous system. *J. Comp. Neurol.* 527, 2573–2598.

Sherman, S.M., Spear, P.D., 1982. Organization of visual pathways in normal and visually deprived cats. *Physiol. Rev.* 62, 738–855.

Shishido, E., Takeichi, M., Nose, A., 1998. *Drosophila* synapse formation: regulation by transmembrane protein with Leu-rich repeats, CAPRICIOUS. *Science* 280, 2118–2121.

Sigrist, S.J., Reiff, D.F., Thiel, P.R., Steinert, J.R., Schuster, C.M., 2003. Experience-dependent strengthening of *Drosophila* neuromuscular junctions. *J. Neurosci.* 23, 6546–6556.

Simpson, J.H., 2009. Chapter 3 Mapping and Manipulating Neural Circuits in the Fly Brain, in:

Genetic Dissection of Neural Circuits and Behavior, *Advances in Genetics*. Elsevier, pp. 79–143.

Sink, H., Whittington, P.M., 1991. Early ablation of target muscles modulates the arborisation pattern of an identified embryonic *Drosophila* motor axon. *Development* 113, 701–707.

Stocker, B., Bochow, C., Damrau, C., Mathejczyk, T., Wolfenberger, H., Colomb, J., Weber, C., Ramesh, N., Duch, C., Biserova, N.M., Sigrist, S., Pflüger, H.-J., 2018. Structural and molecular properties of insect type II motor axon terminals. *Front. Syst. Neurosci.* 12, 5. doi:10.3389/fnsys.2018.00005

Sun, M., Xing, G., Yuan, L., Gan, G., Knight, D., With, S.I., He, C., Han, J., Zeng, X., Fang, M., Boulianne, G.L., Xie, W., 2011. Neuroligin 2 is required for synapse development and function at the *Drosophila* neuromuscular junction. *J. Neurosci.* 31, 687–699.

Sweeney, S.T., Broadie, K., Keane, J., Niemann, H., O’Kane, C.J., 1995. Targeted expression of tetanus toxin light chain in *Drosophila* specifically eliminates synaptic transmission and causes behavioral defects. *Neuron* 14, 341–351.

Tapia, J.C., Wylie, J.D., Kasthuri, N., Hayworth, K.J., Schalek, R., Berger, D.R., Guatimosim, C., Seung, H.S., Lichtman, J.W., 2012. Pervasive synaptic branch removal in the mammalian neuromuscular system at birth. *Neuron* 74, 816–829.

Technau, G., Heisenberg, M., 1982. Neural reorganization during metamorphosis of the corpora pedunculata in *Drosophila melanogaster*. *Nature* 295, 405–407.

Thomas, J.B., Bastiani, M.J., Bate, M., Goodman, C.S., 1984. From grasshopper to *Drosophila*: a common plan for neuronal development. *Nature* 310, 203–207.

Tomàs, J., Garcia, N., Lanuza, M.A., Santafé, M.M., Tomàs, M., Nadal, L., Hurtado, E., Simó, A., Cilleros, V., 2017. Presynaptic Membrane Receptors Modulate ACh Release, Axonal Competition and Synapse Elimination during Neuromuscular Junction Development. *Front. Mol. Neurosci.* 10,

132.

Truman, J.W., 1990. Metamorphosis of the central nervous system of *Drosophila*. *J. Neurobiol.* 21, 1072–1084.

Turney, S.G., Lichtman, J.W., 2012. Reversing the outcome of synapse elimination at developing neuromuscular junctions in vivo: evidence for synaptic competition and its mechanism. *PLoS Biol.* 10, e1001352. doi:10.1371/journal.pbio.1001352

Ulian-Benitez, S., Bishop, S., Foldi, I., Wentzell, J., Okenwa, C., Forero, M.G., Zhu, B., Moreira, M., Phizacklea, M., McIlroy, G., Li, G., Gay, N.J., Hidalgo, A., 2017. Kek-6: A truncated-Trk-like receptor for *Drosophila* neurotrophin 2 regulates structural synaptic plasticity. *PLoS Genet.* 13, e1006968. doi:10.1371/journal.pgen.1006968

Venken, K.J.T., Simpson, J.H., Bellen, H.J., 2011. Genetic manipulation of genes and cells in the nervous system of the fruit fly. *Neuron* 72, 202–230.

Ventimiglia, D., Bargmann, C.I., 2017. Diverse modes of synaptic signaling, regulation, and plasticity distinguish two classes of *C. elegans* glutamatergic neurons. *Elife* 6. doi:10.7554/eLife.31234

Vonhoff, F., Keshishian, H., 2017. Cyclic nucleotide signaling is required during synaptic refinement at the *Drosophila* neuromuscular junction. *Dev. Neurobiol.* 77, 39–60.

Wagh, D.A., Rasse, T.M., Asan, E., Hofbauer, A., Schwenkert, I., Dürbeck, H., Buchner, S., Dabauvalle, M.-C., Schmidt, M., Qin, G., Wichmann, C., Kittel, R., Sigrist, S.J., Buchner, E., 2006. Bruchpilot, a protein with homology to ELKS/CAST, is required for structural integrity and function of synaptic active zones in *Drosophila*. *Neuron* 49, 833–844.

Wairkar, Y.P., Toda, H., Mochizuki, H., Furukubo-Tokunaga, K., Tomoda, T., Diantonio, A., 2009. Unc-51 controls active zone density and protein composition by downregulating ERK

signaling. *J. Neurosci.* 29, 517--528.

Walsh, M.K., Lichtman, J.W., 2003. In vivo time-lapse imaging of synaptic takeover associated with naturally occurring synapse elimination. *Neuron* 37, 67–73.

Wan, H.I., DiAntonio, A., Fetter, R.D., Bergstrom, K., Strauss, R., Goodman, C.S., 2000. Highwire regulates synaptic growth in *Drosophila*. *Neuron* 26, 313–329.

Wang, T., Hauswirth, A.G., Tong, A., Dickman, D.K., Davis, G.W., 2014. Endostatin is a trans-synaptic signal for homeostatic synaptic plasticity. *Neuron* 83, 616–629.

Wang, T., Jones, R.T., Whippen, J.M., Davis, G.W., 2016. $\alpha 2\delta$ -3 Is Required for Rapid Transsynaptic Homeostatic Signaling. *Cell Rep.* 16, 2875–2888.

White, B.H., Osterwalder, T.P., Yoon, K.S., Joiner, W.J., Whim, M.D., Kaczmarek, L.K., Keshishian, H., 2001. Targeted attenuation of electrical activity in *Drosophila* using a genetically modified K(+) channel. *Neuron* 31, 699–711.

White, K., Grether, M.E., Abrams, J.M., Young, L., Farrell, K., Steller, H., 1994. Genetic control of programmed cell death in *Drosophila*. *Science* 264, 677–683.

White, K., Tahaoglu, E., Steller, H., 1996. Cell killing by the *Drosophila* gene reaper. *Science* 271, 805–807.

Wiesel, T.N., Hubel, D.H., 1963. Effects of visual deprivation on morphology and physiology of cells in the cats lateral geniculate body. *J. Neurophysiol.* 26, 978–993.

Wiesel, T.N., Hubel, D.H., 1965. Comparison of the effects of unilateral and bilateral eye closure on cortical unit responses in kittens. *J. Neurophysiol.* 28, 1029–1040.

Williams, D.W., Truman, J.W., 2005. Remodeling dendrites during insect metamorphosis. *J. Neurobiol.* 64, 24–33.

Wilson, A.M., Schalek, R., Suissa-Peleg, A., Jones, T.R., Knowles-Barley, S., Pfister, H.,

Lichtman, J.W., 2019. Developmental Rewiring between Cerebellar Climbing Fibers and Purkinje Cells Begins with Positive Feedback Synapse Addition. *Cell Rep.* 29, 2849–2861.

Wojtowicz, J.M., Marin, L., Atwood, H.L., 1994. Activity-induced changes in synaptic release sites at the crayfish neuromuscular junction. *J. Neurosci.* 14, 3688–3703.

Yoshihara, M., Adolfsen, B., Galle, K.T., Littleton, J.T., 2005. Retrograde signaling by Syt 4 induces presynaptic release and synapse-specific growth. *Science* 310, 858–863.

Yoshihara, M., Ito, K., 2012. Acute genetic manipulation of neuronal activity for the functional dissection of neural circuits—a dream come true for the pioneers of behavioral genetics. *J Neurogenet* 26, 43–52.

Younger, M.A., Müller, M., Tong, A., Pym, E.C., Davis, G.W., 2013. A Presynaptic ENaC Channel Drives Homeostatic Plasticity. *Neuron.* 79, 1183-1196.

Yu, H.-H., Kao, C.-F., He, Y., Ding, P., Kao, J.-C., Lee, T., 2010. A complete developmental sequence of a *Drosophila* neuronal lineage as revealed by twin-spot MARCM. *PLoS Biol.* 8. doi:10.1371/journal.pbio.1000461

Zito, K., Parnas, D., Fetter, R.D., Isacoff, E.Y., Goodman, C.S., 1999. Watching a synapse grow: noninvasive confocal imaging of synaptic growth in *Drosophila*. *Neuron* 22, 719–729.

Zucker, R.S., Regehr, W.G., 2002. Short-term synaptic plasticity. *Annu. Rev. Physiol.* 64, 355–405.

Chapter 3: Conclusions and future directions

Nicole A. Aponte-Santiago

The Picower Institute for Learning and Memory, Department of Biology, Massachusetts Institute
of Technology, Cambridge, MA 02139

Conclusion

My thesis work has begun to define how *Drosophila* tonic and phasic motoneurons respond to changes in activity or the presence of their partner neuron co-innervating the same postsynaptic muscle. My studies identified and characterized several plastic changes that occur in the structure of the tonic Ib neuronal subclass following silencing of their own activity or that of the Is partner neuron. I also identified distinct functional changes in the output of the Ib population that occur in response to ablation of Is motoneurons. A key component of this research moving forward will be directed at dissecting the underlying molecular mechanisms governing this type of plasticity, as well as why they are only observed in the tonic neuronal subclass. Given many forms of synaptic plasticity emerged early in nervous system evolution, defining the underlying molecular pathways could provide insights into plasticity mechanisms across species. *Drosophila* provides a genetically tractable system to define the molecular underpinnings of these synaptic responses. Given many human genes (~75%) have conserved homologs in *Drosophila* (Bier, 2005), we expect some of the molecular pathways used to alter synaptic structure and function in the fly model will be relevant for synaptic plasticity in other species. Therefore, dissecting the molecular pathways of how postsynaptic cells differentially regulate co-innervating inputs from different neuronal subclasses in this relatively simple model will likely provide insight into how neuronal subclasses interact in more sophisticated neuronal circuits.

The initial goal for my thesis work was to examine how postsynaptic cells distinguish and differentially regulate unique presynaptic inputs, as well as to determine if synaptic competition was present at *Drosophila* NMJs as observed at vertebrate motoneuron endplates. The robust developmental plasticity of synapse elimination at vertebrate NMJs provided an informative template for examining if similar types of competitive structural plasticity occurred in *Drosophila*,

and if so, to define the underlying molecular pathways. In hindsight, it is clear that a major difference in vertebrate versus invertebrate NMJ development is the large redundant motoneuron pool that innervates vertebrate muscle fields. While these motoneurons are all of the same type and thus compete within their own subclass for muscle innervation, *Drosophila* lacks this large precursor motoneuron pool and each motoneuron is genetically hardwired to innervate only 1 or a small subset of muscles. Therefore, there is no actual competition between identical motoneuron classes innervating the same muscle as observed in vertebrates. As such, I focused on determining if similar synaptic interactions would apply to neurons innervating the same target muscle that were from different subclasses, namely the tonic Ib and phasic Is motoneurons.

To begin the study, I performed a genetic screen and created a new genetic toolkit by identifying GAL4 drivers specific for the motoneuron subclasses that allowed manipulation of gene expression in a cell-type specific fashion. I then described the development of the tonic Ib and phasic Is motoneurons that co-innervate larval abdominal muscle 1 and characterized their responses to genetic manipulation of their activity or that of the co-innervating input. Unlike the vertebrate NMJ, *Drosophila* motoneurons from these subclasses did not display competition for synaptic innervation. Instead we found that the tonic motoneuron subclass was capable of either structural or functional compensation when the phasic motoneuron was disrupted.

To put the synaptic interactions we discovered in context of how these motoneurons initially innervate muscle 1 and control its contractility, we characterized the development and function of these two neuronal subclasses during development of the larval motor system. We found that Ib motoneurons innervating muscle 1 arrive first and form synapses before the Is growth cone approaches muscle 1. The delayed innervation by the Is input resulted in a shorter time window for maturation of Is NMJs over the 6 days of larval development. Although synaptic

innervation of the Is subtype was delayed compared to the Ib class, Is motoneurons added AZs at a faster rate and the muscle formed larger PSDs apposed to those AZs. It will be interesting in future studies to determine if the enhanced formation of larger PSD fields apposed to Is active zones is due to the high P_r synapses that the phasic Is neurons are known to form. We also found differences in how phasic Is and tonic Ib motoneurons respond to disruption of the Gbb pathway, a known retrograde BMP signal important in NMJ development. Our data indicate this pathway is important for synaptic growth in both Ib and Is motoneurons, but loss of Gbb signaling also reduces the number of muscles that contain any Is innervation at all. In addition, we established that Ib and Is motoneurons form independent inputs that make similar contributions to muscle excitability and contractile force. Finally, we found that the Ib and Is neuronal inputs respond differently to activity mismatch onto a postsynaptic target. Ib synapses showed structural changes following silencing of the Ib neuron itself or the co-innervating Is motoneuron. In contrast, we found that Ib motoneurons displayed functional changes without structural alterations when Is was ablated. Unlike the tonic Ib subclass, Is motoneurons showed no similar changes and were far less plastic to any manipulation we made.

Given the way my project developed during my thesis work, there are several approaches that would have been helpful to employ from the beginning. The MN1-Ib and MNIs GAL4 drivers have sparse expression in the central nervous system as well, including some expression in a few interneurons (Ashley et al., 2019). To make the drivers more specific, I would use the enhancer of the drivers found to create LexA and split GAL4 lines (Pfeiffer et al., 2010). For taking advantage of the split GAL4 technology, I would combine the enhancer regions for MN1-Ib and MNIs drivers with the enhancer region of a motoneuron driver. With this new tool, I would be able to manipulate only specific motoneurons without affecting any CNS interneurons. I would use the split GAL4

system to further characterize the role of these neurons in crawling larvae. To make additional MN1-Ib and MNIs genetic markers, I would have created transgenic lines with the LexA expression system and a GFP or RFP marker in the same insertion site. This change would facilitate the genetics of adding MN1-Ib or MNIs specific GFP or RFP markers in the background of genetic manipulations. For example, this change would facilitate the genetics of creating new lines with double expression systems and facilitate adding genetic mutations involved in NMJ patterning or NMJ plasticity to the motoneuron specific expression toolkit. Finally, in homeostatic plasticity, changes in the Is inputs can only be measured at low calcium, when the release properties of these neurons could be scaled up (Genç & Davis, 2019). Therefore, it would be beneficial to do electrophysiology experiments at low calcium to determine if any functional plasticity could be detected MNIs neurons under these conditions. Additionally, it would have valuable to have identified a few more MN Ib drivers that innervate muscles besides M1. Other muscles might display some unique plasticity, in particular the possibility for ectopic innervation when the MN Ib neuron is silenced or ablated. Given muscle 1 is the most peripheral muscle of each hemi-segment, there may be an inability for other motoneurons to detect potential innervation signals release by this muscle. Additional MN Ib drivers targeting other muscles would also allow to generalize our findings across this population if they behaved similarly to MN1-Ib. Given the phasic Is motoneurons innervate multiple muscles, this wasn't a problem for this subclass. Together, these additional tools would have given us more insight into how tonic and phasic motoneurons interact.

Future Directions

Different levels of plasticity between Ib and Is motoneurons

We found that the phasic MNIs motoneurons did not express any detected plasticity due to changes in their activity or following ablation or silencing of the partner neuron, MN1-Ib. We have interpreted this finding to indicate that the phasic Is motoneurons lack the type of plasticity found in the Ib subclass. However, we cannot rule out that the Is does show plasticity given MNIs innervates multiple muscles, in contrast to MN1-Ib innervating only one muscle. MNIs could be changing all of its synaptic terminals by a small amount that is distributed over a much larger synaptic field onto multiple muscles, and such a distributed change may not be measurable in just one muscle. Therefore, it would be interesting to collectively assay all the NMJs formed by the MNIs to see if one could measure changes emerging from the output of all Is synapses. Another possibility is that there are changes in the function but not the morphology of MNIs. At low calcium, the high releasing active zones of the Is synapse may be unable to potentiate, as previously observed in homeostatic plasticity. Homeostatic plasticity at Is synapses was only found under low calcium conditions when the release properties of these neurons could be scaled up (Genç & Davis, 2019). Therefore, to see if Is motoneurons do display some plasticity, I recommend doing electrophysiology recordings in low extracellular calcium. The higher calcium conditions used in our study are thought to represent physiological levels in the larvae, so it is unlikely the Is would display much plasticity *in vivo*.

Muscle innervation by multiple Ib or Is motoneurons

Another interesting scenario would be to discern what happens when the muscle is innervated by two neurons of the same class similar to what occurs at mammalian NMJs (Doll & Broadie, 2014; Tapia et al., 2012). This would allow us to discern if muscle innervation of two neurons of the same class would show different forms of plasticity, including potential competition

as observed in vertebrates. Poly-innervation of dorsal muscles can be triggered by manipulating the transcription factors of dorsal Ib motoneurons (Meng et al., 2019). Meng et al. showed through GCaMP imaging that poly-innervation does occur and that the duplicated neurons release neurotransmitters onto the muscle. It would be useful to identify if these neuronal inputs compete, compensate, or are independent by differentially labeling each neuron and comparing active zone number and bouton number with respect to each other. A positive correlation between inputs, measured by the number of active zones or synaptic boutons, would indicate that the neurons cooperate. In contrast, a negative correlation would suggest competition, while no correlation would indicate independent inputs as we have observed for the Ib and Is subclasses. I expect the tonic Ib inputs to be more plastic, either competing or cooperating, while the Is input would be more independent given we did not see changes in morphology or function of Is motoneurons in any of our manipulations.

Differences between Ib motoneurons

Silencing or ablating the Is with the MNIs GAL4 driver affects all the muscles innervated by the Is motoneurons. Therefore, it would be interesting to assess if Ib motoneurons innervating other muscles respond to the Is manipulation in the same way as we saw with MN1-Ib. MN1-Ib is capable of functionally compensating for the absence of Is and can increase active zone number in the case when Is is silenced. I would expect to see the same change as MN1-Ib in MN4-Ib since both M1 and M4 are innervated by the same dorsal Is motoneuron and occasionally lack Is innervation. On the other hand, M2 and M3 always have Is input. Therefore, MN2-Ib and MN3-Ib may behave differently. This experiment would allow us to see if there are subtle changes in the

same neuronal type that allows type Ib motoneurons to have different levels of plasticity, or if all Ib neurons are likely to behave the same.

Disruption of retrograde signals involved in muscle-triggered Ib plasticity

Ib responds differently to ablation or silencing of the Is neuron by increasing activity or active zone number, respectively. It is likely these different responses reflect distinct retrograde signals originating from the muscle. Now that we have characterized this type of plasticity, the next crucial step is to elucidate the molecular pathways at play. One way to achieve this would be to do a target screen of mutations disrupting the well characterized WNT, BMP or synaptotagmin 4-mediated retrograde signaling in the background of our manipulations. One could create a MNIs LexA driver to ablate or silence the Is and downregulate components of retrograde signaling with a muscle Gal4 driver. Using these toolkits, one could take advantage of being able to use a double expression system in the same animal. If ablation of one of these retrograde pathways altered either the functional or structural plasticity we observed in Ib, it would allow us to focus on characterizing the downstream receptors and their signaling pathway. It would also allow us to determine if the Is motoneuron lacks these components, thus providing a molecular clue for their inability to display these forms of plasticity. In addition to these well-known synaptic growth pathways, manipulations of protein known to function in structural plasticity could also be tested, including those mediated by Neurexin/Neuroligin, Teneurins, and neurotrophins. It will also be interesting to see if previously identified homeostatic plasticity mechanisms that are triggered following disruption of postsynaptic glutamate receptors may also be engaged following loss of one of the two motoneuron inputs.

Another important remaining question is how the postsynaptic cell detects the two synaptic populations and differentially regulates their properties. The Ib changed its property due to its own silencing and due to silencing or ablation of the Is partner neuron. It is still unknown if the postsynaptic cell differentially regulates the inputs or if the presynaptic neurons reacts differently to signals released by the muscle onto both Is and Ib terminals. For example, the Is may not detect the “increase innervation” signal when the Ib is silenced, and only the Ib neurons respond by extending filipodia-like projections. Another possibility is that the muscle is only sending this signal to the Ib motoneuron. Once the molecular pathways are established that mediate the changes we identified in Ib motoneurons, one could use immunocytochemistry to determine if the retrograde signals are only found at the PSDs apposed to the Ib subclass, or if they are present equally in both postsynaptic regions. RNA profiling of the two neuronal subclasses could also reveal unique expression profiles for presynaptic receptors or downstream signaling components that contribute to the differential plasticity.

One of the robust observations we made was the finding that the Ib motoneuron increased active zone number, but not functional output, following Is silencing. To extend this observation, one could follow with live imaging when more active zones appear at Ib terminal after Is silencing, and measure the maturation of these new active zones by looking at the increasing size of the PSD during development (Akbergenova et al., 2018). It would also be interesting to perform EM under these conditions to examine the distribution of SVs within the terminal. It is possible that although active zone number increases, there is less docked SVs per active zone, which would explain why the structural change does not lead to a functional increase in release. It would also be exciting to examine distribution of the presynaptic voltage-gated calcium channel Cacophony (Cac). Another possibility is that the motoneurons increases the number of active zones, but does not upregulate

Cac production, leading to fewer channels per active zone and lack of a functional increase in output.

Interestingly, the increase in active zone number in Ib motoneurons is not seen when the Is is ablated, suggesting these structural changes require the physical presence of a Is non-functional synapse onto the muscle. This indicates that the muscle is able to distinguish when the Is motoneuron is absent or present in determining how it induces change in the Ib neuron. If there is a signal coming from the Is input that informs the muscle of its presence, one could use a double expression system to silence the Is and downregulate candidate Is signaling components at the same time. If, disruption of this signal triggered a functional change in Ib, it would indicate a molecular component of the switch present in the Is that tells the muscle it is there but non-functional. This experiment can be done by using a double expression system to silence the Is and downregulate unique proteins expressed at the Is terminal, such as the cell adhesion molecule DIP alpha (Ashley et al., 2019; Carrillo et al., 2015; Pérez-moreno & Kane, 2019). Another way that the muscle may know when Is is present is through spontaneous SV release from the Is. One could use genetic approaches to disrupt evoked and spontaneous glutamate release from the Is by deleting the vesicular glutamate transporter, resulting in empty synaptic vesicles (Choi et al., 2014). Decreasing both evoked and spontaneous release from the Is motoneuron would determine if spontaneous release is involved in input identification by the muscle. If we see the same effect when we disrupt both evoked and spontaneous release in Is, similar to that observed following loss of evoked release by tetanus toxin expression, then spontaneous release is not the signal that allows the muscle to identify when Is is physically present. Another possibility is that the Ib neuron responds to Is disruption of both evoked and spontaneous release with a change in activity without a structural change like it would in the case of Is ablation. This second scenario would be a strong

indication that spontaneous release is important for the muscle to identify the presence of the phasic input and subsequently shift the retrograde system it employs to trigger Ib plasticity changes.

Transcriptional profiles of Ib and Is motoneurons

As we gather more information about the Ib and Is motoneurons in *Drosophila*, it is becoming highly relevant to characterize the distinct transcriptional profiles of each neuronal subclass. The intrinsic differences between Ib and Is neurons are likely due in part to differences in their transcription profiles. I would expect to find differences in ion channel expression and ion channel isoforms that would correspond to their different action potential kinetics. In addition, I would expect to see differences in expression pattern of proteins involved in patterning, axonal targeting, and plasticity.

In addition to changes in the transcriptome, it will be important to look at post-synaptic modifications of ion channels and synaptic proteins and their distribution to understand how post-translational changes also control the differences between these two neuronal subpopulations. Identifying the cell surface proteome from each subclass may define why the Ib innervates a single muscle, while Is motoneurons innervate many muscle partners. Finally, the transcription profile would help us determine how these motoneurons express different receptors that might lead to unique responses to retrograde signals or trans-synaptic communication from the muscle. Overall, the work in my thesis brings us closer to understanding the dynamics occurring between multiple inputs onto one postsynaptic cell, and how these inputs may be differentially regulated through activity changes.

Possible Parallels to Mammalian Tonic and Phasic Neurons

It remains to be seen what parallels can be found between our new findings on tonic and phasic synapses in *Drosophila* and synapses in the mammalian CNS. In the prefrontal context in mammals, tonic and phasic dopaminergic neurons are essential for maintaining a learned behavior that is associated with tonic firing patterns, versus changing the behavior due to reward and phasic firing patterns (Ellwood et al., 2017). In the fly system, we see that tonic synapses are more plastic than phasic synapses following activity modifications. Therefore, it would be interesting to study how changes in activity in phasic or tonic neurons would change learning behavior in mammals. Additionally, it remains to be seen if the phasic neurons are also less plastic in the mammalian prefrontal context. Finally, disruption in the balance of tonic and phasic inhibition has been implicated in several neurological disorders, such as epilepsy, depression, and anxiety (Brickley & Mody, 2012; Fritschy, 2008; Hines et al., 2012; Macdonald et al., 2010). Understanding the interactions of tonic and phasic synapses in different systems is likely to yield insights into how distinct synapses in the brain can be differentially regulated.

Bibliography:

- Akbergenova, Y., Cunningham, K. L., Zhang, Y. V., Weiss, S., & Littleton, J. T. (2018). *Characterization of developmental and molecular factors underlying release heterogeneity at Drosophila synapses*. 1–37.
- Ashley, J., Sorrentino, V., Lobb-rabe, M., Nagarkar-jaiswal, S., Tan, L., Xu, S., Xiao, Q., Zinn, K., & Carrillo, R. A. (2019). *Transsynaptic interactions between IgSF proteins DIP- a and Dpr10 are required for motor neuron targeting specificity*. 1–24.
- Bier, E. (2005). Drosophila, the golden bug, emerges as a tool for human genetics. *Nature Reviews Genetics*, 6(1), 9–23. <https://doi.org/10.1038/nrg1503>
- Brickley, S. G., & Mody, I. (2012). Extrasynaptic GABA A Receptors: Their Function in the CNS and Implications for Disease. *Neuron*, 73(1), 23–34. <https://doi.org/10.1016/j.neuron.2011.12.012>
- Carrillo, R. A., Özkan, E., Menon, K. P., Nagarkar-Jaiswal, S., Lee, P. T., Jeon, M., Birnbaum, M. E., Bellen, H. J., Garcia, K. C., & Zinn, K. (2015). Control of Synaptic Connectivity by a Network of Drosophila IgSF Cell Surface Proteins. *Cell*, 163(7), 1770–1782. <https://doi.org/10.1016/j.cell.2015.11.022>
- Choi, B. J., Imlach, W. L., Jiao, W., Wolfram, V., Wu, Y., Grbic, M., Cela, C., Baines, R. A., Nitabach, M. N., & McCabe, B. D. (2014). Miniature Neurotransmission Regulates Drosophila Synaptic Structural Maturation. *Neuron*, 82(3), 618–634. <https://doi.org/10.1016/j.neuron.2014.03.012>
- Doll, C. A., & Broadie, K. (2014). Impaired activity-dependent neural circuit assembly and refinement in autism spectrum disorder genetic models. *Frontiers in Cellular Neuroscience*, 8. <https://doi.org/10.3389/fncel.2014.00030>

- Ellwood, I. T., Patel, T., Wadia, V., Lee, A. T., Liptak, A. T., Bender, K. J., & Sohal, V. S. (2017). Tonic or phasic stimulation of dopaminergic projections to prefrontal cortex causes mice to maintain or deviate from previously learned behavioral strategies. *Journal of Neuroscience*, 37(35), 8315–8329. <https://doi.org/10.1523/JNEUROSCI.1221-17.2017>
- Fritschy, J. M. (2008). Epilepsy, E/I balance and GABAA receptor plasticity. *Frontiers in Molecular Neuroscience*, 1(MAR). <https://doi.org/10.3389/neuro.02.005.2008>
- Genç, Ö., & Davis, G. W. (2019). Target-wide Induction and Synapse Type-Specific Robustness of Presynaptic Homeostasis. *Current Biology*, 29(22), 3863-3873.e2. <https://doi.org/10.1016/j.cub.2019.09.036>
- Hines, R. M., Davies, P. A., Moss, S. J., & Maguire, J. (2012). Functional regulation of GABA A receptors in nervous system pathologies. *Current Opinion in Neurobiology*, 22(3), 552–558. <https://doi.org/10.1016/j.conb.2011.10.007>
- Macdonald, R. L., Kang, J. Q., & Gallagher, M. J. (2010). Mutations in GABAA receptor subunits associated with genetic epilepsies. *Journal of Physiology*, 588(11), 1861–1869. <https://doi.org/10.1113/jphysiol.2010.186999>
- Meng, J. L., Marshall, Z. D., Lobb-Rabe, M., & Heckscher, E. S. (2019). How prolonged expression of hunchback, a temporal transcription factor, re-wires locomotor circuits. *ELife*, 8, 1–30. <https://doi.org/10.7554/eLife.46089>
- Pérez-moreno, J. J., & Kane, C. J. O. (2019). *GAL4 Drivers Specific for Type Ib and Type Is Motor Neurons in Drosophila*. 9(February), 453–462. <https://doi.org/10.1534/g3.118.200809>
- Pfeiffer, B. D., Ngo, T.-T. T. B., Hibbard, K. L., Murphy, C., Jenett, A., Truman, J. W., & Rubin, G. M. (2010). Refinement of tools for targeted gene expression in *Drosophila*. *Genetics*, 186(2), 735–755. <https://doi.org/10.1534/genetics.110.119917>

Tapia, J. C., Wylie, J. D., Kasthuri, N., Hayworth, K. J., Schalek, R., Berger, D. R., Guatimosim, C., Seung, H. S., & Lichtman, J. W. (2012). Pervasive Synaptic Branch Removal in the Mammalian Neuromuscular System at Birth. *Neuron*, 74(5), 816–829. <https://doi.org/10.1016/j.neuron.2012.04.017>